

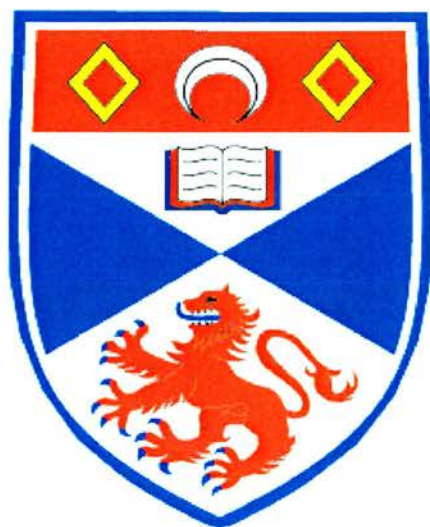
University of St Andrews



Full metadata for this thesis is available in
St Andrews Research Repository
at:

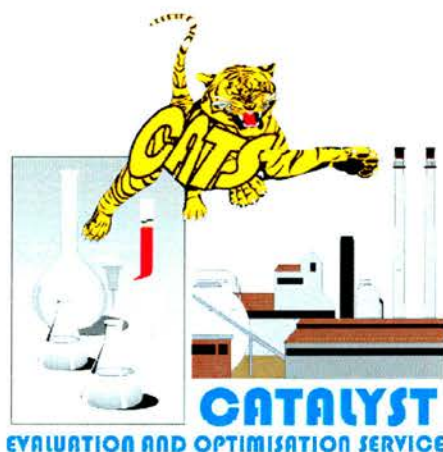
<http://research-repository.st-andrews.ac.uk/>

This thesis is protected by original copyright



Studies in Carbonylation Catalysis

A thesis presented to the University of St. Andrews in fulfilment of
the requirements for the degree of Master of Philosophy



Gary Paul Schwarz

February 2000



DECLARATION

I, Gary Paul Schwarz, hereby certify that this thesis, has been written by me, that it is the record of work carried out by me and that it has not been submitted in any previous application for a higher degree.

Signed _____

Date 24/02/00

I was admitted as a research student in September 1997 and as a candidate for the degree of Master of Philosophy in September 1997; the higher study for which this is a record was carried out in the University of St. Andrews between September 1997 and February 2000.

Signed _____

Date 24/02/00

I hereby certify that the candidate has fulfilled the conditions of the Resolution and Regulations appropriate for the degree of Master of Philosophy in the University of St. Andrews and that the candidate is qualified to submit this thesis in application for that degree.

Signed _____

Date 24th February, 2000

In submitting this thesis to the University of St. Andrews I wish access to it to be subject to the following conditions: for a period of five years from the date of submission, the thesis shall be withheld from use. I understand, however, that, the title and abstract of the thesis will be published during this period of restricted access; and after the expiry of this period the thesis will be made available for use in accordance with the regulations of the University Library for the time being in force, subject to any copyright in the work not being affected thereby, and a copy of the work may be made and supplied to any *bona fide* library or research worker.

Signed

Date 24/02/99



ACKNOWLEDGEMENTS

ACKNOWLEDGEMENTS

I would first like to thank Professor David Cole-Hamilton, for his guidance, inspiration and encouragement, not to mention for giving me the opportunity to study whilst working for CATS. Thanks also to Dr. Doug Foster for his guidance as CATS coordinator and for allowing me use of the reports.

I would also like to express my gratitude to Dr. Russell Morris for help with the POSS work and to all the research groups who supplied ligands to test, there simply would be nothing to write without them: Professor Eric Hope (Leicester), Dr. Tom Welton (Imperial), Professor J. Derek Woollins (St. Andrews), Professor Roger Alder (Bristol), and Dr. Martin Wills (Warwick)

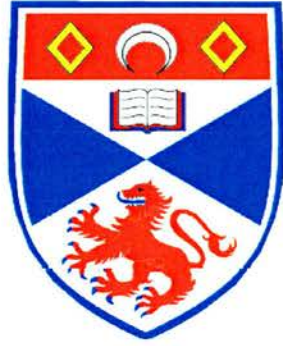
A big thank you to the entire DCH group, both past and present, who I have shared lab - and pub - time with. Gratitude is also extended to all the technical and services staff at the school of chemistry, especially Jim Rennie and Bobby Cathcart in the workshop for endless help with the rig.

To the St. Andrews 'sanity squad' – the people who kept me 'normal' ...or at least from going completely *meshugga*... during my time in St. Andrews (in order of appearance) Andy and Patricia Marr, Alisdair Brown, Ruth Robertson, Joshua Paul, Louis Rogers, Linda MacInnes, Dan White and Ann McConnell.

A certain amount of gratitude is also owed to all the others in who have put up with me at various stages of my stay (you know who you are!). To the people who are too numerous to mention – in St. Andrews, Glasgow, London, New Zealand and various other parts of the globe – don't worry, I haven't forgotten you. To all of you: thank you for making my stay in Britain a memorable one.

As always, I owe my family a huge debt of gratitude, and even though they have been on the other side of the world, they have always given me more support than anyone would expect – Gillian, Gordon, Greg and Gavin – I couldn't have done it without you, Thanks heaps.

I am also very grateful to the Scottish Higher Education Funding Council (SHEFC) for funding CATS (through a research development grant) and for providing me with a salary for the past 2 ½ years.



ABSTRACT

ABSTRACT

Catalyst testing is an important aspect of process development. Often potential catalysts remain undiscovered after synthesis and are never tested. This may be due to the research group's focus not being on catalysis, or it may be caused by a lack of local testing facilities. The CATS service was established to provide a solution to this problem. The St. Andrews branch of this service tested the potential of a variety of compounds, mainly for homogeneous hydroformylations sourced from academic and industrial research groups.

The role of the CATS service is explained in the first chapter. The facilities available to the customer from the entire service as well as the facilities in St. Andrews are discussed. This is analysed as all the research carried out in this work was done under the CATS umbrella.

Catalytic hydroformylation of alkenes is covered in the second chapter. It is the major catalytic reaction tested, and its history, processes, design, and applications are presented. The general mechanism and kinetic processes of this catalytic reaction are also discussed.

The third chapter focusses on POSS molecules as building blocks for dendrimers to design ligands for easily recyclable catalysts. The concept is discussed and some results reported.

Chapter four discusses all of the projects carried out for customers, introduces their aims, and reports their results. These projects include catalysis using fluorous biphasic catalysis, large ring biphosphines, dendrimer based diphosphine units, palladium catalysed copolymerisation, cobalt based methanol carbonylation, and rhodium catalysed carbonylation of methyl acetate. Asymmetric hydroformylation of vinyl acetate and styrene is also explored.

TABLE OF CONTENTS

Declaration	<i>i</i>
Acknowledgements	<i>iii</i>
Abstract	<i>iv</i>
Table of Contents	<i>v</i>
List of Figures	<i>viii</i>
List of Tables.....	<i>x</i>
Abbreviations	<i>xi</i>
Foreword	1

CHAPTER ONE: THE CATS SERVICE

1.1 The Service.....	2
Facilities available through CATS.....	2
1.2 Facilities in St. Andrews	3
1.2.1 Kinetics Rig.....	3
1.2.2 GC-MS	6
1.2.3 The Laboratory.....	6

CHAPTER TWO: INTRODUCTION TO HYDROFORMYLATION

2.1 Introduction	7
2.2 History	8
2.3 Hydroformylation Processes	9
2.3.1 First Generation Processes	9
2.3.2 Second Generation Processes.....	9
2.3.3 Third Generation Processes.....	10
Biphasic Systems	11
Solid Supports	11
Supercritical fluids	12
2.4 Catalyst Design	12
2.4.1 Variation of Metal	13
Monometallic Catalysts.....	13
Polymetallic Catalysts.....	13
2.4.2 Modification by Ligands.....	14
Phosphines.....	14
Phosphites	16
2.4.3 Rhodium Organometallic Catalyst Deactivation	16
2.5 Substrates	18
2.5.1 Substrates with Industrial importance.....	19
2.6 Asymmetric Hydroformylation.....	21
2.7 Mechanism	22
2.7.1 Unmodified Cobalt and Rhodium Catalysts	22
Selectivity.....	23
2.7.2 Phosphine-Modified Catalysts	24
2.7.3 Substrate influenced isomers.....	26

2.8 Kinetics of Hydroformylation	27
2.8.1 Unmodified Catalysts.....	28
2.8.2 Ligand Modified Catalysts.....	29
2.9 Process Parameters.....	30
2.9.1 Unmodified Catalysts.....	30
Temperature	30
Pressure	30
Catalyst Concentration.....	31
2.9.2 Modified Catalysts	31
Temperature	31
Pressure	31
Catalyst Concentration.....	32
Ligands.....	32
2.10 Conclusion.....	32

CHAPTER THREE: SILSESQUIOXANE DENDRIMERS

3.1 Introduction	33
3.2 Silsesquioxanes	34
3.2.1 The History of Silsesquioxanes.....	35
3.2.2 The Chemistry of Silsesquioxanes:.....	35
3.2.3 The Role of Silsesquioxane molecules in Catalysis.....	37
3.3 Dendrimers.....	38
3.5 Catalyst Design	40
3.5.1 Strategy	40
3.5.2 Why use a dendrimer supported catalyst?.....	40
3.5.3 Metal Selection.....	40
Rhodium.....	40
Cobalt.....	41
3.5.4 Ligand Design.....	41
3.5.3 Binding Catalytic Species to Ligand.....	43
3.6 Results.....	44
3.7 Experimental for chapter Three.....	47
POSS Phosphine Ligand	47
Catalytic run:.....	47
3.8. Conclusion:	48

CHAPTER FOUR: CATALYTIC RUNS

4.1 Fluorous Biphasic Catalysis (Leicester).....	49
Hexene.....	51
Nonenes.....	53
4.2 Large Ring Diphosphines (Bristol)	57
Hex-1-ene.....	58
Styrene and Vinyl Acetate.....	59
4.3 Dendrimer based diphosphine units (Imperial).....	64
Rhodium Complexes.....	65
Ruthenium Complexes.....	66
4.4 Asymmetric Hydroformylation (Warwick).....	71

Vinyl Acetate	72
Styrene.....	75
4.5 Other reactions	83
4.5.1 Palladium Catalysed Copolymerisation	83
4.5.2 Cobalt Based Methanol Carbonylation Catalysis	86
4.5.3 Rhodium Catalysed Carbonylation of Methyl acetate	90
CHAPTER FIVE: EXPERIMENTAL	
5.1 General Experimental.....	93
5.2 Charging the Autoclave.....	94
Air Sensitive compounds	94
Non-Air Sensitive Compounds	95
5.3 Analysis.....	95
Afterword.....	96
References	97

LIST OF FIGURES

CHAPTER ONE:

Figure 1: Schematic diagram of the CATS kinetic rig.	3
Figure 2: Photograph showing autoclave and injection port.	4
Figure 3: Photograph of CATS kinetics rig.	5
Figure 4: The CATS PC and GC-MS system.	6
Figure 5: The Wolfson Centre for Catalysis.	6

CHAPTER TWO:

Figure 6: Examples of hydroformylation reactions.	7
Figure 7: Compounds accessible through hydroformylation.	8
Figure 8: Phase transfer and immobilised catalysis at the border between homogeneous and heterogeneous catalysis.	11
Figure 9: General Composition of Catalytic System for hydroformylation and orders of metal activity and ligand modifying effect.	13
Figure 10: Structures of BISBI and DIPHOS.	15
Figure 11: Possible mechanisms of catalyst degradation.	17
Figure 12: The order of olefin reactivity in hydroformylation reactions.	18
Figure 13: Hydroformylation pathway of 2,3-dimethyl-2-butene.	18
Figure 14: Bis-phosphite ligand used to modify a rhodium catalyst precursor.	19
Figure 15: Hydroformylation of allyl alcohol to 1,4-butanediol.	20
Figure 16: The hydroformylation step in the synthesis of the Vitamin A precursor (b).	20
Figure 17: Generic asymmetric hydroformylation.	20
Figure 18: The structure of (R,S)-BINAPHOS phosphine-phosphite ligand.	21
Figure 19: Catalytic cycle of hydroformylation with unmodified cobalt catalyst.	22
Figure 20: Isomerisation of the acylcobalt carbonyl species.	23
Figure 21: Initial equilibria forming the active catalyst species.	24
Figure 22: The hydroformylation cycle for modified rhodium catalysts.	24
Figure 23: General scheme for metal insertion determining <i>n/i</i> products.	25
Figure 24: Alkene isomerisation during hydroformylation.	26
Figure 25: General scheme depicting alkene coordination equilibrium.	29

CHAPTER THREE:

Figure 26: POSS molecule based on a cubane structure.	34
Figure 27: An example of an open cage POSS molecule.	36
Figure 28: Synthesis of Octavinyl octasilsesquioxane ($(\text{CH}_2=\text{CH}_2)_8\text{Si}_8\text{O}_{12}$).	36
Figure 29: The synthesis of a 24-Br functionalised dendrimer in one step.	37
Figure 30: Schematic diagram of a dendritic macromolecule functionalised on the external surface with a catalytic group 'A'.	38
Figure 31: A catalyst based dendrimeric species built on a single silicon atom as the core.	39
Figure 32: Reaction catalysed by the dendrimeric supported nickel catalyst.	39
Figure 33: Proposed three-step synthesis of a 72-Br functionalised dendrimer.	42
Figure 34: Two examples of POSS molecules with phosphorous functional groups on the outer layer.	43
Figure 35: Functionalisation of the chain ends of a dendrimer using NaPR_2 facilitating the possible coordination of a metal species ('M') leading to a potentially non-leaching catalyst.	43
Figure 36: Reaction of vinyl-POSS with HPeEt_2 and a radical initiator.	44
Figure 37: Kinetic graph of POSS dendrimer based catalyst.	45
Figure 38: Reaction of 24 and 72-vinyl functionalised POSS with HPeEt_2	46
Figure 39: Reaction of 24-Cl functionalised POSS with $\text{LiCH}_2\text{P}(\text{CH}_3)_2$	46

CHAPTER FOUR:

Figure 40: Principle of biphasic reactions.....	50
Figure 41: Solvent (PP3) and examples of ligands used in the perfluorous biphasic study.....	51
Figure 42: Photograph showing the fluoruous (bottom) and organic (top) layers of the biphasic reactions. ...	52
Figure 43: Kinetics of Hydroformylation of Nonenes.....	53
Figure 44: Large ring diphosphines studied for hydroformylation reactions.....	57
Figure 45: Alkene binding step of hydroformylation reactions.....	57
Figure 46: Catalyst precursors FJS 343 – FJS 351.....	64
Figure 47: Dendrimer core for generation = 1 dendrimer (n=8). Generation =3 is not shown (n = 32).....	64
Figure 48: Kinetics Graph for Imperial Experiment 7.....	65
Figure 49: Graph of induction period for experiment 4.	67
Figure 50: Graph of gas uptake for experiment 4 showing odd shape.	68
Figure 51: Structures of the ESPHOS and SEMI-ESPHOS ligands.....	71
Figure 52: Scheme illustrating the formation of straight and branched Rh-Alkyl species.....	72
Figure 53: Vinyl acetate used as a building block for the synthesis of the α -amino acid threonine.	73
Figure 54: Production of 2Ac1ol and 1Ac2ol from vinyl acetate under hydroformylation conditions.	73
Figure 55: Hydrolysis of 1-acetoxy-2-propanol and 2-acetoxy-1-propanol to give 1,2-propanediol.	74
Figure 56: Thermal decomposition of 3-acetoxypropanal.....	74
Figure 57: Structures of Naproxen and Ibuprofen.....	75
Figure 58: Copolymerisation of ethene and CO in methanol.	83
Figure 59: End groups of the copolymerisation products.....	84
Figure 60: The catalyst precursors and active catalytic cobalt species (a & b).	86
Figure 61: Kinetic graph of methanol carbonylation	87
Figure 62: Rhodium Catalysed carbonylation of methyl acetate	90

LIST OF TABLES

CHAPTER TWO:

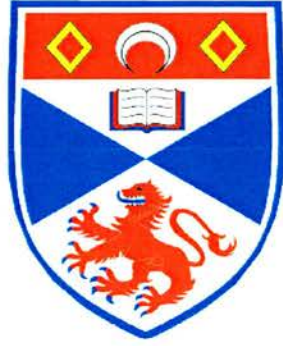
Table 1: Hydroformylation of alkenes: Relative Rate and Isomer ratios	26
Table 2: Parameters of the hydroformylation kinetics of terminal alkenes	27

CHAPTER FOUR:

Table 3: Hydroformylation of hex-1-ene catalysed by rhodium complexes.	55
Table 4: Hydroformylation of nonenes.	56
Table 5: Results from the hydroformylation of 1-Hexene by large ring diphosphines	60
Table 6: Attempted asymmetric hydroformylation of styrene.	62
Table 7: Attempted asymmetric hydroformylation of vinyl acetate.	63
Table 8: Catalytic hydroformylation of 1-hexene using the catalyst precursors FJS 343 – FJS 351.	69
Table 9: Asymmetric hydroformylation of vinyl acetate using ESPHOS.	76
Table 10: Asymmetric hydroformylation of vinyl acetate using SEMI-ESPHOS.	78
Table 11: Hydroformylation of vinyl acetate using PPh ₃ for comparison	78
Table 12: Asymmetric hydroformylation of styrene using ESPHOS diphosphine.	79
Table 13: Asymmetric hydroformylation of styrene using SEMI-ESPHOS.	80
Table 14: Hydroformylation of styrene using PPh ₃ for comparison.	81
Table 15: Copolymerisation of ethylene and CO using diphosphine ligands.	85
Table 16: Kinetic runs for Cobalt Based Methanol Carbonylation Catalysis.	89
Table 17: Rhodium Catalysed Methyl Acetate Carbonylation runs.	92

ABBREVIATIONS

1Ac2ol	1-acetoxy-2-propanol
2Ac1ol	2-acetoxy-1-propanol
2Acal	2-acetoxypropanal
acac	η^2 -acetylacetone
Ac	acetate
AIBN	azoisobutylnitrile
Ar	aryl
CATS	Catalyst Evaluation and Optimisation Service
Cp*	pentamethylcyclopentadienyl
ee	enantiomeric excess
<i>n/i</i>	branched/straight chain isomers
Ph	phenyl
POSS	polyhedral oligomeric silsesquioxanes
PP3	perfluoromethylcyclohexane
PPh ₃	triphenylphosphine
ppm	parts per million
rpm	revolutions per minute
THF	tetrahydrofuran
TOF	turnover frequency



FOREWORD

FOREWORD

Why is it necessary to study homogeneous catalysis?

Heterogeneous catalysis has advantages in application but homogeneous catalysis provides a far better mechanistic understanding of catalytic cycles and the possibility of influencing steric and electronic properties. It is feasible to optimise homogeneous catalysts step-by-step for a particular problem. Processes can be developed to avoid disadvantages such as catalyst recycling and leaching. This would lead to a new generation catalyst that has the advantages of both systems, whilst minimising the drawbacks. At first glance this may seem very optimistic. However, current research shows that such gains are not unrealistic. Given the industrial and economic importance of catalysed reactions this would provide financial as well as environmental benefits.

Having recognised the potential of such modified homogeneous catalysis, it was considered appropriate to engage in studies in this area in concert with other contemporary research programmes under the CATS service umbrella.



CHAPTER ONE:
THE CATS SERVICE

CHAPTER ONE: THE CATS SERVICE

The CATS (Catalytic Evaluation and Optimisation Services) service is aimed at evaluating, optimising and commercialising new compounds and materials as catalysts. The projects I conducted were under the umbrella of the services and the core of my research was performed as part of the CATS program.

1.1 THE SERVICE

The services aims are to:

- Evaluate new compounds and materials for their catalytic potential
- Optimise promising catalysts for their activity, selectivity, stability and lifetime
- Open up routes to commercialisation of catalysts via direct contacts with appropriate industries
- Bridge the gap between the Science base and the Applied Catalysis Industry.

CATS is run by a consortium of Scottish Universities: St. Andrews (homogeneous catalysis), Dundee (heterogeneous catalysis), Edinburgh (Surface Area Measurements) and Glasgow (heterogeneous catalysis). This chapter focuses on the facilities based in St. Andrews used to evaluate and optimise homogeneous catalytic reactions.

FACILITIES AVAILABLE THROUGH CATS

The four centres in the CATS framework each specialise in a different area of catalysis. The equipment available to the consortium is as follows:

- Heterogeneous reactor for liquid-phase hydrogenations
- Two dedicated reactors for evaluating metals, supported metals, metal oxides or supported metal complexes, each with on-line GCMS detection
- Homogeneous batch reactor with efficient gas/liquid mixing and the capability for kinetic measurements at constant pressure
- Instrument for measuring total (BET) surface area, metal surface area, and pore size
- A wide range of other techniques from within the research groups running the service
- There is a large range of reactions able to be supported by the service.

1.2 FACILITIES IN ST. ANDREWS

The facilities available at the St. Andrews catalysis centre are for the optimisation and evaluation of homogeneous reactions. The CATS service owns a range of hardware and they will be introduced here. There are other facilities and services available within the group and the university which will not be mentioned in this section (eg. elemental analysis, atomic absorption spectrometry, NMR, FT-IR, etc.).

1.2.1 KINETICS RIG

The service owns a purpose built kinetics autoclave that is used to perform catalytic runs under various pressures.

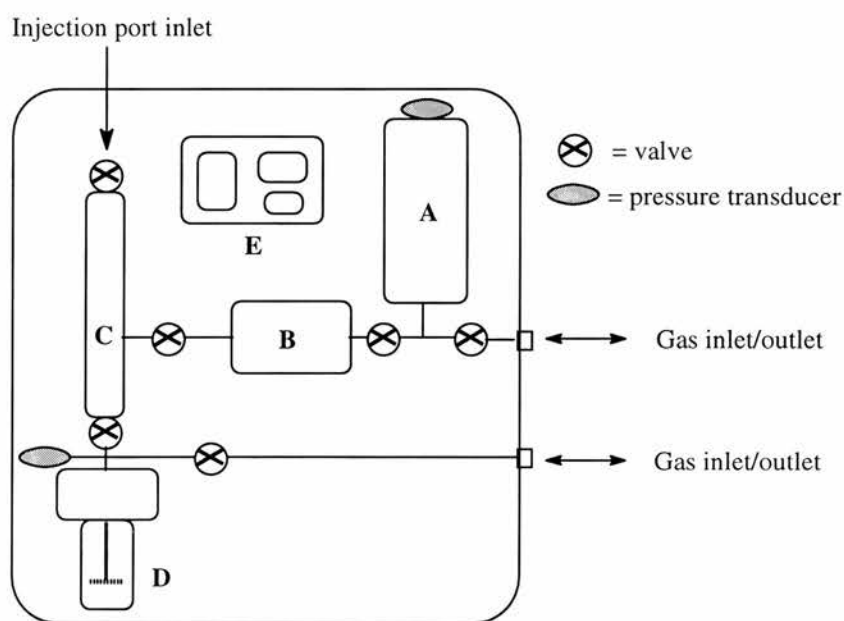


Figure 1: Schematic diagram of the CATS kinetic rig.

The rig, shown schematically in Figure 1, consists of a ballast vessel (A), a pressure controller and transducer (B), an injection vessel (C), the autoclave (D) and a control panel (E). The hardware was manufactured by Baskerville and assembled by the University of St. Andrews, School of Chemistry workshop.

Each section can be isolated from the others by using valves. As the reaction proceeds the pressure in the autoclave is kept constant by the pressure controller, which in turn is fed by gas stored in the ballast vessel. The gas uptake is monitored by recording the drop in pressure in the ballast vessel. Data obtained allows the calculation of the rates of reaction.

The autoclave and ballast vessel can be vented or filled independently, and the pressures in the autoclave, ballast vessel and injection port are all monitored by pressure transducers. There is an inbuilt pressure monitor in the flow controller that records the pressure in the injection port (and autoclave when the valve is open).

Data is transferred via a link from data logging hardware (Pico Monitor model ADC16) fitted to a COM port in the CATS PC. The computer uses data logging software (PicoLog for Windows version 5.04.2) to monitor and record the pressures. Printouts of all data are then available in graph or raw forms. This can be saved and used in other applications if needed.

The Ballast vessel (Figure 1A) is filled directly from the cylinder and has been tested to 7500 Psig. The volume of the ballast vessel was calculated as 37.8 mL

The pressure and mass flow controller (Figure 1C) is manufactured by Bronkhorst Hi-Tec (Model F032C) and is linked to a digital readout and control system (Model E-7000). This controls the pressure in the injection port (and in the reaction vessel during runs when the valve is open).

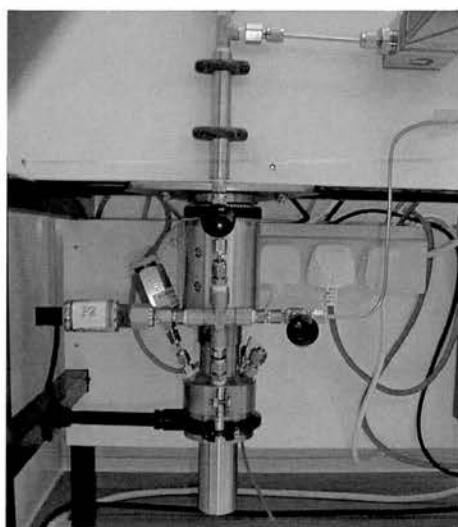


Figure 2: Photograph showing autoclave and injection port.

The injection port (Figure 1C and Figure 2) has a large bore valve able to accommodate syringe needle to facilitate substrate injection and is tested to 7500 Psig. The lower valve has a tube that extends deep into the reaction vessel to ensure the substrate is injected directly into the reaction mixture.

The autoclave is fitted with a temperature probe and mechanical stirrer. It can also accommodate a sampling probe (with needle valve) for manual sample extraction if samples need to be taken during the course of a reaction. The stirrer is driven by a DC Motor and the revolution rate is monitored using a hand held Lutron Digital Photo Tachometer (Model DT-2234B). The volume of the reaction vessel is 30 mL and all wetted parts are made from Hasteloy C. It is heated by an external heating band controlled by an independent temperature controller. The temperature within the autoclave is monitored using the internal temperature probe linked by a thermocouple to a Fluke 51 K/J digital thermometer. For safety reasons, a bursting disc is fitted and has a maximum pressure of 5240 Psig.

The control panel (Figure 1E) houses the digital readout and control system, the pressure readouts from the pressure transducers and the event switch which sends a signal to the data logger when it is activated. The event switch is used to record the exact injection time or other significant events during the run. The full reaction rig is shown in Figure 3.



Figure 3: Photograph of CATS kinetics rig.

The rig is charged using high pressure gasheads built by the School of Chemistry workshop.

1.2.2 GC-MS

The CATS service in St. Andrews runs an HP 6890 GC System (Gas Chromatography - Mass Selective detector or GC-MS) manufactured by Hewlett Packard (Model 5973 MS) (Figure 4).

The system is linked to a Hewlett Packard Vectra XA PC system running under the Windows 95™ operating system with an HP Laserjet 5 laser printer installed. The mass spectrometer is controlled by Enhanced Chemstation software (G1701AA version A.03.00).



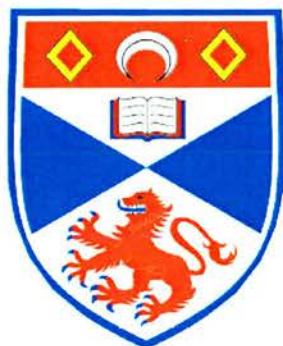
Figure 4: The CATS PC and GC-MS system.

1.2.3 THE LABORATORY

The Cats equipment is housed in a purpose built laboratory (Figure 5). This catalysis suite is called the “Wolfson Centre for Catalysis” and was refurbished with funding from the Wolfson Foundation.



Figure 5: The Wolfson Centre for Catalysis



CHAPTER TWO:
INTRODUCTION TO HYDROFORMYLATION

2.2 HISTORY

The first hydroformylation reaction on record is the experiment performed by Otto Roelen in 1938² when he passed a mixture of ethylene and synthesis gas over a fixed-bed cobalt containing catalyst. Roelen detected and isolated small amounts of propanal and diethyl ketone that had formed. It took some time to recognise the general principles and the broad applicability of metal-carbonyl catalysed reactions, and the homogeneous nature of the catalysis was proven.³

Hydroformylation did not become a significant industrial process until the 1950's, almost 20 years after its discovery. Two factors played a part in its development. The first was the rapid growth of the petrochemical industry and the second was the emergence of the PVC and detergent industries. These sectors remain the largest users of alcohols produced via hydroformylation/hydrogenation. The aldehydes formed in the *oxo* reaction play a vital role in the bulk and speciality chemical businesses. Typical chemicals obtainable from aldehydes are shown below (Figure 7). This prompted the development of a number of hydroformylation processes.

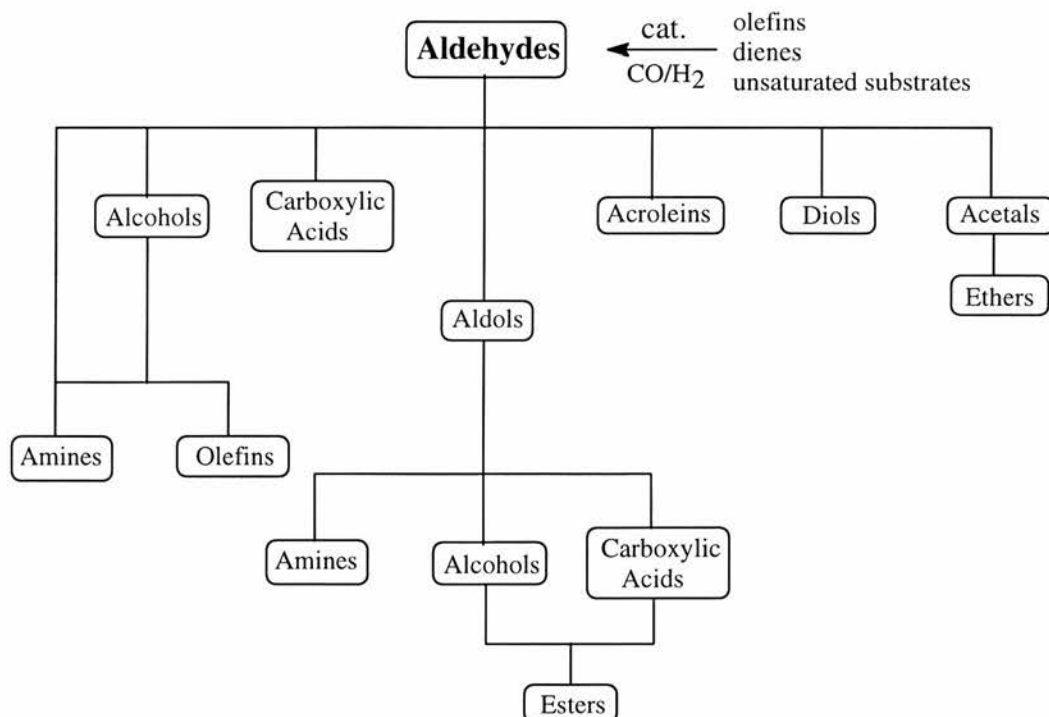


Figure 7: Compounds accessible through hydroformylation (adapted from Ref. 4).

Hydroformylation production capacity is somewhere in the region of more than six million ton a year and so it can be considered a major homogeneously catalysed

production process. The vast majority of the products are used in the polymer industry as plasticisers, but the detergent industry is also a large consumer.

2.3 HYDROFORMYLATION PROCESSES

2.3.1 FIRST GENERATION PROCESSES

The processes of hydroformylation can be categorised into three generations. The first was based upon cobalt as catalyst metal. This evolved due to the stability of cobalt carbonyl hydrides. The reaction conditions were harsh with a pressure of between 200 and 300 bar to avoid catalyst decomposition and metal deposition. Correspondingly high temperatures (between 150-180°C) were used to ensure an acceptable rate of reaction. The various methodologies were very similar and only differed in how they tried to deal with the problem of separation of catalyst and product to recycle the catalyst.⁴ Several modes were developed and had essentially similar results but managed to facilitate the rapid growth in both capacity and importance of the hydroformylation process.

There was, however, an urgent need to upgrade the general procedure. Milder conditions, increased selectivity to linear aldehydes and a reduction in by-product formation were all required. In the early 1960's it was discovered that phosphines (or arsines) enhanced metal-carbonyl-catalysed reactions. The replacement of π -acceptor carbon monoxide by these electron donating ligands gave access to tailor made catalysts via the electronic and steric influences of the ligand. A further advantage was that the metal carbonyls had enhanced stability which lead to reduced carbon monoxide pressure.

2.3.2 SECOND GENERATION PROCESSES

The first generation complexes were superseded at this point by what can be called the second generation processes. The advantages gained by ligand modification were retained. The most significant change was that the primary metal for catalysts was also changed from cobalt to rhodium. Rapid progress was attained in the application of rhodium-phosphine catalysis on a laboratory scale. It was, however, almost a decade before it was used in a commercial role (Celanese Corporation in 1974).⁵ Other companies followed in 1976 and this then lead to an aggressive licensing policy which drastically changed the picture of propene hydroformylation during the following few years. The low pressure oxo (LPO) process soon became the dominant method. Its success can be

attributed to its often cited advantages as well as the mineral-oil supply crisis in the 1980's favoured the processes with high raw material use.

It is important to note, however, that cobalt based catalytic systems were by no means rendered obsolete. An example of a process that still relies on cobalt is the hydroformylation of higher alkenes. Although higher alkenes make up about only 6% of total hydroformylation production, this is nevertheless a very significant volume overall. Part of the reason why cobalt is favoured over rhodium for the hydroformylation of higher alkenes is due to the boiling point of the substrate. The high boiling points of the product aldehydes. The usual method for separating products from the reaction is distillation. This presents no great problems when low molecular weight products are produced as the temperatures required to separate them does not adversely affect the catalyst. However, as the alkenes used become heavier the separation becomes more of a problem and the temperatures required would thermally decompose the rhodium catalyst resulting in great expense. Cobalt is still occasionally used for short chain alkene reactions due to economic reasons.

2.3.3 THIRD GENERATION PROCESSES

The second generation processes soon took over from their cobalt based predecessors due to several distinct advantages. Material and energy conservation was greatly enhanced and not much room was left for major improvements.

However, some progress was achieved with the introduction of a third process that uses variations in the solvent systems in which the reaction is carried out. The first area explored was to use a biphasic but still homogeneous system. The idea is based on using an immiscible solvent system in which the product is soluble in one phase with the catalyst being soluble in the other. The advantages of the second generation processes would be retained and enhanced by minimising catalyst leaching and recycling as well as aiding product separation.

It is argued that the problems associated with catalyst leaching and ligand degradation add more costs to a process in recovery and recycling than is saved in process simplification. The third generation processes are addressing this issue by attempting to bridge the gap between homogeneous and heterogeneous catalysis by designing systems that exploit the advantages of both techniques (Figure 8).⁶ These can be sub-divided into further

categories: homogeneous catalyst immobilisation using solid supports, biphasic systems and the latest development: the use of supercritical fluids.

BIPHASIC SYSTEMS

The most promising approach to conquering the recycling problem is the liquid-liquid biphasic catalysis. The catalyst retains its beneficial molecularity but becomes immobilised by forming a second liquid phase as a “liquid support”.

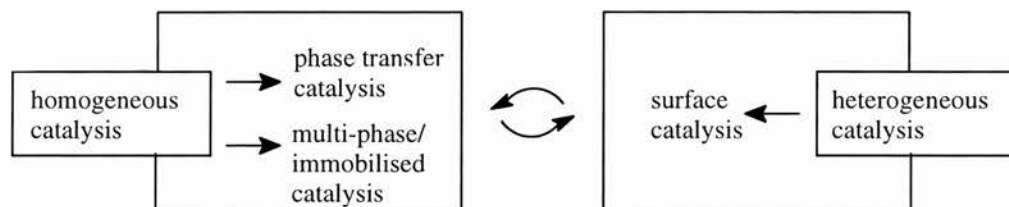


Figure 8: Phase transfer and immobilised catalysis at the border between homogeneous and heterogeneous catalysis (Adapted from Ref. 6).

Organometallic catalysis in biphasic media is of growing interest in present academic and industrial work.^{7,8} Most of the research has focussed on the use of water as the second phase. Phosphane ligands, modified with hydrophilic groups to make them water soluble, are used for this purpose.⁹ Biphasic systems with amphiphilic ligands have also been employed, hence forming micelles and/or reverse micelles, which protect and transport the catalyst in the biphasic system.¹²

The second, more recent approach is to use fluorocarbons as second phase. The resulting fluororous biphasic system (FBS) is based on the limited miscibility of partially or fully fluorinated compounds with most common organic solvents. When the two phases mix above a threshold temperature, single phase catalysis with biphasic separation of products and catalyst is possible. This technique is explored further in Chapter 4 (section 4.1).

SOLID SUPPORTS

The idea of applying soluble polymers in catalysis instead of the more common insoluble ones date back to the mid 1970's.¹⁰ The reactions are carried out under homogeneous reaction conditions. Catalyst recovery and separation is achieved by membrane filtration or precipitation. This area of research has been slow in the past but there has been a resurgence in recent years. In the early 1990's studies have focused on attaching transition metal catalysts to suitable polymers.¹¹ Studies of catalyst immobilisation have also been explored using catalysts trapped in the pores of zeolites (ship in the bottle

technique).¹² Part of the attraction of this class of catalysts is a minimisation of leaching into the reaction mixture. Thus, not only is the catalyst easily recovered, but its lifetime is significantly extended as well. The use of dendrimers as soluble catalyst supports is a current area of research and is discussed more extensively in Chapter 3.

SUPERCRITICAL FLUIDS

Although supercritical fluid technology is well established in the industry (for example in the extraction of coffee, tea, hops and natural flavours) it has not been extensively explored in the area of homogeneous catalysis. Supercritical conditions can dramatically change the solubility profile of solvents and the reactivity of certain species in homogeneous catalysis.¹³ There have been recent studies specifically in the use of rhodium catalysed hydroformylation using supercritical systems.¹⁴ Supercritical fluids like scCO₂ and scH₂O are increasingly investigated to replace organic solvents due to their environmentally friendliness, low cost, low toxicity, ease of solvent removal and recycling. Also the miscibility with gaseous reactants is high and mass transport limitations are avoided.¹⁵

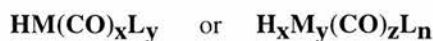
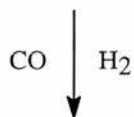
2.4 CATALYST DESIGN

The oxo catalyst is usually made up of a transition metal atom (M) that allows a metal carbonyl hydride complex to be formed. These compounds may also be modified by ligands (L). A general composition can be given as:



When $n = 0$ the catalyst is said to be “unmodified”. When the metal has ligands other than CO or hydrogen the catalyst is said to be “modified”. It is important to note that various precursor compounds may form the active hydroformylation species under the right conditions. With high enough temperature and pressure (in the presence of a base) even transition metal chlorides

Catalyst Precursor + [M] + Modifying Ligand [L]



M = Rh >> Co > Ir, Ru > Os > Pt > Pd > Fe > Ni

L = PPh₃, P(OR)₃ > P(n-C₄H₉)₃ >> NPh₃, SbPh₃ > BiPh₃

Figure 9: General Composition of Catalytic System for hydroformylation and orders of metal activity and ligand modifying effect. ¹⁶⁻¹⁹

2.4.1 VARIATION OF METAL

MONOMETALLIC CATALYSTS

Most research into hydroformylation processes is based almost entirely on cobalt, rhodium, platinum and to a lesser extent ruthenium.²⁰ As shown in Figure 9, that corresponds to three of the four most active metals in the series. Hydroformylation plants operate exclusively with catalysts based on rhodium or cobalt, namely $\text{HCo}(\text{CO})_4$, $\text{HCo}(\text{CO})_3(\text{PBU})_3$ and $\text{HRh}(\text{CO})(\text{PR}_3)_3$.²¹ Platinum and ruthenium catalysts are mainly areas of academic interest. Other carbonyl-forming metals (such as Mo, Cr, Mn, Ir, Fe and Os)^{21,22} have been claimed to be active oxo catalysts but their activities and lifetimes are much lower than those of cobalt and rhodium catalysts. Although less attractive, these other metals can create unexpected catalytic activity if properly designed and selected. Results of comparative tests between catalysts, modified and unmodified by phosphines, in the hydroformylation of alkenes have been discussed in the literature.^{4,23}

POLYMETALLIC CATALYSTS

Hydroformylation catalysts with bi- or polymetallic centres have been explored extensively. Research in polymetallic cluster oxo catalysts structure and reactivity has revealed a wealth of information. It has been shown that, under hydroformylation conditions, clusters are degraded to at least bi-metallic species, sometimes reversibly.²⁴ These species can then perform the oxo reaction.²⁵ Cluster catalysts have not exhibited significant advantages in the oxo reaction.

2.4.2 MODIFICATION BY LIGANDS

PHOSPHINES

The only classes of ligands used in industrial hydroformylation plants are phosphines PR_3 ($\text{R} = \text{C}_6\text{H}_5$, $n\text{-C}_4\text{H}_9$), triphenylphosphine oxide and in some cases phosphites, $\text{P}(\text{OR})_3$. Nitrogen containing ligands such as amines, amides or isonitriles showed exclusively lower reaction rates. This may be explained by the phosphines stronger coordination to the metal centre. The order of reactivity of Ph_3E ($\text{E} = \text{main group V element}$) has been illustrated by a comparative study of the hydroformylation of 1-dodecene at 90°C (8 bar CO/H_2). The resulting reactivity scheme showed that phosphine ligands were superior (Figure 9). Other heteroatom containing ligands have been tested, but were proven, without exception, to have a poorer performance than phosphines.⁴ Water soluble systems are promising as very selective (high *n/iso*) and environmentally friendly.

Phosphines and their coordination chemistry have been studied extensively.²⁶ Tolman introduced the cone angle Θ and the electronic parameter χ to classify phosphine ligands with respect to their steric demand and coordination ability.²⁷ For chelating diphosphines the *natural bite angle*, based on molecular mechanics calculations, has been developed.²⁸ In some cases *n/iso* selectivities are now predictable by the diphosphine structure, but it is still not clear to what extent the phosphorous ligands control the selectivity.²⁹ There is, however, little data on the structure of phosphines and its influence on the catalysis.

An example of the recent research is a study that has focused on differences in electronic symmetry between ligands to try explain increased *n/i* regioselectivity.³⁰ The hypothesis tested was that very different regioselectivities might be obtained from diequatorial-diphosphine and apical-equatorial rhodium complexes. The mode of chelation could be controlled by using chelating diphosphines with varying natural bite angles. A strong correlation was found between regioselectivity for *n*-aldehyde formation and natural bite angle in the past.²⁸ This study compared BISBI and DIPHOS (Figure 10) which have wide ($\beta_n = 113^\circ$, $n/i = 66$) and narrow ($\beta_n = 85^\circ$, $n/i = 2.6$) bite angles respectively.

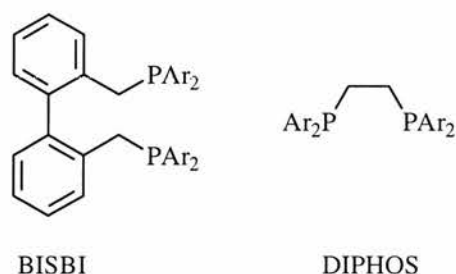


Figure 10: Structures of BISBI and DIPHOS.

The correlation between regioselectivity and chelation mode suggests that the diequatorial diphosphines such as BISBI and apical-equatorial chelating diphosphines such as DIPHOS have significantly different steric and/or electronic properties. It was deduced that electron-withdrawing aryl substituents in the equatorial position (as for BISBI) increase the *n/i* selectivity. The apical-equatorial coordinating DIPHOS ligand showed decreased *n/i* ratios with electron-withdrawing aryl substituents (-3,5-CF₃). Hence an electron-withdrawing substituent on an equatorial phosphine increases the *n/i* ratio while an electron-withdrawing substituent on an apical phosphine decreases the *n/i* ratio.

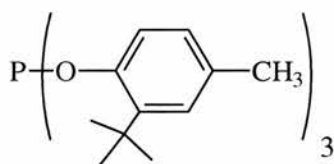
The phosphine ligands can also affect the overall function of the catalyst. Trialkylphosphine complexes of rhodium have been shown to catalyse the direct production of alcohols from alkenes under hydroformylation conditions (in protic solvents).³¹ Mechanistic studies showed that there were no aldehyde intermediates in the reactions and this suggests a different mechanistic pathway is followed.

Most studies deal with ligands and their influence on activity and selectivity in homogeneous hydroformylation catalysis. Initial reports recorded high *n/i* selectivities, but coordination of phosphine makes the metal-hydrogen bond more hydridic leading to formation of hydrogenation products. In general the *n/i* ratio of modified catalysts increases with increasing ligand/metal ratio. When a ligand is coordinated to a metal centre its steric bulkiness is increased and the formation of linear products is favoured. The structure of the ligand determines how pronounced the effect is. Hydrogenation and isomerisation reactions are suppressed when an excess of phosphine ligand is used. At constant ligand/metal ratios, closely related phosphines show lower *n/i* ratios when their bulk is increased. This trend is due to the formation of unsaturated HM(CO)₂L species in cases where the bulky group on the ligand is positioned close to the metal centre. The steric demand of the ligand favours formation of dicarbonyl species which generate the

branched products. It is important to note that these trends are only reliable if the ligands being compared have similar electronic structures as electronic structures have an influence on selectivity as well.

PHOSPHITES

Recent progress has been made by using phosphites (general formula $(RO)_3P$) as ligands in rhodium catalysed oxo synthesis. Rhodium catalysts with phosphites such as the structure illustrated below show high activities in the hydroformylation of long-chain alkenes.³²



Less reactive alkenes such as 2,2-dialkyl-1-alkenes are hydroformylated at much higher rates than those achieved with triphenylphosphine-modified rhodium catalysts. Activities of 15 000 mol (aldehyde)/ mol (Rh) per hour have been reported (90°C , 10-30 bar).³² 1-Alkenes are converted with even higher rates (160 000 mol/mol per hour). At these high rates the reaction becomes mass-transfer limited. The lack of CO dissolved in the liquid layer leads to the formation of unsaturated rhodium species which rapidly isomerise the alkene. This leads to a low n/i ratio (20 – 30 % linear product). The first step in the synthesis of nonvolatile plasticisers is hydroformylation of a long chain alkene, for which rhodium phosphite catalysts have useful properties. The current use of sterically hindered phosphites as antioxidants for polyalkenes, along with their simpler synthesis, makes them more attractive than phosphines. Chiral phosphites can also be useful in asymmetric hydroformylation.¹⁸

2.4.3 RHODIUM ORGANOMETALLIC CATALYST DEACTIVATION

The deactivation (or lifetime) of homogeneous catalysts is one of the most important factors limiting the practical application of many very active but chemically unstable catalysts. Studies on deactivation of catalysts facilitate the design of not only selective but also stable homogeneous hydroformylation catalysts. It is valuable to note that a major running cost of a hydroformylation process is triphenylphosphine replacement.

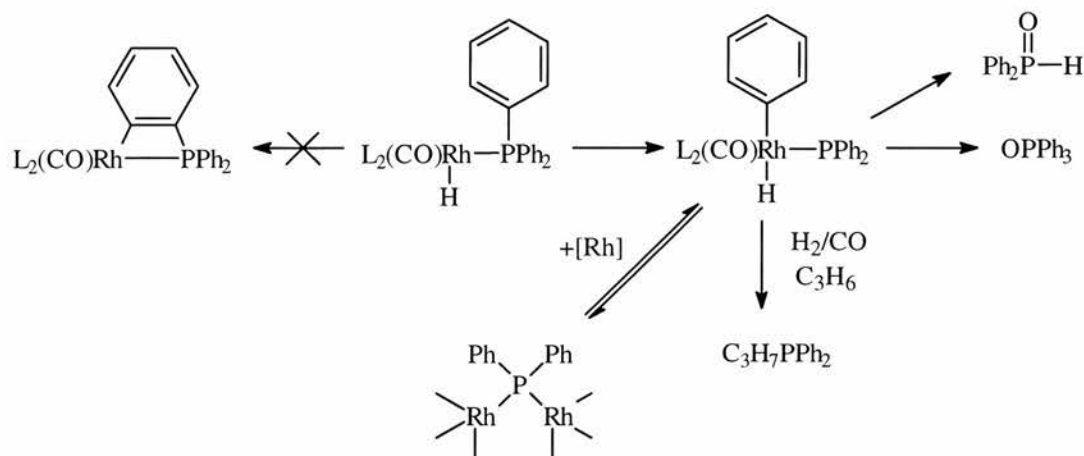


Figure 11: Possible mechanisms of catalyst degradation

Widely used rhodium catalysts, modified with monodentate triarylphosphines can be used to illustrate the sorts of deactivation reactions that can occur (Figure 11)³³. The process most probably proceeds via degradation of the phosphorous ligand which leads finally to a decrease in catalyst activity. The formation of less active phosphido-bridged rhodium carbonyl species is usually used to explain the deactivation process.^{34,35} Catalyst degradation can also be initiated by the insertion of rhodium(I) into the carbon-phosphorous bond of PPh_3 followed by a two electron transfer from $Rh(I)$ to the C-P bond. These processes lead to a decrease in catalyst activity due to the following:

1. the formation of a less active rhodium complex with $C_3H_7PPh_2$ or binuclear, bridged phosphido species $-Rh-PPh_2-Rh-$;
2. elimination of PPh_3 from the coordination sphere as $OP(H)Ph_2$ or $OPPh_3$.

Deactivation of the $HRh(CO)(PPh_3)_3$ active form of the catalyst at high temperature ($>100^\circ C$) is probably caused mainly by the formation of a phosphido-bridged dimeric rhodium complex.³⁵ Orthometallated or dimeric complexes with Rh-Rh bonds at these conditions are unlikely but have been observed in other reactions.³⁶

The process involved when triphenyl phosphite as precursor seems to be a stimulating step in the catalytic process rather than a degrading one.³³ The catalytically active species $HRh\{P(OPh)_3\}_3$ and $HRh(CO)\{P(OPh)_3\}_3$ are easily formed 'in situ' from corresponding orthometallated complexes. Only traces or orthometallated species are detected in the reaction mixtures.

The discrepancies between similar species degradation (even comparing simple catalysts) suggest that there is still no general explanation for a degradation mechanism of the

rhodium-phosphorus ligand modified catalytic system. Hence, this is an area of further research to facilitate effective catalyst design.

2.5 SUBSTRATES

The hydroformylation reaction is applicable to a broad range of substrates. On a laboratory scale most unsaturated carbon-carbon bonds and some heteroatom-carbon double bonds can be hydroformylated. Reaction rates vary with catalyst and conditions. From an industrial perspective the most important substrates are unbranched terminal alkenes such as propene, 1-butene, 1-octene etc. although some selected functionalised alkenes are used. The relative reactivity of unfunctionalised alkenes decreases with increased internalisation and branching (Figure 12).¹⁸

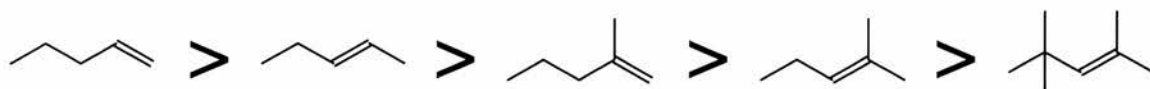


Figure 12: The order of olefin reactivity in hydroformylation reactions.

A similar reactivity order results for unmodified rhodium catalysts and in general the activity of rhodium based homogeneous catalysts modified with different phosphorus ligands depends on the structure of the unsaturated substrates.

A formyl group formed during the hydroformylation reaction of unfunctionalised alkenes is unlikely to be attached to a quaternary carbon atom (the *Keulemans rule*). An example of this general rule is the oxo reaction with 2,3-dimethyl-2-butene where 3,4-dimethylpentanal is formed exclusively. For both rhodium and cobalt catalysis, isomerisation of the substrate occurs, followed by hydroformylation (Figure 13):³⁷

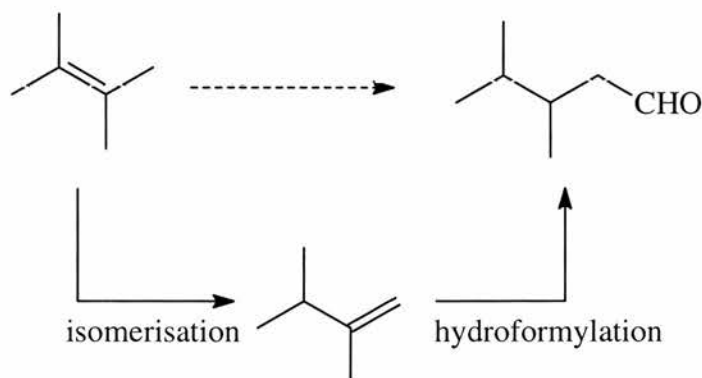


Figure 13: Hydroformylation pathway of 2,3-dimethyl-2-butene

It is important to note that the industrial importance of hydroformylation is not limited to simple alkenes. The reaction may also be applied to some complex unsaturated substrates with one or more functional groups. Rhodium catalysts used for this task are usually modified with complex ligands.³³ The structure shown in Figure 14 is an example of a bis-phosphite ligand used for such a task producing over 94% of n-pentanal from a C₄ feedstock containing a mixture of butenes.³³

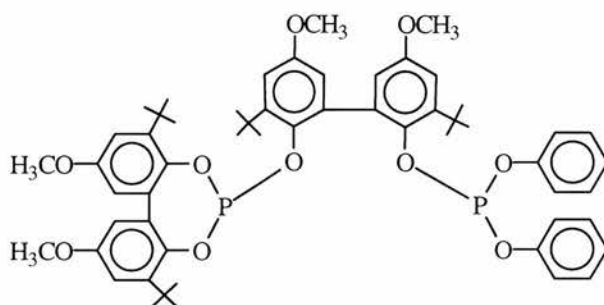


Figure 14: Bis-phosphite ligand used to modify a rhodium catalyst precursor.

2.5.1 SUBSTRATES WITH INDUSTRIAL IMPORTANCE

Alkenes that are converted in commercial hydroformylation plants can be divided by chain length into four groups: ethylene (C₂), propene (C₃), butene to dodecene (C₄ to C₁₂) and longer chains (>C₁₂). The share of overall production capacity is: C₂ (~2%), C₃ (73%), C₄–C₁₂ (19%) and >C₁₂ (6%).¹⁸

There are a variety of compounds prepared on an industrial scale other than these ‘simple’ hydroformylation products. For example in 1963 Ajinomoto started to produce the sodium salt of L-Glutamic acid (monosodium glutamate - a food additive) from 3-cyanopropanal obtained in 80% yield by regioselective cobalt-catalysed hydroformylation of acrylonitrile.³⁸ The directing effect of the functional group ensured high linearity of the product. An annual capacity of 12 000 tons was maintained during almost 10 years of production. The process was discontinued after the availability of superior microbial synthesis and concerns over using acrylonitrile in food additive production.

Allyl alcohol can be converted to 1,4-butanediol by phosphine modified rhodium catalysed hydroformylation and hydrogenation of 2-hydroxytetrahydrofuran (Figure 15).³⁹ In 1990 ARCO launched a production plant based on the technology developed by Kuraray with a 30 000 tons/year 1,4-butanediol capacity.⁴⁰

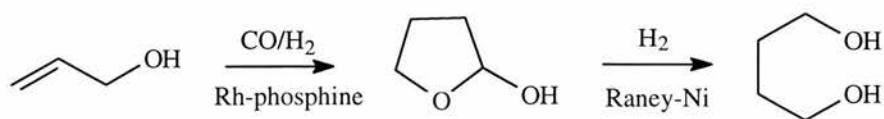


Figure 15: Hydroformylation of allyl alcohol to 1,4-butanediol.

The branched aldehyde illustrated in Figure 16(b) is an intermediate in the manufacture of vitamin A. The annual demand for vitamin A is about 3000 tons. Major producers are BASF, Hoffmann-La Roche and Rhône-Poulenc Animal Nutrition.¹⁸ At an early stage in the synthesis BASF and Hoffmann-La Roche used hydroformylation to synthesise (b) starting from 1,2,-diacetoxy-3-butene (a) and 1,4-diacetoxy-2-butene (c), respectively.⁴¹ The selectivity towards the branched product in the BASF process is achieved by using an unmodified rhodium carbonyl catalyst at a high reaction temperature. The symmetry of (c) in La Roche's process does not lead to regioselectivity problems. Elimination of acetic acid and isomerisation of the *exo* double bond (La Roche) yields the product (b) in both cases.

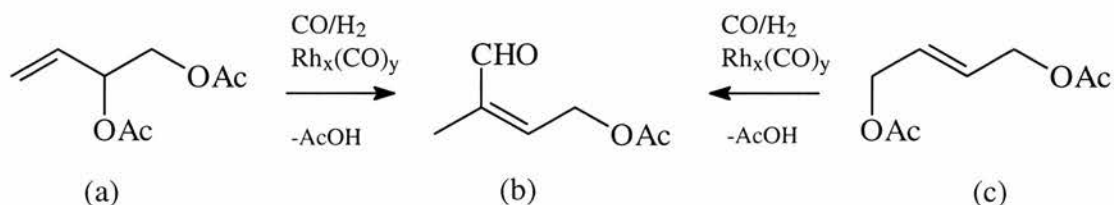


Figure 16: The hydroformylation step in the synthesis of the Vitamin A precursor (b).

2.6 ASYMMETRIC HYDROFORMYLATION.

A range of chiral molecules are accessible through asymmetric hydroformylation. These include valuable precursors for pharmaceuticals and agrochemicals. The potential market for bulk synthetic chiral products is estimated to exceed more than US\$ 2 billion.⁴² To synthesise pure compounds, high regioselectivity and high enantioselectivity have to be combined. The branched aldehyde with an asymmetric carbon atom in Figure 17 is the target molecule.

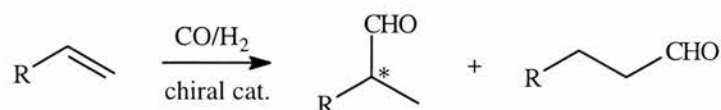


Figure 17: Generic asymmetric hydroformylation

For a long time platinum was considered the most superior metal in asymmetric hydroformylation. To achieve high activity and to improve the *n/i* ratio, platinum-phosphine complexes were used together with Lewis acid co-catalysts such as SnCl_2 .⁴³

With chelating chiral diphosphines, very high enantioselectivities (>96% *ee*) were achieved.⁴⁴ Despite the high *ee* values achieved using platinum catalysts extensive isomerisation and hydrogenation are major disadvantages, along with a low regioselectivity for the branched products. A very strong influence of the reaction temperature on the enantioselectivity was also observed.⁴⁵

Advances gleaned by using rhodium catalysed hydroformylations overcame these disadvantages. And by 1993 there had been advances in the use of phosphine-phosphite (eg. BINAPHOS) and diphosphite ligands that gave enantioselectivities up to 95% in the hydroformylation of substituted styrene derivatives.⁴⁶ The branched/linear ratios were as high as 86:14 with >99% conversions at substrate/catalyst ratios of 300-2000:1.

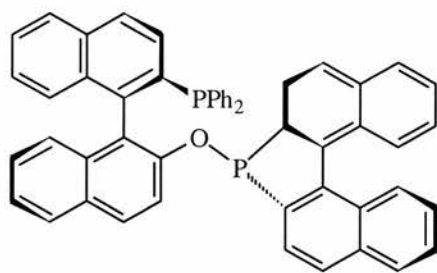


Figure 18: The structure of (R,S)-BINAPHOS phosphine-phosphite ligand

Progress in rhodium catalysed hydroformylations, encouraged by reactions such as those mentioned above have been the focus of current asymmetric hydroformylation research.

2.7 MECHANISM

Even though the reaction has been used for over 50 years on an industrial level, there are many aspects of the hydroformylation reaction mechanism which are not well understood. There is on going investigation of the proposed reaction pathways.

2.7.1 UNMODIFIED COBALT AND RHODIUM CATALYSTS

Although the exact mechanism of hydroformylation is still under investigation, the generally accepted hydroformylation cycle was formulated in the early 1960's. Originally

only for cobalt catalysts (Figure 19),⁴⁷ the mechanism can also be applied to unmodified rhodium complexes.

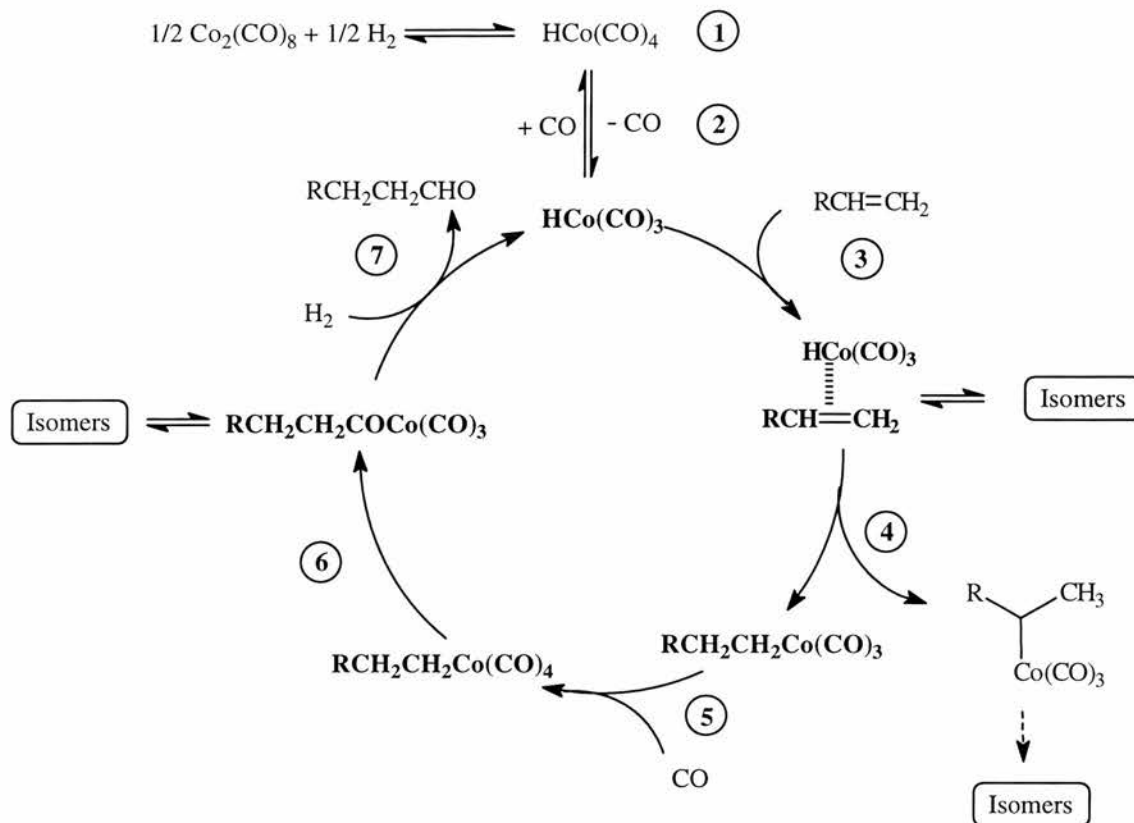


Figure 19: Catalytic cycle of hydroformylation with unmodified cobalt catalyst (Taken from ref. 47).

The key steps in this cycle are:

1. Reaction of the metal carbonyl $\text{Co}_2(\text{CO})_8$ with hydrogen to form the hydrido-metal carbonyl species $\text{HCo}(\text{CO})_4$;
2. Dissociation of CO to generate the unsaturated $16e^-$ species $\text{HCo}(\text{CO})_3$;
3. Coordination of the alkene $\text{RCH}=\text{CH}_2$ ($18e^-$);
4. Formation of the alkylmetal carbonyl species ($16e^-$);
5. Coordination of CO ($18e^-$);
6. Insertion of CO to form the acylmetal carbonyl $\text{RCH}_2\text{CH}_2\text{COCCo}(\text{CO})_3$ ($16e^-$);
7. Cleavage of the acylmetal species by hydrogen to form the aldehyde and regeneration of the hydridometal carbonyl $\text{HCo}(\text{CO})_3$.

SELECTIVITY

The *n/i* ratio of aldehydes formed by unmodified metal carbonyl catalysis is influenced by:

- Catalyst concentration (slightly);

- Temperature (strongly);
- H₂ partial pressure (slightly);
- CO partial pressure (very strongly).

Variations of the *n/i* ratio from 1.6 to 4.4 have been reported, but the determining factors are still obscure.⁴⁸ The selective reaction of the hydridocobalt carbonyl with the alkene via *Markovnikov* and *anti-Markovnikov* addition gives rise to the branched and linear acylcobalt carbonyl isomers. The less sterical demanding HCo(CO)₃ favours the formation of the branched isomer, whereas HCo(CO)₄ generates the linear isomer preferentially. This corresponds to the increased selectivity observed at higher CO partial pressure. As HCo(CO)₄ is the less reactive catalyst, the catalytic activity drops at the same time.

Thermodynamic data has been reported for the isomerisation of the acylcobalt carbonyl species (Figure 20).⁴⁹ With $\Delta H = 0.47 \pm 0.2$ kcal/mol (2.0 ± 0.8 kJ/mol) and $\Delta S = 2.13 \pm 0.6$ cal/mol °C (8.91 ± 2.5 KJ/mol °C), the isomerisation rate varies in proportion to the alkene concentration and inversely with *p*(CO). The higher the *p*(CO), the slower the isomerisation rate and the higher the *n/i* ratio. Thus the equilibrium dynamics are influenced by the ability of the acyl intermediate to rearrange. How facile this rearrangement is relies on carbon monoxide pressure. At *p*(CO) = 2.5 and 90 bar, *n/i* was found to be 1.6 and 4.4 respectively. This gives a clue to which reaction, at a molecular level, is responsible for determining the *n/i* ratio.

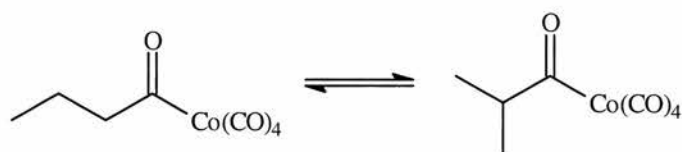


Figure 20: Isomerisation of the acylcobalt carbonyl species.

2.7.2 PHOSPHINE-MODIFIED CATALYSTS

The hydroformylation mechanism for phosphine modified rhodium catalysts is similar to the above cycle (Figure 19) with slight modifications. The precursor of the active hydroformylation species is HRh(CO)(PPh₃)₃⁵⁰ and was first synthesised and characterised in 1963.⁵¹ Five years later Wilkinson introduced the species as a catalyst.⁵² There are two possible pathways: associative and dissociative. Preceding the catalytic

cycle are several equilibria which generate the key intermediate, $\text{HRh}(\text{CO})_2(\text{PPh}_3)_2$ (Figure 21).

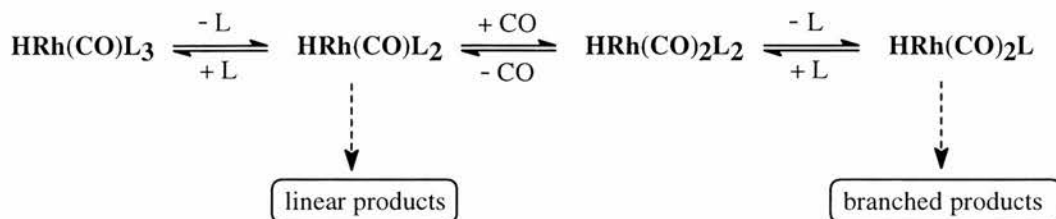


Figure 21: Initial equilibria forming the active catalyst species ($\text{L} = \text{PPh}_3$).

The associative mechanism is initiated by the coordination of an alkene to $\text{HRh}(\text{CO})_2(\text{PPh}_3)_2$ to form a six coordinate species which is in turn converted in a fast irreversible reaction to the alkylrhodium complex $\text{RRh}(\text{CO})_2(\text{PPh}_3)_2$ ($18e^-$). The latter species is derived through the dissociative pathway as well (Figure 22).

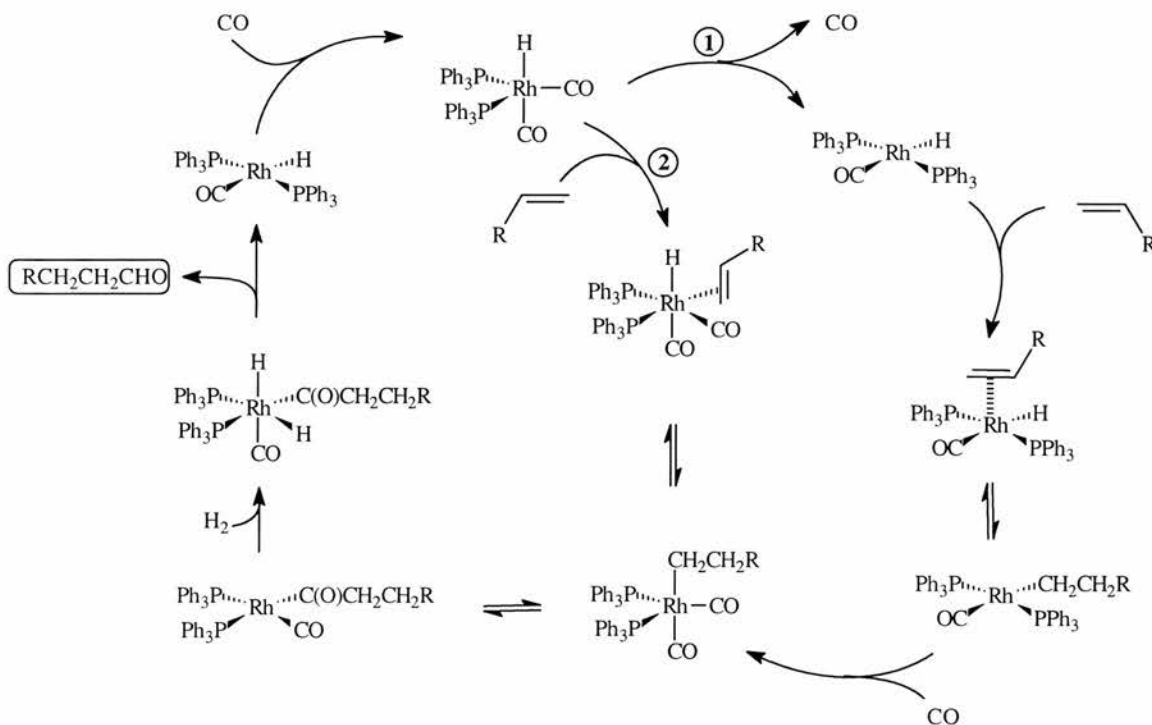


Figure 22: The hydroformylation cycle for modified rhodium catalysts. (1 = dissociative, 2 = associative).

When the dissociation of a carbon monoxide ligand from $\text{HRh}(\text{CO})_2(\text{PPh}_3)_3$ is the first step in the reaction then it is said to be following the dissociative pathway. Subsequent alkene coordination, formation of the alkyl complex and coordination of a carbon monoxide ligand generates the alkylrhodium complex $\text{RRh}(\text{CO})_2(\text{PPh}_3)_2$. For both the associative and dissociative pathways the next steps are the same. Firstly CO inserts to form the acyl complex $\text{RC}(\text{O})\text{Rh}(\text{CO})(\text{PPh}_3)_2$, and then oxidative addition of hydrogen.

This second step is believed to be rate determining in the hydroformylation pathway. Reductive elimination to form the aldehyde followed by coordination of an additional CO ligand regenerates $\text{HRh}(\text{CO})_2(\text{PPh}_3)_3$ and the cycle can begin again.

The dissociative mechanism is considered the major pathway, especially under industrial conditions. The associative mechanism is preferred at very high concentrations of catalyst and phosphine. The number of CO and phosphine ligands in the intermediates is still not clear. Loss of a phosphine ligand (instead of a CO) at the beginning of the cycle may be the first step instead. This may happen particularly at high CO partial pressure and low ligand concentrations. The species generated ($\text{HRh}(\text{CO})_2(\text{PPh}_3)$) is less sterically hindered and would direct the reaction towards the branched product (Figure 21).

The n/i selectivity of modified catalysts increases with lower partial pressure of CO and with high ligand concentration. Temperature effects are less. The predominant catalytic species under these circumstances is coordinated by more than one phosphine ligand. Hence the metal is more sterically hindered and so the alkene prefers to form a linear alkyl and acyl species.

2.7.3 SUBSTRATE INFLUENCED ISOMERS

In general terms the direction of insertion of the alkene into the metal-hydride bond can take place to yield the normal or branched metal alkyl which determines the n/i ratio of aldehydes (Figure 23).

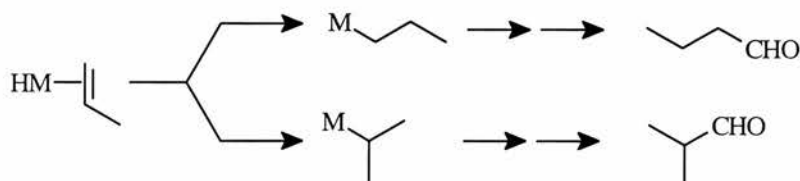


Figure 23: General scheme for metal insertion determining n/i products.

In some cases, such as using a Shell Higher Olefin Process (SHOP) feed, the product can be determined by the reaction of the feedstock. The process was developed to produce linear α -olefins from ethylene metathesis for detergent production.⁵³ Isomerisation of internal to terminal alkene occurs and is drawn over by reaction with CO to produce linear aldehydes.

However, the n/i ratios are also affected by the alkene structure and are sensitive to steric hindrance. For example, dicobaltoctacarbonyl hydroformylates longer chain 1-alkenes more slowly than the shorter alkenes. Methyl substitution on the alkene chain not only slows the reaction as the methyl group is moved closer to the double bond, but the n/i ratio increases (Table 1).⁵⁴

Once metal hydride addition has taken place, β -elimination and readdition can occur. Accordingly alkene isomerisation can take place in the hydroformylation process (Figure 24). This is especially apparent in hydroformylations of internal alkenes, as not only does (E)/(Z)-isomerisation take place, but n -aldehydes are obtained. This isomerisation is suppressed with the phosphine modified catalyst, in the presence of excess phosphine and at high CO pressures. Thus internal isomerisation (especially in longer chain alkenes) can cause the production of isomers during the hydroformylation reaction..

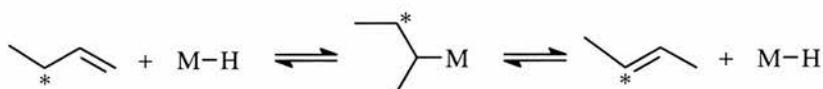


Figure 24: Alkene isomerisation during hydroformylation.

Alkene	Relative rate constant	Substitution (%)	
		Carbon 1	Carbon 2
	1	82	18
	0.97	86	14
	—	96	4
	0.11	100	0
	0.088	—	—

Table 1: Hydroformylation of alkenes: Relative Rate and Isomer ratios (ref. 54).

2.8 KINETICS OF HYDROFORMYLATION

Although extensive studies have been published dealing with catalysts, ligands, substrates and product distributions, very few have dealt with the kinetic aspects and their consequences in reaction. Most knowledge gained has been that about *macrokinetics*. This includes how the rate is affected by temperature, pressure, synthesis gas composition and catalyst concentration. Little information is available on *microkinetics* and

conclusions about the rate determining step have been deduced from spectroscopic observations.

Some examples of parameters determined for triphenylphosphine-modified and unmodified rhodium and cobalt catalysts in the hydroformylation of terminal olefins are shown in Table 2.¹⁸ The general reaction rate equation used is:

$$r = k \times [\text{substrate}]^v \times [\text{catalyst}]^w \times [p(\text{CO})]^x \times [p(\text{H}_2)]^y \times [\text{ligand}]^z$$

	<i>v</i>	<i>w</i>	<i>x</i>	<i>y</i>	<i>z</i>	<i>ref.</i>
Co ₂ (CO) ₈	1	1	-1	1	0	55 a
Co ₂ (CO) ₆ L ₂ ^{a)}	1	1	Negative	Positive	≈0	55 b
Rh ₄ (CO) ₁₂	1	1	-1	1	0	55 c
HRh(CO)L ₃ ^{b)}	0.6	1	-0.1	0.05	-0.7	55 d
HRh(CO)L ₃ ^{b)}	1	1.2	Negative	1.5	0	55 e

^{a)}L = P(n-C₄H₉)₃, ^{b)}L = P(C₆H₅)₃.

Table 2: Parameters of the hydroformylation kinetics of terminal alkenes (ref. 18).

2.8.1 UNMODIFIED CATALYSTS

The generally accepted equation for the high pressure catalysts Co₂(CO)₈ and Rh₄(CO)₁₂ is:⁵⁶

$$r = k \times [\text{substrate}] \times [\text{catalyst}] \times \frac{[p(\text{H}_2)]}{[p(\text{CO})]}$$

Thus the rate of reaction is positively influenced by an increase in concentration of catalyst, alkene or hydrogen but a negatively effect is seen with an increase in carbon monoxide. However at low partial pressures ($p(\text{CO}) < 10$ bar) an increasing concentration of carbon monoxide enhances the overall reaction rate. This shows it is necessary for CO to generate hydridocobalt carbonyls (ie. HCo(CO)₃). At higher CO partial pressures, the less reactive HCo(CO)₄ is formed leading to the negative order of reaction. Unmodified rhodium catalysts behave similarly but with a higher critical $p(\text{CO})$ (≈ 30 bar).

The dominant variables under high pressure conditions are the catalyst concentration and temperature. The transport of the gases across the liquid-gas interface is rapid in such cases but for low pressure runs it may have to be taken into account. There is a large gap

between the solubilities of gaseous reactants and their conversion rates and this implies the influence of transportation on the overall reaction rate add to the difficulties in determining precise kinetics. Furthermore, if the stirring of the solution is not effective, the reaction may appear to be zero order due to inadequate transport of gas into the solution. This means that rate expressions are usually derived under restricted conditions for example for temperature, pressure and conversion.

2.8.2 LIGAND MODIFIED CATALYSTS

The rate for phosphine modified rhodium catalysts (namely $\text{HRh}(\text{CO})(\text{PPh}_3)_3$) is dependent on the following different parameters:

1. first order in catalyst concentration;
2. first order in hydrogen partial pressure;
3. at low alkene concentrations, positive order, and at high alkene concentrations, negative order (substrate inhibition);
4. at low CO partial pressure (<10 bar), positive order, at high CO partial pressure, negative order;
5. at low ligand concentrations, positive order, and at high ligand concentrations, zero order.

Solvents have a significant influence on the rate of hydroformylation. For example alcohols lead to higher rates than nonpolar solvents like toluene or hexane. The negative order dependence of the reaction rate at higher carbon monoxide pressure is mainly due to the formation of the di- and tri-carbonyl acyl rhodium complexes $\text{RCORh}(\text{CO})_2(\text{PPh}_3)_2$ and $\text{RCORh}(\text{CO})_3(\text{PPh}_3)$, which, being coordinatively unsaturated, do not undergo oxidative addition of hydrogen. At lower CO partial pressures, the formation of these species is negligible. A positive order dependence of the rate is seen as the monocarbonyl $\text{RCORh}(\text{CO})(\text{PPh}_3)_2$ is stabilised.

The effect of PPh_3 concentration on the activity and selectivity of the Rh/PPh_3 catalyst in the hydroformylation of 1-decene in toluene was studied.⁵⁷ It was found that the TOF/[1-decene] and product selectivities are independent of the P/Rh ratio and solely depend on the concentration of the phosphine. This is true as long as the CO/H_2 ratio, total pressure, solvent and temperature are the same.

Although the rate determining step is almost always hydrogen oxidative addition, if saturation kinetics plays a role in the reaction then the coordination of alkene to rhodium equilibrium may be important kinetically (Figure 25). At the beginning of the reaction when the equilibrium lies to the right (ie. high alkene concentration) all the rhodium is present in an active form and the rate is zero order in substrate. After some of the alkene has been consumed and the reaction shifts to the left (ie. low alkene concentration) the reaction becomes first order in alkene because the concentration of the active species is proportional to the alkene concentration.

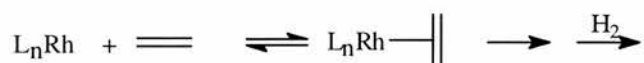


Figure 25: General scheme depicting alkene coordination equilibrium.

2.9 PROCESS PARAMETERS

A range of parameters influence the hydroformylation process with respect to conversion, selectivity and operation. By fine tuning the operating conditions a broad band of product compositions can be achieved. The reactions can also be tuned to maximise the production of certain products.

2.9.1 UNMODIFIED CATALYSTS

TEMPERATURE

The initial rate of the hydroformylation reaction, as with most homogeneously catalysed reactions, increases with increasing temperature. With higher temperatures the *n/i* ratio decreases for almost all alkenes. This is reversed for α -alkenes bearing a functional group which directs the regioselectivity towards linear products. In addition by-product formation generally increases with higher temperatures. The most important side reactions are:

- isomerisation of the starting alkene;
- hydrogenation of aldehydes and
- aldol type condensation reactions

PRESSURE

As shown in the equation in section 2.8.1 the overall reaction rate is independent of the total pressure as long as the ratio of $p(\text{CO})$ to $p(\text{H}_2)$ is 1:1 and a minimum carbon monoxide pressure is maintained to stabilise the metal carbonyl species. Low $p(\text{CO})$ initially increases the reaction rate whereas at higher partial pressures the rate drops. If the hydrogen partial pressure is increased then the speed of reaction increases⁵⁸ as does the n/i ratio to some extent.⁵⁹ This effect is less pronounced than for $p(\text{CO})$. Above a $p(\text{H}_2)$ of 60-80 bar almost no improvement in the n/i ratio is seen. Hence high n/i ratios and reaction rates can be achieved using high pressures,⁶⁰ where the rate retarding effect of $p(\text{CO})$ is compensated by $p(\text{H}_2)$ and the n/i ratio is determined by $p(\text{CO})$ alone.

CATALYST CONCENTRATION

The catalyst concentration controls the conversion and formation of by-products. Temperature, residence time as well as the catalyst feed are all important factors in the hydroformylation conversions using unmodified catalyst. High conversions are achieved at high catalyst feed.⁴ The extent to which catalyst concentrations under industrial conditions affect the n/i ratio are still unclear.¹⁸ The uncertainty may be a result of the various experimental designs applied.

2.9.2 MODIFIED CATALYSTS

TEMPERATURE

Phosphine modified cobalt catalysts lead to an increased selectivity towards linear products, to increased thermal stability and hydrogenation activity but also to lower reactivity compared with cobalt carbonyl. Thus to compensate for this loss of activity the reaction temperatures need to be kept at 180°C. At higher temperatures the n/i selectivity drops. Less steric demand around the metal centre causes increased branched aldehyde formation. The modified cobalt catalysts have by-product formation similar to their unmodified derivatives.

When rhodium catalysts are used the decrease of n/i ratio at higher temperatures is more pronounced. Industrial plants operate at temperatures of 120°C to keep the n/i ratios high. Although the reactivity at these temperatures is low compared to unmodified rhodium catalysts they are still high enough to keep the reaction fairly fast.

PRESSURE

Ligand modified catalysts follow the following general equilibrium (M = Co, Rh):



At low $p(\text{CO})$ the equilibrium is shifted to the right. When the metal is coordinated by the ligands it becomes more sterically hindered, hence unbranched product formation is favoured. When $p(\text{CO})$ is increased the n/i ratio drops. Only at higher pressures ($p(\text{CO}) > 15$ bar) is the catalytic cycle pushed to the left of the equilibrium hence favouring the unbranched product again. Rates and hydrogenation activity both go up when the partial pressure of hydrogen is increased.

CATALYST CONCENTRATION

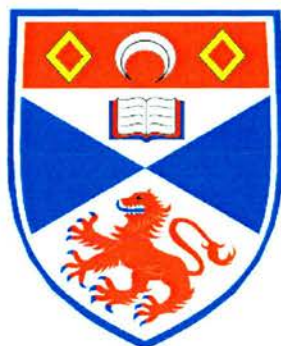
No general rules for the role of catalyst concentration have yet been found for modified catalysts. There are conflicting reports on the effects of the concentration¹⁸ but it can be deduced from Table 2 that the rate and conversion of hydroformylation is improved by increasing the amount of catalyst. The effect is not linear over the range of catalyst concentration, but more pronounced at low concentrations (<6.0 mmol).^{52(c)}

LIGANDS

The catalytic activity depends on the absolute concentration of the ligand [L] and independent of the rhodium concentration. Furthermore the more basic the phosphine (ie. the higher the pK_a) the less active they are. As they coordinate strongly to the metal they lower rates by “blocking” the centre. Increased rates have been observed when more electron withdrawing ligands are used.⁶¹ The activity of the catalyst is dependent. The use of phosphites tend to give high n/i ratios along with high isomerisation rates as they are fairly basic and have high χ values.

2.10 CONCLUSION

Although metal catalysed homogeneous hydroformylations have had a fairly long history and has a high level of implemented commercial processes there is still much research to be done in the field. A lot of areas are not yet understood comprehensively but this need not stifle progress as enough is understood about catalyst design to facilitate development in both research and applications. Furthermore, the exciting prospects offered by the third generation catalysts as well as progress in ligand research have opened up the field and are far from being fully exploited.



CHAPTER THREE:
SILSESQUOXANE DENDRIMERS

CHAPTER THREE: SILSESQUOXANE DENDRIMERS

3.1 INTRODUCTION

The advantages of designing and synthesising a catalyst that would bridge the gap between homogeneous and heterogeneous catalysts make it an attractive proposition. Heterogeneous catalysis has the distinct advantage over its counterpart in that the catalyst is easily separated from the reaction mixture and products, hence it is easily recycled and the cost is less of an issue. Its sibling, homogeneous catalysis has, in general, a superior turnover and selectivity but has a distinct drawback: it is sometimes very difficult to separate the catalyst from the product and hence may impart a prohibitive cost. The ideal situation would be to have a catalyst that encompasses the qualities of both, the ease of separation of the heterogeneous model and the catalytic ability of the homogeneous.

It is envisaged that a catalyst supported by a macromolecule would allow the tuning of the system so that this can be achieved. Studies in the area of giant molecules have shown three possible catalytic 'carriers'. Linear, crosslinked and dendritic polymers can all be modified to encompass multiple catalytic sites. A linear polymer would be soluble and hence homogenous, however, there is reduced activity due to the random distribution of catalytic sites and it would be difficult to separate due to the non-persistent nanoscopic size of the molecules. A cross-linked polymer is able to overcome the separation problem by being insoluble in the reaction medium. This is a mixed blessing as it again highlights the problem of heterogeneous catalysts; the reaction is dependent on mass transport leading to reduced activity. The use of a dendritic polymer could provide a greater catalytic activity coupled with not only a homogenous system but, due to persistent nanoscopic size, easy separation from the products by ultra filtration. In addition, the controlled activation of the metal bonding sites may give enhanced stability constants for complex formation and reduced catalyst leaching.

In tackling this project a number of factors need to be considered, the design of the dendrimer itself, the selection of the catalytic species to be incorporated into it and the tuning of the surface functional groups to allow it to ligate in the desired way.

Once the species has been designed and synthesised, it then needs to be tested for the desired catalytic properties. At this stage it is envisaged that a hydroformylation process will be considered but a large scope of reactions may be possible. This chapter focuses primarily on the design of the ligand (i.e. the dendrimeric species)

3.2 SILSESQUIOXANES.

The use of a silsesquioxane as the core of the dendrimer has been chosen as it will pass on certain advantageous characteristics to the entire molecule, namely a rigid framework that has similar properties to heterogeneous siloxane catalyst supports. There is also the added advantage, that being cubic, a functional group can be accommodated at each corner. Hence there are eight sites from which to develop the dendrimer. Most of the dendrimers are based on tetragonal silane with only four such sites.

The term silsesquioxanes describes a class of compound that has quite a broad range. They are three-dimensional oligomeric organo-silicon compounds with the general formula $(\text{RSiO}_{3/2})_n$ ($n = 6, 8, 10, 12, \dots$). Their structures are polyhedral frameworks with various degrees of symmetry (Figure 26). The silicon atoms reside at the corners bridged by oxygen atoms.⁶² Substituents on silicon (R) can include hydrogen as well as alkenyl, alkoxy and aryl functional groups. The name is derived from the one and a half, or *sesqui*, stoichiometry of oxygen bound to silicon. When the R group is polymerisable or graftable, the result is a novel class of compounds known as **polyhedral oligomeric silsesquioxanes** commonly called POSS monomers.⁶³ The forms of silsesquioxanes have been reported as random, ladder, cage and partial cage structures.

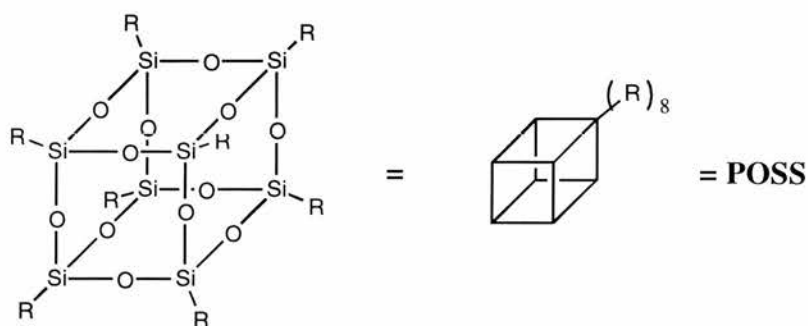


Figure 26: POSS molecule based on a cubane structure.

Although there are a variety of possible structures of silsesquioxanes the compounds that are based upon a cage structure with a general formula $\text{Si}_8\text{O}_{12}\text{R}_8$ will be discussed here.

The silicon atoms are situated on each of the eight corners of the cube bridged by oxygen. Each silicon contains a pendant group 'R' (Fig. 1). Detailed studies of other types of structures are available.⁶⁴

3.2.1 THE HISTORY OF SILSESQUIOXANES

The first commercialisation of silicones began with silsesquioxane chemistry. The silicone industry started with commercialisation of silicone resins consisting primarily of silsesquioxanes for electrical insulation at high temperature. Today, however, polydimethylsiloxane is the predominant material used.

Silsesquioxane chemistry spans over half a century but interest in the area has steadily increased. A survey has been done showing that between 1955 and 1993 there has been an approximate exponential growth in the number of publications.⁶⁴

There are numerous applications for substituted silsesquioxanes, including their use as models for silica surfaces, Wittig reagents as well as heterogeneous silica supported transition metal and rare earth catalysts. They can also be utilised as preceramic coatings that can be pyrolysed to silicon carbide, nitrated glass, silicon oxynitride, aluminosilicates, silica-reinforced composites, and a variety of microporous materials.

3.2.2 THE CHEMISTRY OF SILSESQUIOXANES:

An extensive discussion of this class of compounds is beyond the scope of this chapter, hence a description of some aspects will be briefly covered to introduce the work done in the area.

Most of the recent advances have been focussed around the POSS molecule, both the open and closed chain varieties. Not only has the impetus been on varying the 'R' groups bound to the silicon but also the incorporation of other elements into the framework. Extensive work has been done on the open cage (incompletely condensed) variety of the POSS molecule (Figure 27). As shown, one of the silicon groups is missing and hydroxide groups remain on silicon. Controlled cleavage, synthesis and reactions of the POSS molecules and framework silicons in both the open and closed cage systems have stirred interest.⁶⁵ The reaction of the pendant groups in the incompletely condensed species has resulted in the isolation of stable anionic species.⁶⁶

Reaction of $R_8Si_8O_{12}$ with strong protic acids (HX) affords $R_8Si_8O_{11}X_2$ via selective cleavage of one Si–O–Si linkage and subsequent hydrolysis affording $R_8Si_8O_{11}(OH)_2$.⁶⁷

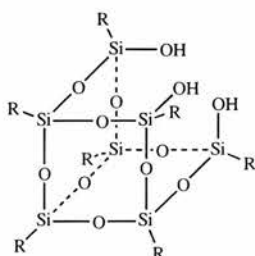


Figure 27: An example of an open cage POSS molecule.

$R_8Si_8O_{12}$ systems can also be used as precursors to incompletely condensed Si/O frameworks with important implications for the manufacture of hybrid organic-inorganic materials that are particularly valuable in the synthesis of sol-gels.⁶⁸

Numerous methods are known for the synthesis of highly functionalised silsesquioxane and spherosilicate frameworks. The main methods are:

- Direct synthesis via hydrolytic condensation of $RSiX_3$ (Figure 28),
- Hydrosilylation of hydrosilsesquioxanes (Figure 29),
- Synthetic manipulations of organic substituents on other readily available frameworks
- Silylation of spherosilicates
- Cross metathesis reactions of alkenes with readily available vinyl substituted silsesquioxane.⁶⁹

Octavinyltasilsesquioxane is commercially available and easily synthesised (Figure 28).⁷⁰

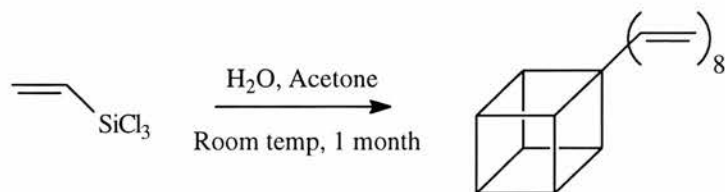


Figure 28: Synthesis of Octavinyltasilsesquioxane $(CH_2=CH)_8Si_8O_{12}$

The POSS molecule can easily be reacted and used as a building block to create a range of dendrimeric species (Figure 29).

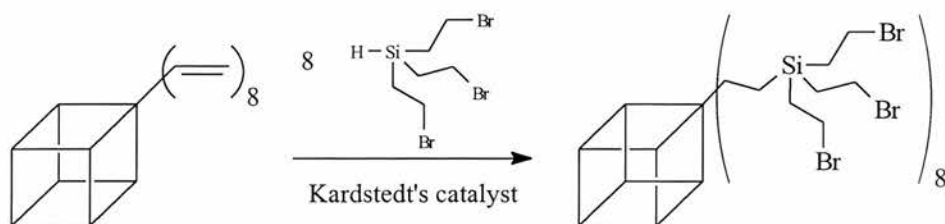


Figure 29: The synthesis of a 24-Br functionalised dendrimer in one step from Octavinyl octasilsesquioxane Kardstedt's catalyst = (bis(divinyltetramethyldisiloxane)platinum(0), Pt(DVTMDS)_x)

3.2.3 THE ROLE OF SILSESQUIOXANE MOLECULES IN CATALYSIS

Heterogeneous catalysis plays an important role in the petrochemical industry and a wide range of processes such as hydrocarbon reforming and oxidation, olefin polymerisation and metathesis rely on this type of species. While it has been shown that this is a valuable area, surface catalysis and in particular the mechanistic pathway has proven difficult to study. Homogeneous systems on the other hand are more easily studied. For this reason there is scope for homogeneous models that mimic heterogeneous catalysts.

Some work has been done in this area^{66,70c,71} using incompletely condensed POSS molecules. They exhibit a number of features that make them suited to this task, in particular they have a sufficient degree of oligomerisation to be considered a model for highly siliceous materials. The POSS molecules possess an extensive Si–O framework and hence may have more similar electronic properties to silica and siliceous solids than simpler siloxide ligands.

The rigid framework of the POSS species rather than the functional group to which it is bound may allow it to dictate its coordination to a certain extent and is hence similar to a surface in that respect. Open cage structures have been used directly in catalytic systems e.g. a silsesquioxane with molybdenum incorporated in the cage has been shown to rapidly catalyse the metathesis of alkenes.⁷² The catalytic polymerisation of alkenes using a vanadium containing silsesquioxane has also been reported.⁷³

It is believed that silicon atoms of a silsesquioxane framework are approximately as electron withdrawing as CF₃ groups⁷⁴ and most silsesquioxanes coordinate to metals with acute M–O–Si bond angles which limits the extent of O_(pπ)–M_(dπ) bonding possible.

The POSS based catalyst was shown to exhibit similar properties to analogous non-silsesquioxane bound catalytic species. Hence, it may be possible that the silicon framework is able to provide a useful platform upon which a catalyst is built.

3.3 DENDRIMERS

Dendritic polymers, also known as arborols, fractal polymers or cascade molecules, are structures with a globular form in which well defined branches radiate from a central core. As the system extends it becomes more branched and crowded. There has been a great deal of interest in dendrimeric macromolecules and the complexes have been known since the 1920's.

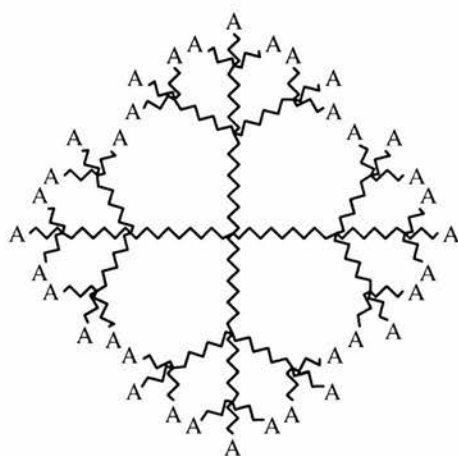


Figure 30: Schematic diagram of a dendritic macromolecule functionalised on the external surface with a catalytic group 'A'

Since the advent of Mandelbrot fractal geometry and similar theories there has been a relative explosion of ideas in this area and a number of reviews summarise this well.⁷⁵ Much of the work has focussed on new materials and their molecular architecture as well as design and synthesis of regular networks of branched systems.

The historical interest in well defined macromolecules stems from their relevance in biochemistry and the dendrimeric systems found in nature. A related area of study is the generation of micelles, liposomes, vesicles and oligomers. There are many potential uses of these entities in such diverse areas as drug delivery agents, synthetic vaccines, synthetic cells to macromolecular templates.⁷⁶ Thus, there is a plethora of exciting areas to be explored, catalytic systems being only one of them.

Using the POSS as a framework, the species can be built upon as dendrimers in three dimensions. This would provide an ordered array of functional groups crowded on the surface of a 'dandelion-clock' like structure.

The idea of using a soluble polymer as a catalyst support is not unheard of. Problems with accurate control of the number and location of catalytic metal sites have been encountered.⁷⁷ A silane based dendrimer system has been designed to alleviate these problems.⁷⁸ The core of this macromolecule is simpler than the POSS dendrimer proposed. It consists of a single silicon atom with four functional groups radiating out from it, which in turn branch into one to three groups leading to a dendrimeric species. The ends of the branches consist of a nickel based catalyst (Figure 31).

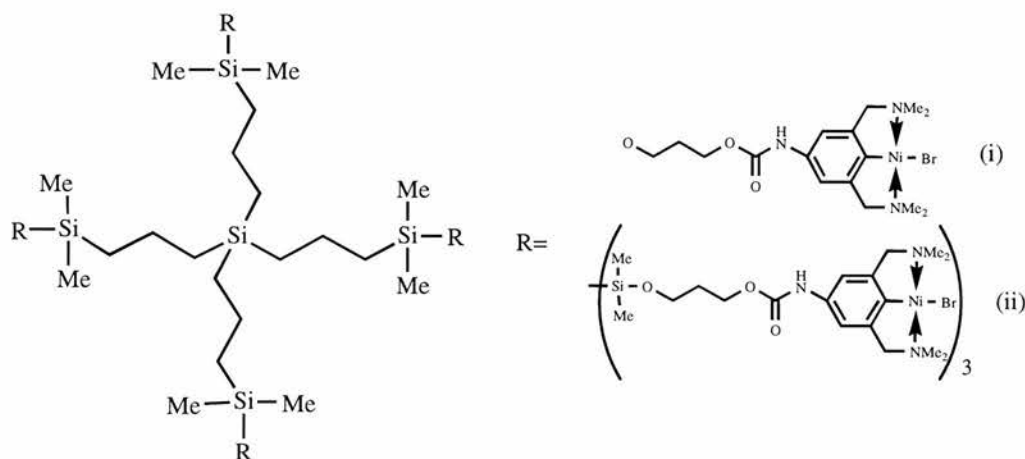


Figure 31: A catalyst based dendrimeric species built on a single silicon atom as the core.⁷⁸

These dendrimers showed regiospecific catalytic activity for the Kharasch addition of poly haloalkanes to carbon—carbon double bonds (Figure 32). It was hypothesised that the catalytic macromolecule would be able to be separated from the reaction mixture but the report does not state if this was attempted.

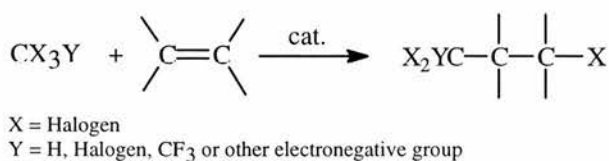


Figure 32: Reaction catalysed by the dendrimeric supported nickel catalyst.

3.5 CATALYST DESIGN

The dendrimeric based catalytic systems need a certain amount of design to ensure that all criteria are fulfilled so that an effective catalyst can be synthesised. Various methods have been used to characterise POSS and dendrimeric systems, they include solid state and solution NMR, single crystal X-ray crystallography, FTIR, gel-permeation chromatography, electrochemistry and MALDI-TOF mass spectroscopy. The high symmetry of the molecules could make NMR spectroscopy particularly diagnostic and solution NMR would be the first method of choice for characterisation.

3.5.1 STRATEGY

When designing the POSS catalysts there are a number of goals: These include the synthesis of a range of POSS frameworks with varying degrees of dendritic branching, to functionalise them with catalytic sites, characterise the species and to assess their catalytic properties. The catalytic system could then be optimised.

3.5.2 WHY USE A DENDRIMER SUPPORTED CATALYST?

The advantages of a dendrimer-supported catalyst include: the easy recycling of the catalyst (using ultra filtration), precise control of the number of catalytic sites, and the production of a multidentate system that could produce a non-leaching catalyst. Certain other environmental properties could also be influenced, such as designable solubilising properties and the tailoring of interiors to suit the environment.

3.5.3 METAL SELECTION

RHODIUM

Using rhodium within a homogeneous catalytic system has shown some very promising advances in a range of reactions. This type of catalyst shows very high activity, selectivity and stability and addresses two major drawbacks, namely the expense of rhodium and the difficulty in separating the catalyst from products after the completion of the process under most circumstances.

Despite the very high cost of rhodium, it is often preferred over cobalt in catalytic systems because it can operate under very mild conditions and give better selectivity. The cost requires that the metal must be recycled with no attrition. This problem has been

overcome in some cases but in many remains the reason why more homogeneous processes based on rhodium cannot be commercialised (*cf.* problem of long chain alkene catalytic hydroformylation in section 2.3).

A POSS dendrimer supported catalyst would help to overcome separation difficulties and hence provide a very valuable addition to the arsenal of rhodium catalysts. This would be done by the ability to recover the catalyst using ultrafiltration and hence facilitate separation from the reaction mixture. As the rhodium is recovered and recycled, its expense becomes less of an issue.

COBALT

The use of a cobalt based catalyst may also be considered. The relative inactivity of this metal compared to rhodium has limited its extensive use in industry in recent years. The distinct advantage it does have is that it is significantly cheaper than rhodium. If the reactivity, stability and selectivity of the complexes can be improved using the dendrimer supported system then the use of cobalt will be investigated.

3.5.4 LIGAND DESIGN.

A recent study of heterogeneous metallocene based catalysts has clearly shown (using structural as well as spectroscopic evidence) that the accessibility of the catalytically active site is crucial.⁷⁹ The design of the catalyst support needs to ensure that the active species is exposed enough to perform its duty, but at the same time that it is sufficiently bound to ensure leaching is kept to a minimum. The number of catalytic sites can be controlled by the design of the dendrimer. As the number of branches increases radially, the number of potential metal binding sites also increases. As the crowding of the outer surface of exposed functional groups is directly related to the degree of branching, the potential for producing a multidentate ligand is evident. Thus, the size of the dendrimer will allow it to function as a tuneable ligand with the ability to vary the number of metals bound. The dendritic species can be considered a large ligand able to act as a multidentate species. The most logical place to start is with the simplest possible core, increasing the branching and complexity as understanding of the system proceeds.

Extension of the silicon based framework is possible (Figure 33).⁸⁰

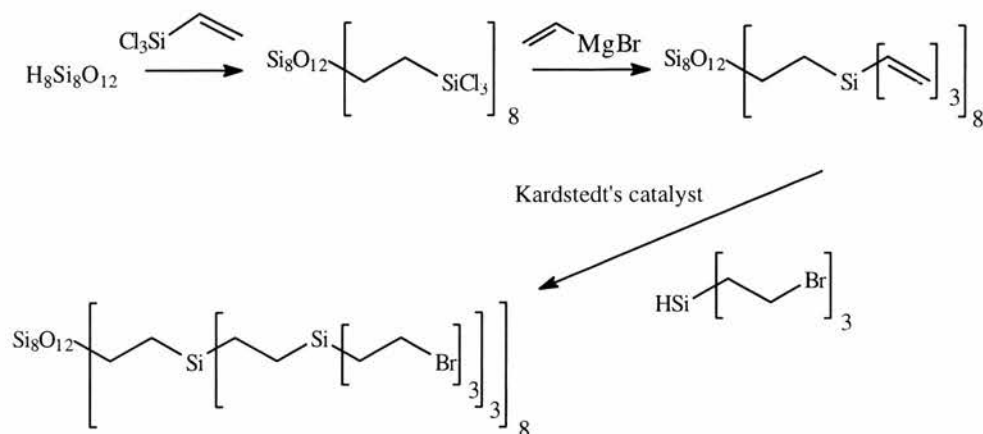


Figure 33: Proposed three-step synthesis of a 72-Br functionalised dendrimer.

Preliminary results in this area show that the first two steps work well and the 24-vinyl dendrimer has been characterised using single crystal x-ray diffraction.⁸¹ The alternative method of starting with octavinyl derivatised POSS molecules and using HSiCl_3 as the hydrolysing agent works equally well.

Various sizes of dendrimers can be synthesised using similar methods. This will consequently vary the density and number of functional groups on the exterior hence allowing the number and nature of the coordination sites to the metal to be varied.

The most predominant phosphine in the catalytic hydroformylation and hydrogenation type reactions proposed has been aryl phosphines. Alkyl phosphines, on the other hand, have been studied less extensively. It has recently become apparent that some of their properties, in particular the greater electron donating ability compared to arylphosphines, can be utilised, and different products (alcohols rather than aldehydes) can be obtained (see Chapter 2)

The POSS/dendrimer system lends itself to the use of rhodium trialkyl phosphine complexes and a number of key advantages are evident. They can be easily attached to the outside of dendrimers using standard organometallic chemistry and perhaps more significantly the resulting dendrimers are predicted to have similar chemical (and electronic properties) to 'small molecule' trialkylphosphine complexes. This latter point is important when considering the design of a catalyst that is effective but not too influenced by the ligand to which it is attached. Hence the dendrimer is acting merely as a means to enlarge the catalyst sufficiently so that it can be recovered by ultrafiltration, but does not significantly influence catalytic properties.

There has not been much work in the POSS dendrimer systems involving phosphorous as the outer shell of functional groups (i.e. all eight silicon ‘corners’ being substituted by a chain with phosphorous as the end group). The work that has been carried out has used aryl phosphine groups (Figure 34).^{82,83}

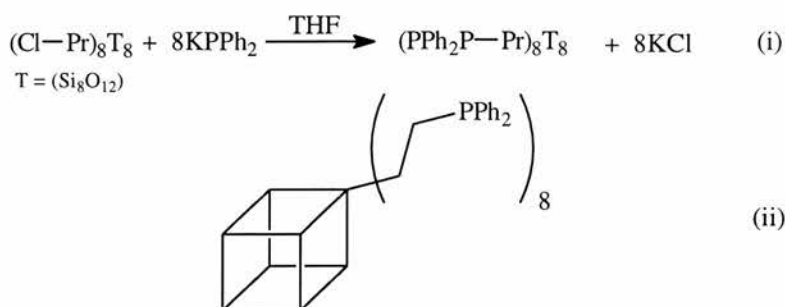


Figure 34: Two examples of POSS molecules with phosphorous functional groups on the outer layer

Other work with phosphorous has involved the incorporation of group 15 atoms into the POSS framework⁸⁴ and Ph_3PCH_2 bound to one silicon group within an incompletely condensed silsesquioxanes.⁸⁵ Reactions of phosphoranes with hydrosilsesquioxanes and chlorosilsesquioxanes have also been successful.⁸⁶

3.5.3 BINDING CATALYTIC SPECIES TO LIGAND

The key to this project is the metal containing catalytic species and the nature of the interaction with the POSS dendrimer ligand. It is crucial that they are bound strongly to minimise the leaching of the metal whilst also providing an easily accessible active site.

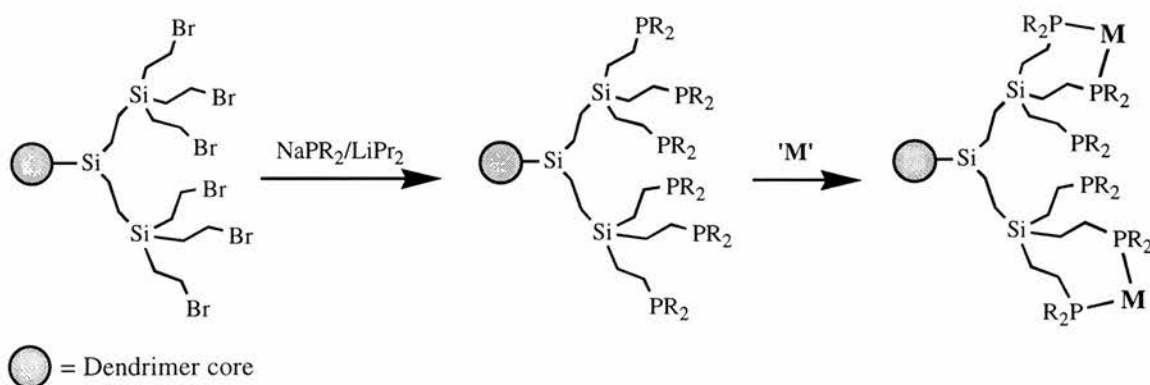


Figure 35: Functionalisation of the chain ends of a dendrimer using NaPR_2 facilitating the possible coordination of a metal species ('M') leading to a potentially non-leaching catalyst

The illustration above (Figure 35) shows how the catalytic species could be reacted with the dendrimer to affect ligation. The precise nature in which the metal would bind is not

yet known but it is thought that there will be more than one binding site so that the system can take advantage of a chelation effect enhancement of stability.

3.6 RESULTS

The work performed has incorporated the first step of the project aims. The simple vinyl-POSS molecule has been reacted with an alkyl phosphine (Figure 36). This was done as a radical reaction with AIBN (azoisobutylnitrile) as the initiator. A radical reaction was performed to affect an anti-Markownikoff type addition of the phosphine to the alkene so that it would give terminal phosphine groups as desired. The reaction was performed in this way at 50°C for 3 days. The long reaction time was deemed necessary as shorter times resulted in incomplete reaction as shown by a multiplet centred at 6 ppm in the ^1H NMR spectrum. These peaks correspond to the unreacted vinyl groups on the POSS molecule and this is confirmed by comparison to the ^1H NMR spectrum of the starting material. The product, a colourless oil, is very thermally stable but decomposes rapidly in air or non-degassed solvent. The ^{31}P NMR spectrum clearly shows if any oxidation has taken place and is also the most informative nucleus to examine. There are two peaks clearly evident in the spectrum, a strong signal at -14.6 ppm is attributed to the bound diethyl phosphine, and a small peak at 48.3 ppm indicative of the formation of diethylphosphine oxide (this is in the region where an oxide would be expected to be found). Thus the purity of the sample can be qualitatively estimated by the intensity of the second peak relative to the one further upfield. It is significant that the peak due to triethylphosphine would be predicted to be found at -20 ppm and that of the starting phosphine (HPEt_2) at -55 ppm. Hence the absence of these materials is confirmed.

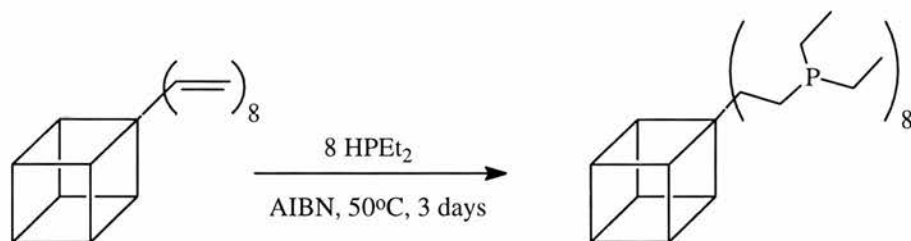


Figure 36: Reaction of vinyl-POSS with HPEt_2 and a radical initiator.

The sample catalytic reaction needed to prove that the ligand did actually coordinate to the metal. Hence, it was decided to use conditions which would produce alcohols if the POSS ligand had coordinated to the rhodium and the catalyst had successfully formed (see

section 2.4.2).³¹ The reaction was carried out in a protic solvent (methanol) using $\text{Rh}(\text{OAc})_2$, with 36 bar CO/H_2 at 120°C . The substrate was 1-hexene. If the catalyst had not successfully formed, the rhodium would be expected to catalyse the normal hydroformylation reaction and produce heptanal only. The reaction was stopped after five hours and the products analysed after cooling. The results of the GC-MS showed the formation of 1-heptanol (60.5%), heptanal (1.5%) and 2-hexanal (7.5%). Some unreacted hexene (3.28%) was present, and other peaks from the methanol (used in the reaction itself and for dilution of the analysis solution) were detected. As the vast majority of the products were alcohols it can be deduced that the catalyst formed and successfully catalysed the reaction. Not all of the substrate had been consumed and hence the reaction conditions may still be improved.

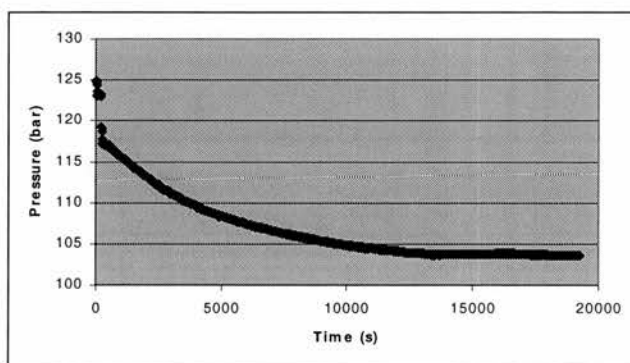


Figure 37: Kinetic graph of POSS dendrimer based catalyst.

The kinetics graph (Figure 37) shows the gas uptake had slowed considerably in the latter part of the reaction but had not stopped completely. This, along with the presence of a dark precipitate in the final solution at the end of the reaction, indicates the possibility of catalyst decomposition. The reaction was first order with respect to the substrate. The kinetics calculated suggests a number of possibilities. If the curve is fitted with a single exponential $k = 2.06 \times 10^{-4} (\pm 3.5 \times 10^{-7}) \text{ s}^{-1}$. It could also be shown that the curve can be fitted with a double exponential decay, in which case $k = 3.15 \times 10^{-4} (\pm 1.16 \times 10^{-5}) \text{ s}^{-1}$ for the first part of the curve and $k = 8.53 \times 10^{-5} (\pm 1.21 \times 10^{-5}) \text{ s}^{-1}$ for the second. Both the single and double exponential decays are plausible. If the reaction is slowing due to catalyst decomposition, the single exponential might be expected. If there are two reactions occurring then the double exponential may describe the reaction better. There are two possibilities if this is the case. The first may involve the hydroformylation of the hexene to the aldehyde which is followed by hydrogenation. The second possibility is if isomerisation of the substrate is followed by a slower hydrolysis of the newly formed

isomer. In either case the second reaction is slower than the first and may explain why all of the substrate had not been consumed.

Studies have continued within the research group and further advances in this area have been achieved.⁸⁷ The main areas focus on radical reaction of dialkylphosphine onto the double bonds of vinyl-functionalised dendrimers and a second route was explored which utilises nucleophilic substitution of the chlorine atoms of Cl-functionalised dendrimers by a lithium salt. The following reactions summarise the types of compounds that have been prepared.

The 24 and 72 vinyl-POSS molecules have been reacted with HPeEt_2 in a similar fashion to the above reaction, resulting in the phosphine functionalised outer layer of the dendrimer (as illustrated in Figure 38).

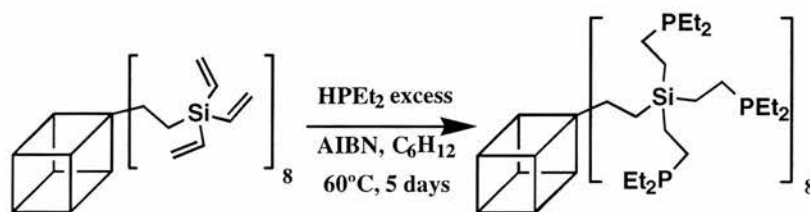


Figure 38: Reaction of 24 and 72-vinyl functionalised POSS with HPeEt_2 .

Nucleophilic substitution of chlorine on Cl-functionalised POSS molecules has been achieved using lithium alkylphosphine or arylphosphine salt (Figure 39). Other similar reactions have been performed, such as the methylphosphination of the 72 Cl-substituted POSS by $\text{LiCH}_2\text{P}(\text{CH}_3)_2$.

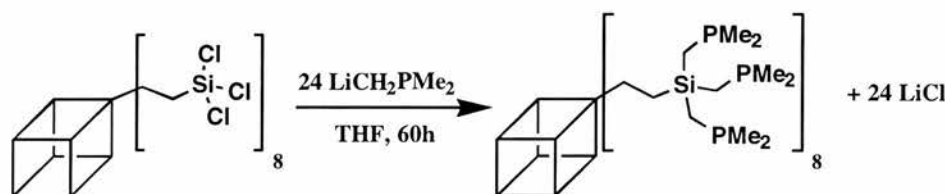


Figure 39: Reaction of 24-Cl functionalised POSS with $\text{LiCH}_2\text{P}(\text{CH}_3)_2$

Preliminary catalytic activity studies have been performed on some of the compounds mentioned above. The results have shown that the rhodium-dendrimer complexes with 24 and 72 branches have good activity for hydroformylation at optimal conditions prescribed for similar reactions.⁸⁸ Some successful catalytic hydrocarbonylation reactions were done using $-\text{CH}_2\text{PMe}_2$ and $-\text{CH}_2\text{P}(\text{C}_6\text{H}_{13})_2$ derivatives of the rhodium-dendrimer complexes.

3.7 EXPERIMENTAL FOR CHAPTER THREE

POSS PHOSPHINE LIGAND

Octavinyl octasilsesquioxane (0.300 g, 4.7×10^{-4} mol L⁻¹) was added to a dry 2 necked 100 mL round bottomed Schlenk flask. AIBN (0.0078 g, 4.7×10^{-4} mol L⁻¹) was added and the flask was charged with dry degassed cyclohexane (10 mL). A second Schlenk flask was charged with dry degassed cyclohexane (10 mL) and diethylphosphine (0.34 g, 3.8×10^{-3} mol L⁻¹) added. The HPET₂ solution was slowly added to the POSS/AIBN solution via cannula. Once all had been transferred, the flask was charged with a further aliquot of cyclohexane (5 mL) to rinse the emptied vessel. A condenser was fitted to the flask and its contents were heated to 50°C for 60 hours.

The resulting solution was allowed to cool and evaporated to dryness *in vacuo*. The resulting product was a viscous, colourless oil.

NMR Data (Varian 300 n.m.r. spectrometer):

¹H CDCl₃ δ_H 1.0 ppm, m, (P-CH₂CH₃); 1.34 ppm, m, (P-CH₂CH₃); 0.66 ppm, m, (Si-CH₂CH₂-P)

¹³C CDCl₃ δ_C 18.1 ppm, d, *J*_{cp} 4.0 Hz (P-CH₂CH₃); 17.78 ppm, d, *J*_{cp} 16.0 Hz (Si-CH₂CH₂-P); 9.4 ppm, d, *J*_{cp} 11.9 Hz (P-CH₂CH₃); 5.75 ppm, d, (Si-CH₂CH₂-P)

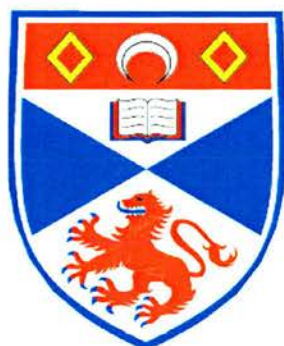
³¹P CDCl₃ δ_P -14.6 ppm

CATALYTIC RUN:

The reaction vessel was charged with Rh(OAc)₂ (0.026 g; 1.16×10^{-3} mol L⁻¹) and the POSS based phosphine ligand (0.1678 g; 4.64×10^{-3} mol L⁻¹) dissolved in methanol (4 mL) was injected under a stream of argon via the side port. After the vessel had been flushed with 3 cycles of CO/H₂ (*ca.* 15 bar) it was pressurised to 30 bar and sealed. The stirrer was activated and the internal temperature raised to 120°C. Once stabilised, the substrate (1-hexene; 1 mL) was injected, the pressure brought up to 36 bar and the gas uptake monitored. The reaction was stopped after 5 hours by immersing the reaction vessel in cold water and allowing to cool whilst stirring. The autoclave was vented and the final solution was diluted in methanol and a GC-MS analysis carried out.

3.8. CONCLUSION:

The development of a support structure that is able to allow a metal species to function as a homogeneous catalyst whilst incorporating the greatest advantages of a heterogeneous system is a promising area. Earlier studies show that it is possible to design a dendrimer based on a POSS skeleton and incorporate a 'layer' of catalyst on the outside. This is an area which, although not studied in detail to date, could have powerful implications for the future. Further advances are being achieved at a rapid rate and interest in this area has increased rapidly over the last few years. Studies have continued in the current research group and the results suggest that the future of this class of compound's use as an easily recoverable catalyst is very promising.



CHAPTER FOUR:
CATALYTIC RUNS

CHAPTER FOUR: CATALYTIC RUNS

This chapter discusses the catalytic reactions performed, the nature of the ligands and work done in the CATS service. Each section involves a number of repeated experiments and the overall results are discussed and tabulated. A brief outline of operational procedure for each section is given but is dealt with in greater detail in the experimental chapter that follows.

4.1 FLUOROUS BIPHASIC CATALYSIS (LEICESTER)

Long chain aldehydes are required for the manufacture of soaps and detergents. The current industrial process involves an older $\text{Co}_2(\text{CO})_8$ based catalysed process operating at high temperature and pressure, resulting in low selectivity and poor catalyst recovery. Rhodium based catalysts cannot be used as their thermal instability precludes the use of distillation for the separation from the high boiling products. One way of circumventing this problem is to use a two phase system with the catalyst dissolved in water. Since the substrate and products are immiscible in water, separation can be easily effected. However, substrates with chain lengths >6 have such low solubility in water that the rate of hydroformylation is too low for the aqueous process to be of commercial interest. It is these substrates ($\text{C}_9\text{-C}_{14}$) that are most valuable to the soap and detergent industry.

A solution to these problems requires a new approach. One such idea is to use fluoruous biphasic systems (FBS), first suggested by Horváth and Rábai working at Exxon Laboratories in 1994.⁸⁹ The term 'fluoruous' (by analogy with aqueous) has been proposed for any of a range of fully fluorinated hydrocarbon solvents that are immiscible with conventional organic solvents under ambient conditions. In essence, the approach is very similar to that in the aqueous biphasic system. Metal catalysts are rendered preferentially soluble in the fluoruous phase by derivatisation with ligands that incorporate long perfluoroalkyl substituents. By contrast, the organic substrate/product is insoluble in this fluorocarbon phase.

There has been increased interest in this area, and a number of recent publications deal with fluoruous biphasic reactions or separation techniques.⁹⁰ Apart from the ease of separation, an obvious attraction is the environmental advantages gleaned from this type

of reaction. Simpler, more efficient recycling of catalysts is an obvious point to make here, but it is also valuable to note that some of the perfluorinated solvents themselves have incredibly low toxicity. This, along with good gas solubility, has led to proposals that they be used as synthetic blood substitutes.⁹¹

By carefully selecting the two solvents, the system can be immiscible at room temperature but homogeneous under reaction conditions. If the catalyst is designed to be soluble only in the fluorinated phase, the reaction can be carried out in the monophasic higher temperature regime. Cooling effects phase separation such that the catalyst remains in the fluorinated phase and the products are in the organic phase. Separation can then be easily carried out and the catalyst recycled (Figure 40). Ideally the catalyst needs to have very low (preferably zero) solubility in the organic phase and must work for terminal and internal alkenes (with significant *n*-aldehyde from the internal substrate).

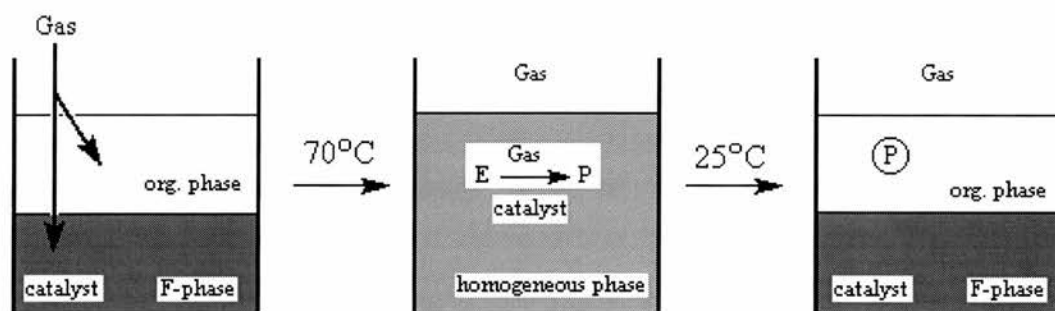


Figure 40: Principle of biphasic reactions (F-phase = perfluorinated solvent, E = reactants, P = product)
Adapted from ref. 91e.

An example of a study using a biphasic system is the recent kinetic set of experiments performed using $\text{Rh}(\text{acac})(\text{CO})_2$ and triphenylphosphine (P/Rh ratio of ca. 10).⁹² The reactions were performed in a 50:50 biphasic mixture of toluene and perfluoromethylcyclohexane ($\text{C}_6\text{F}_{11}\text{CF}_3$ or PP3) with 1-decene as substrate. It was concluded that the kinetic response of the Rh/ PPh_3 catalyst is not uniform with respect to the substrate. At high concentrations of PPh_3 (ca. 0.2 mol/L) only first order kinetics were observed. At low phosphine concentrations (ca. 0.02 mol/L) saturation kinetics occur. Mass transfer limitation was excluded as the maximum rate of gas consumption was well below the experimentally determined mass-transfer limit and the maximum TOF is independent of the concentration of rhodium. Data obtained were consistent with a kinetic first order for rhodium.

Because 1-decene saturation kinetics were observed, it appears that there is a rate limiting step at the saturation limit before which there is a quasi-equilibrium involving the substrate. It was suggested that the equilibrium step is the formation of $\text{HRh}(\text{C}_7\text{H}_{15}\text{CH}=\text{CH}_2)(\text{CO})_x(\text{PPh}_3)_{3-x}$ ($x = 1$ or 2), but could also involve the alkyl or acyl intermediates as well. The corresponding rate-limiting steps are alkene and CO insertion or H_2 activation, respectively.

In collaboration with the research group of Professor E.G. Hope (University of Leicester) a new range of such ligands have been developed and tested. The solvents used were toluene and perfluoro-1,3-dimethyl-cyclohexane (PP3). Various perfluorinated ligands were evaluated, including $\text{P}(\text{C}_6\text{H}_4\text{-4-C}_6\text{F}_{13})_3$ and $\text{P}(\text{OC}_6\text{H}_4\text{-4-C}_6\text{F}_{13})_3$ (Figure 41) and some similar isomers.

HEXENE

All results for this section are summarised in Table 3. Several reactions were performed using PPh_3 , the industrial ligand of choice for short chain alkene hydroformylations (experiments 1-3). The unmodified triphenylphosphine ligand was reacted in toluene (experiments 1 and 2) as well as the standard toluene/PP3 biphasic conditions. When comparing these results to those attained using the ligand with fluoruous ponytails, $\text{P}(\text{C}_6\text{H}_4\text{-4-C}_6\text{F}_{13})_3$ (experiment 4). The rate for the fluorinated ligands was significantly higher with enhanced n/i ratio.

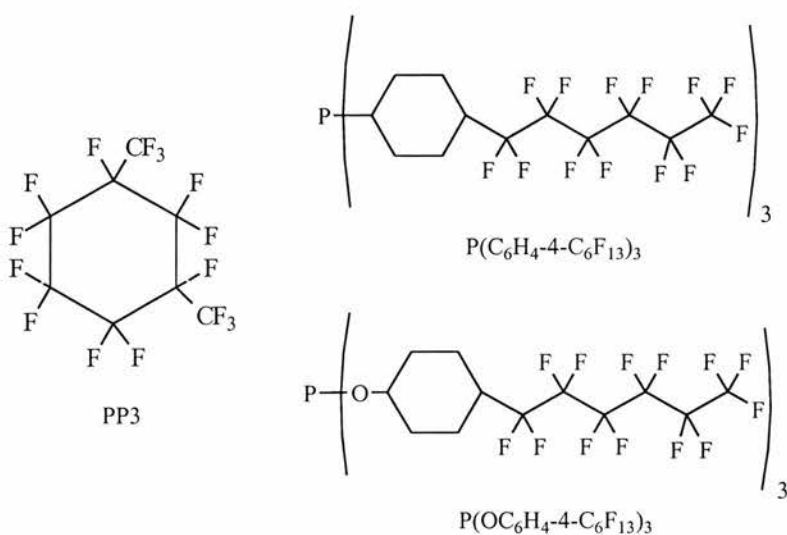


Figure 41: Solvent (PP3) and examples of ligands used in the perfluorous biphasic study.

The rate constant for the internal alkene was 70% of that for the straight chain. Furthermore, reaction of the internal alkene produced significant amounts of straight chain aldehyde. Visual inspection of the resulting two phase mixture showed that the bottom (fluorous) phase is yellow/orange in colour, whilst the top (organic) phase was completely colourless (Figure 1).

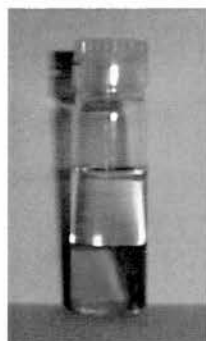


Figure 1: Photograph showing the fluorous (bottom) and organic (top) layers of the biphasic reactions.

The reactions were performed at 70°C and allowed to proceed for 1 hour. To minimise mass transfer problems the stirring rate was high. Qualitative analyses were by GC-MS and quantitative analyses by GC using *n*-octanol as an internal standard.

When comparing the ‘standard’ phosphite ligand, $\text{P}(\text{OPh})_3$ to similar fluorinated ligands, rate increases were also observed. The rate for $\text{P}(\text{OPh})_3$ under standard conditions (experiment 5) rose considerably, with higher initial turnover frequency (TOF), when replaced with $\text{P}(\text{OC}_6\text{H}_4\text{-4-C}_6\text{F}_{13})_3$ (experiments 6 and 7). Furthermore, there was a large increase in the *n/i* ratio but selectivity towards aldehyde was slightly reduced. If a lower concentration of catalyst was used (experiment 8) the rate and *n/i* ratio were reduced but the selectivity to aldehyde increased. Lowering the pressure at the higher concentration (experiment 9) does not improve the *n/i* ratio. This is because the rate of the hydroformylation falls but the rate of isomerisation remains high so there are more products derived from the isomerised alkene.

When changing the *para*-substituted fluorinated ligand (relative to the phosphorous) $\text{P}(\text{OC}_6\text{H}_4\text{-4-C}_6\text{F}_{13})_3$ to the *meta*- and *ortho*-isomers (experiments 10 and 11) significant differences in rate are observed. The *meta*-substituted ligand results in a lowered rate but an increase in the selectivity. The *n/i* ratio obtained is slightly lower than the standard reaction. When reacting the *ortho*-ligand the rate is dramatically enhanced, as is the selectivity to aldehyde, but at the expense of *n/i* ratio, which is very poor indeed.

NONENES

As longer chain products are more valuable in industry, reactions with nonene were performed to assess the ligand's performance. The species tested in these initial runs was $P(C_6H_4-4-C_6F_{13})_3$. The results from these tests are summarised in Table 4.

Under the reaction conditions necessary, isomerisation of longer chained substrates is observed. The most valuable product is the linear aldehyde and ideally the catalytic reaction will preferentially react with the terminal alkene only, thus forcing the products to be linear. The reaction of 1-nonene (experiment 13) shows a fast reaction rate with a good n/i ratio and good selectivity. A certain amount of isomerisation to 2-, 3- and 4-nonene is also observed and a small amount of the corresponding branched hydroformylation products are formed. The reaction is almost complete within the standard reaction conditions and time (99% conversion).

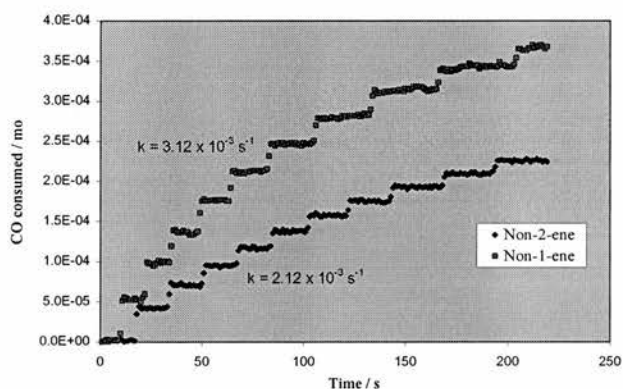


Figure 43: Kinetics of Hydroformylation of Nonenes

The key to the success of the ligand is how effectively the internal alkene's isomerisation can be exploited to form the terminal aldehyde. The way to test this is to react the internal substrate under standard conditions and analyse the products to detect how much isomerisation leads to the linear product. The isomerisation to the terminal alkene is thermodynamically unfavourable, but if the catalyst preferentially reacts with the terminal isomer then the reaction equilibrium will be pushed to the linear products. The reaction products (experiments 14 –16) under these conditions showed that there is a certain amount of exploitation of the isomerisation to produce the linear product. Decanal was produced in significant quantities, and in fact was one of the dominant species (using low pressure and high temperature conditions). Comparing the kinetics between 1-nonene and

2-nonene (Figure 43), it can be seen that the rate of reaction of the internal isomer is about 70% that of the terminal alkene.

These results are positive, the ligand seems to favour reaction to the linear aldehyde. Further tests and optimisation may allow the development of these ligands as effective hydroformylation catalysts for long chain alkenes.

This section concentrates on using the fluorinated ligands on hydroformylation catalysis as it is a convenient system to test. Fluorous biphasic systems need not be limited to this type of reaction. Due to the gas solubility and miscibility properties of perfluorous solvents, they may be adapted to a large range of systems where gases serve as reactants. This area of research is still in its infancy and the potential has only recently been explored, an exciting new area of catalysis awaits.

Table 3: Hydroformylation of hex-1-ene catalysed by rhodium complexes

Conditions (unless otherwise stated): [Rh(CO)₂(acac)] (0.01 mol dm⁻³), phosphine (0.03 mol dm⁻³), hex-1-ene (1 mL) in toluene (2 mL) and PP3 (2 mL), 70°C, 20 bar, 1 hour.

No.	Ligand	hexene / %	isom / %	2EtP / %	2MeH / %	H / %	Conv / %	Selectivity to al / %	<i>n</i> : <i>i</i>	Initial TOF / s ⁻¹	Rate Constant / s ⁻¹	Initial Rate / mol dm ⁻³ s ⁻¹
1	PPh ₃ ^a	0.8	6.1	1.9	23.2	67.9	99.2	93.9	2.7	0.25	<i>b</i>	2.5x10 ⁻³
2	PPh ₃ ^a	0.4	3.9	6.4	21.2	68.1	99.6	96.1	2.5	0.25	<i>b</i>	2.5x10 ⁻³
3	PPh ₃	1.0	1.8	0.3	23.7	73.3	99.0	98.2	3.1	0.32	<i>b</i>	3.2x10 ⁻³
4	P(C ₆ H ₄ -4-C ₆ F ₁₃) ₃	1.7	10.6	0.9	17.3	69.6	98.3	89.2	3.8	1.0	6.3x10 ⁻³	1.0x10 ⁻²
5	P(OPh) ₃	0.4	8.0	4.1	19.6	67.9	99.6	92.0	2.9	0.48	<i>b</i>	4.8x10 ⁻³
6	P(OC ₆ H ₄ -4-C ₆ F ₁₃) ₃	0.3	17.7	1.4	9.7	70.9	99.7	82.3	6.4	0.99	6.2x10 ⁻³	9.9x10 ⁻³
7	P(OC ₆ H ₄ -4-C ₆ F ₁₃) ₃	0.8	14.6	0.7	8.3	75.6	99.2	85.3	8.4	0.74	4.6x10 ⁻³	7.4x10 ⁻³
8	P(OC ₆ H ₄ -4-C ₆ F ₁₃) ₃ ^c	1.4	9.3	3.2	18.6	67.5	98.6	90.6	3.1	0.29	1.8x10 ⁻³	2.9x10 ⁻³
9	P(OC ₆ H ₄ -4-C ₆ F ₁₃) ₃ ^d	0.3	10.7	1.4	10.3	77.2	99.7	89.3	6.6	0.51	3.2x10 ⁻³	5.1x10 ⁻³
10	P(OC ₆ H ₄ -3-C ₆ F ₁₃) ₃	0.1	3.9	2.5	12.9	80.6	99.9	96.1	5.2	0.26	1.6x10 ⁻³	2.6x10 ⁻³
11	P(OC ₆ H ₄ -2-C ₆ F ₁₃) ₃	0.1	0.8	14.5	39.1	45.5	99.9	99.2	0.9	14.0	8.5x10 ⁻²	1.4x10 ⁻¹
12	P(OC ₆ H ₄ -4-C ₆ F ₁₃) ₂ (CF=CF ₂)	25.7	14.6	0.2	15.8	43.7	74.3	80.4	2.7	0.24	1.5x10 ⁻³	2.4x10 ⁻³

al = aldehyde; isom = isomerised hexenes, 2EtP = 2-ethylpentanal, 2MeH = 2-methylhexanal, H = heptanal, TOF = turnover frequency (moles of hex-1-ene consumed per mole of rhodium per second), *n*:*i* = ratio of straight to total branched aldehydes.

^a In toluene (4 mL);

^b Zero order throughout most of the reaction;

^c [Rh(acac)(CO)₂] (0.001 mol dm⁻³), P(OC₆H₄-4-C₆F₁₃)₃ (0.003 mol dm⁻³);

^d Pressure = 8 bar CO/H₂.

Table 4: Hydroformylation of nonenes

Conditions (unless otherwise stated): $[\text{Rh}(\text{acac})(\text{CO})_2]$ (0.01 mol dm⁻³), $\text{P}(\text{C}_6\text{H}_4\text{-4-C}_6\text{F}_{13})_3$ (0.03 mol dm⁻³), 1-nonene (1 mL) in toluene (2 mL) and PP3 (2 mL), 70°C, 20 bar, 1 hour.

No.	1-nonene /%	2-nonene /%	3- & 4-nonene /%	2PrH /%	2EtO /%	2MeN /%	Decanal /%	Conv. /%	Selectivity to al /%	n:i	Rate Const /s ⁻¹
13 ^a	1.0	12.8	1.2	-	1.0	9.8	74.2	99.0	85.9	6.9	3.1x10 ⁻³
14 ^{b,c}	0.2	11.8	20.3	7.3	12.0	33.0	15.4	88.2	76.8	0.29	4.7x10 ⁻⁴
15 ^b	0.2	13.9	11.0	7.2	17.8	39.5	10.4	86.1	87.0	0.16	2.1x10 ⁻³
16 ^{b,c,d}	0.4	21.0	38.7	4.2	5.2	16.3	14.2	79.0	50.5	0.55	2.6x10 ⁻³

2PrH = 2-propylhexanal, 2EtO = 2-ethyloctanal, 2MeN = 2-methylnonanal.

^a 1-nonene as substrate;

^b 2-nonene as substrate;

^c Pressure = 8 bar CO/H₂;

^d T=90°C.

4.2 LARGE RING DIPHOSPHINES (BRISTOL)

The catalytic potential of a range of large ring diphosphines (Figure 44), sent by the research group of Professor R. Alder (University of Bristol), were tested under the CATS service. A variety of conditions for the hydroformylation of hex-1-ene, styrene and vinyl acetate were employed and evaluated.

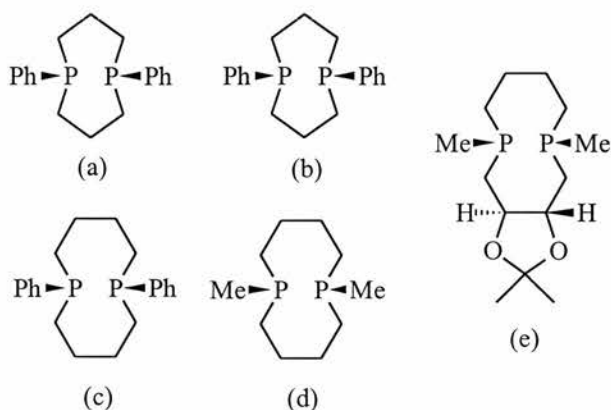


Figure 44: Large ring diphosphines studied for hydroformylation reactions.

Tables 3-5, which follow this discussion, list details and commentary for each reaction. Standard experimental procedures were used. All total solvent volumes were 4 mL and either toluene, ethanol or a 1:1 toluene/ethanol mixture was used. The substrate (1 mL) was injected into the autoclave containing the reaction solution (ligand, metal source and solvent) which was at the required temperature, stirring rate and *ca.* 15 bar below the operating pressure. On injection the pressure was raised and the kinetic data collected. At the end of the reaction, the reactor was cooled by immersion in cold water and the stirrer stopped. The liquid products were analysed by GC (quantitative) and GC-MS (qualitative).

Heating the ligand and rhodium complex, $[\text{Rh}(\text{CO})_2(\text{acac})]$, under CO/H_2 forms the catalytically active species. The reaction should start immediately after the substrate is introduced and no induction period observed. First or zero order kinetic behaviour is usually seen. Information about the alkene binding step (Figure 45) can be deduced from the order of the reaction as long as the rates are not dictated by mass transfer limitations.

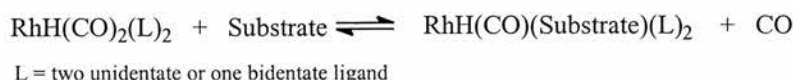


Figure 45: Alkene binding step of hydroformylation reactions.

The reaction is first order in substrate if the equilibrium is not completely to the right. If it is, then the reaction will be zero order. When reacting PPh_3 under similar conditions (70°C , 40 bar), the rate is zero order with $k = 2.5 \times 10^{-3} \text{ mol dm}^{-3} \text{ s}^{-1}$. Other phosphines with average activity show first order kinetics with rates of $1 - 10 \times 10^{-3} \text{ s}^{-1}$.

HEX-1-ENE

The ligands used all show activity for the catalytic hydroformylation of hex-1-ene. The rates have first order dependence on the substrate with a significant induction period. These periods of inactivity may be attributed to the active species not being fully formed before the substrate is injected. Some ligand degradation may also be necessary before the species activates. It is possible that the substrate could also play a role in this induction period as it may need some pre-reaction before the catalyst is activated towards it. Typically, rhodium based catalysts do not have induction periods, unlike ruthenium catalysts in which these intervals may last up to an hour.

Once the reaction has started, the kinetics were stable with rate constants ≤ 0.1 times that for other ligands tested by the CATS service. The rates usually increase in proportion to temperature. Reactions at 120°C do not follow this trend and the presence of unreacted substrate in the final solution although the gas uptake had stopped, suggests the catalyst may not be stable at higher temperatures.

When the reaction is done in toluene, aldehydes are the major product with a small amount of alcohols produced by hydrogenation. When a protic solvent is used (ethanol), hydrogenation dominates the overall reaction and alcohols are produced in abundance. The hydrogenation occurs sequentially (ie. after the hydroformylation) and the kinetics of the reaction are best fit by a double exponential decay (experiment 7, Table 5). The aldehyde hydrogenation (the second step of the overall reaction) has a rate similar to or faster than the hydroformylation (experiment 8, Table 5). Reactions with double exponential decays are associated with faster hydroformylation rates when compared to other ligands. However, the experiments for these other systems use lower temperatures so caution is needed when comparing them. The overall n/i ratios for the reactions are 2 – 3 which is close to the thermodynamic value and may be due to the ligands not being bulky enough to control the reaction at the metal centre. The n/i ratios of the alcohols

relative to the aldehydes (e.g. Experiments 4, 7, and 8, Table 5) suggest that the linear aldehyde is hydrogenated fastest.

STYRENE AND VINYL ACETATE

Both styrene and vinyl acetate commonly react to give high n/i ratios with the major product containing a chiral centre. Thus, ligand E (Figure 44) was tested to see if it could react to produce asymmetric products. Reactions with both substrates were slower than when hex-1-ene was used, but there was no induction period. This shows that the hexene reaction may well require pre-reaction, leading to the induction period. Styrene and vinyl acetate both react to yield mainly branched chain products, although the branched selectivity is less for styrene at lower CO/H₂ pressure. There is little support showing the products undergo subsequent hydrogenation to alcohols for styrene in toluene.

These substrates generally give high n/i ratios and the major product contains a chiral centre. Ligand E was hence tested for its ability to perform these reactions asymmetrically. Both reactions occurred more slowly than for hex-1-ene but without an induction period. This strengthens the argument that the hexene reaction requires some pre-reaction which causes the induction period. Both give mainly branched chain product although the branched selectivity is less for styrene at lower CO/H₂ pressure. There appears to be little tendency for subsequent hydrogenation to alcohols for styrene in toluene. The branched selectivity for vinyl acetate is very high (~95%) and there is significant hydrogenation even in toluene (alcohol:aldehyde = 61.1 : 41.4). The hydrogenation rate constant is much lower than that seen for hydroformylation. Under all conditions essentially racemic mixtures of the chiral products are produced.

The ligands role in the catalytic hydroformylation of styrene and vinyl acetate is not promising. However, reaction with hex-1-ene is more favourable. The resulting rhodium based catalysts show slightly unusual behaviour, in that they have an induction period, but they do show activity. The catalysts are not stable under the conditions used, but there is some potential. Alcohols production using rhodium based catalysts in similar processes are rare. Rarer still when they are modified with multidentate phosphorous. This behaviour deserves more attention. It could lead to a better understanding of the process and to the design of an effective catalytic system to exploit it.

Table 5: Results from the hydroformylation of 1-Hexene by large ring diphosphines

Conditions Solvent (4mL): pure toluene (Tol), pure ethanol (EtOH) or a 1:1 mixture (Tol/EtOH). Gas: CO/H₂, Rh = Rh(CO)₂(acac) = 5x10⁻⁵ mol, hexene = 1 mL (Hexene:Rh = 160:1).

No.	CATALYST SYSTEM	CONDITIONS	t/hr	1-H/ %	i-H/ %	EtPa I/%	MeH al/%	Hal/ %	MeH ol/%	Hol/ %	al:ol	n:i al	n:i ol	Conv /%	REMARKS
1	Ligand A (P ₂):Rh = 1.5:1	Tol/EtOH 80°C, 20 bar	2.3	52.7	1.7	0.0	11.5	25.3	2.3	6.5	4.2	2.2	2.8	47.3	Good quality graph with an induction period of ca. 1/4 hr followed by ca. zero order kinetics, k=6.7x10 ⁻⁵ mol dm ⁻³ s ⁻¹ . Note: gas uptake steady when reaction stopped. Although reaction only partially complete the catalyst is still active. Traces of dibenzyl etc in GCMS of product mixture indicates some ligand decomposition.
2	Ligand A (P ₂):Rh = 1:1	EtOH 80°C, 40 bar	2.1	13.1	6.2	0.2	25.3	46.5	1.8	6.9	8.3	1.8	3.8	86.9	Good quality graph with an induction period of several mins. followed by first order kinetics, k=1.2x10 ⁻⁴ s ⁻¹ . Note: gas uptake steady when reaction stopped. Although reaction only partially complete the catalyst is still active. Traces of dibenzyl etc in GCMS of product mixture indicates some ligand decomposition.
3	Ligand A (P ₂):Rh = 1:1	Tol 80°C, 40 bar	2.8	29.2	4.5	0.2	20.6	41.8	0.8	2.8	17.4	2.0	3.5	70.8	Good quality graph with an induction period of several mins. followed by first order kinetics, k=1.3x10 ⁻⁴ s ⁻¹ . Note: gas uptake steady when reaction stopped. Although reaction only partially complete the catalyst is still active. Traces of dibenzyl etc in GCMS of product mixture indicates some ligand decomposition.
4	Ligand B (P ₂):Rh = 1.5:1	Tol/EtOH 100°C, 20 bar	2.1	70.5	1.9	0.0	6.9	16.4	0.7	3.7	5.3	2.4	5.3	29.5	Good quality graph with an induction period of several mins. followed by ca. zero order kinetics, k=6.5x10 ⁻⁵ mol dm ⁻³ s ⁻¹ . Note: gas uptake steady when reaction stopped. Although reaction only partially complete the catalyst is still active. Traces of dibenzyl etc in GCMS of product mixture indicates some ligand decomposition.
5	Ligand B (P ₂):Rh = 1:1	EtOH 120°C, 40 bar	2.1	0.5	7.2	0.6	8.8	6.6	20.0	56.2	0.2	0.7	2.8	99.5	Good quality graph with an induction period of several mins. followed by first order kinetics, k=6.8x10 ⁻⁴ s ⁻¹ . Note: gas uptake essentially stopped after 1 hr 40 min suggests that catalyst deactivated (towards hydrogenation of the aldehyde into alcohols). This may confirm the catalyst is unstable at this temperature and explains the lower rate constant compared to the identical reaction at lower temperature (expt 6). Traces of dibenzyl etc in GCMS of product mixture indicates some ligand decomposition.
6	Ligand B (P ₂):Rh = 1:1	EtOH 100°C, 40 bar	2.1	0.3	11.7	1.7	9.2	8.1	16.5	52.4	0.3	0.7	3.2	99.7	Good quality graph with an induction period of several mins. followed by a double exponential fit of gas uptake fitting two first order reactions, k=1.4x10 ⁻³ s ⁻¹ (hydroformylation) and k=1.8x10 ⁻⁴ s ⁻¹ (hydrogenation). Note: there is still slow but steady gas uptake when reaction stopped (hydrogenation of aldehyde). Traces of dibenzyl etc in GCMS of product mixture indicates some ligand decomposition.
7	Ligand B (P ₂):Rh = 1:1	EtOH 80°C, 40 bar	2.0	1.6	13.4	1.1	16.8	27.7	8.9	30.6	1.2	1.6	3.4	98.4	Good quality graph with an induction period of several mins. followed by first order kinetics, k=3.7x10 ⁻⁴ s ⁻¹ (no differentiation between hydroformylation and hydrogenation rates). Note: there is still slow but steady gas uptake when reaction stopped (hydrogenation of aldehyde). Traces of dibenzyl etc in GCMS of product mixture indicates some ligand decomposition.

Table 5: Continued.

No.	CATALYST SYSTEM	CONDITIONS	t/hr	1-H/ %	i-H/ %	EtPa l/%	MeH al/%	Hal/ %	MeH ol/%	Hol/ %	al:ol	n:i al	n:i ol	Conv /%	REMARKS
8	Ligand B (P ₂):Rh = 1:1	Tol 120°C, 40 bar	2.2	0.5	5.0	0.1	24.5	68.8	0.2	1.0	77.8	2.8	n/a	99.5	Graph has odd shape with two distinct regions so that kinetics not reliable. Best fit has an induction period of several mins. followed by first order kinetics, $k=1.7 \times 10^{-3} \text{ s}^{-1}$ (up to 400s) and $k=4.2 \times 10^{-4} \text{ s}^{-1}$ (after 400s). Note: gas uptake essentially stopped after 2 hr - as expected in toluene i.e. little activity towards hydrogenation of aldehyde into alcohols. Traces of dibenzyl <i>etc</i> in GCMS of product mixture indicates some ligand decomposition.
9	Ligand B (P ₂):Rh = 1:1	Tol 80°C, 40 bar	2.0	24.6	8.5	0.1	21.2	45.4	t	0.1	>600	2.1	n/a	75.4	Graph has odd shape with two distinct regions so that kinetics not reliable. Best fit has an induction period of several mins. followed by apparent zero order kinetics, $k=3.2 \times 10^{-4} \text{ mol dm}^{-3} \text{ s}^{-1}$ (up to 80 mins), $k=2.0 \times 10^{-4} \text{ mol dm}^{-3} \text{ s}^{-1}$ (after 80 mins). Note: gas uptake still steady when reaction stopped. Although reaction only partially complete the catalyst is still active. Traces of dibenzyl <i>etc</i> in GCMS of product mixture indicates some ligand decomposition.
10	Ligand C (P ₂):Rh = 1:1	Tol 120°C, 40 bar	2.0	0.3	2.3	2.3	31.2	63.3	t	0.6	160	1.9	n/a	99.7	Good quality graph of gas uptake with an induction period of several mins. followed by first order kinetics, $k=7.9 \times 10^{-3} \text{ s}^{-1}$. Note: gas uptake essentially stopped after 10 minutes i.e. reaction complete with little tendency to hydrogenate the aldehyde to alcohols. Traces of dibenzyl <i>etc</i> in GCMS of product mixture indicates some ligand decomposition.
11	Ligand C (P ₂):Rh = 1:1	Tol 80°C, 40 bar	2.0	0.3	3.9	0.8	31.0	64.0	t	0.1	>900	2.0	n/a	99.7	Good quality graph with an induction period of several mins. followed by first order kinetics, $k=9.2 \times 10^{-4} \text{ s}^{-1}$. Note: gas uptake essentially stopped after 1 hr i.e. reaction complete with little tendency to hydrogenate the aldehyde to alcohols. Traces of dibenzyl <i>etc</i> in GCMS of product mixture indicates some ligand decomposition.
12	Ligand D (P ₂):Rh = 1:1	Tol 120°C, 40 bar	2.0	0.1	9.8	1.2	25.2	62.8	0.2	0.7	100	2.4	n/a	99.9	Good quality graph with an induction period of several mins. followed by first order kinetics, $k=7.4 \times 10^{-3} \text{ s}^{-1}$. Note: gas uptake essentially stopped after 10 minutes i.e. reaction complete with little tendency to hydrogenate the aldehyde product through to alcohols.
13	Ligand E (P ₂):Rh = 1:1	Tol 80°C, 40 bar	2.0	0.3	4.0	6.0	25.6	63.5	t	0.6	160	2.0	n/a	99.7	Good quality graph with an induction period of several mins. followed by first order kinetics, $k=4.1 \times 10^{-3} \text{ s}^{-1}$. Note: gas uptake essentially ceased after 2 hr i.e. reaction complete with little tendency to hydrogenate the aldehyde to alcohols.

1-H = 1-Hexene; i-H = Isomerised Hexenes; EtPal = 2-Ethylpentanal; MeHal = 2-Methylhexanal; Hal = n-Heptanal; MeHol = 2-Methylhexanol & Hol = n-Heptanol.

t = trace (generally <0.03%); n/a means that the % of alcohol in final product mixture was so low that the determination of n:i for the alcohol is not possible.

Conversion = 100 - % of residual 1-Hexene (i.e. isomerised hexenes are regarded as products).

Table 6: Attempted asymmetric hydroformylation of styrene.

Conditions: Styrene = 1 mL, Styrene:Rh = 170:1, Gas is CO/H₂, Rh = Rh(CO)₂(acac) = 5x10⁻⁵ mol

No.	CATALYST SYSTEM	CONDITION S	t /hr	STY /%	2PPal /%	3PPal /%	2PPol /%	3PPol /%	ACET /%	1PEol /%	A /%	B /%	al: ol	n:i al	n:i ol	Conv /%	REMARKS
14	Ligand E (P ₂):Rh = 1:1	Tol 80°C, 40 bar	2.0	0.7	72.3 ee<1%	13.5	2.3 ee n/a	0.7	4.7	3.8 ee n/a	0.5	1.5 ee n/a	28.6	0.1 9	n/a	99.3	Good quality graph with no induction period and first order kinetics, k=1.2x10 ⁻³ s ⁻¹ . Note: gas uptake essentially ceased after 1 hr i.e. reaction complete with little tendency to hydrogenate the aldehyde to alcohols.
15	Ligand E (P ₂):Rh = 1:1	Tol 80°C, 10 bar	21	2.4	66.4 ee<1%	26.5	1.7 ee n/a	1.0	1.0	0.6 ee n/a	0.2	0.2 ee n/a	34.4	0.4 0	n/a	97.6	Good quality graph with no induction period and first order kinetics, k=2.3x10 ⁻⁴ s ⁻¹ . Note: gas uptake still occurring at steady rate after 6 hr when gas uptake data collection stopped.

STY = Styrene; 2PPAL = 2-Phenylpropanal; 3PPal = 3-Phenylpropanal; 2PPol = 2-Phenyl-1-propanol; 3PPol = 3-Phenyl-1-propanol; ACET = Acetophenone; 1PEol = 1-Phenylethanol; A represents two minor products, one of which is 2-Phenyl-1-ethanol and the other remains unidentified. B is an unidentified minor product which forms as a racemic mixture (B was also found as an impurity in 2-Phenylpropanal purchased from Aldrich).
Conversion = 100 - % of residual styrene.

Note: where ee is defined as n/a, the % of the particular product in the final product mixture is so low that the accurate determination of ee from the resultant GC peaks is not possible with any degree of certainty. However, in all cases where ee is stated as n/a both visual and semi-quantitative inspection of the two enantiomer peaks for each product suggest racemic mixtures.

Table 7: Attempted asymmetric hydroformylation of vinyl acetate.**Conditions:** Vinyl acetate = 1 mL, Vinyl acetate:Rh = 215:1, Gas used: CO/H₂, Rh = Rh(CO)₂(acac) = 5 × 10⁻⁵ mol

No.	CATALYST SYSTEM	CONDITIONS	t /hr	VA /%	AA /%	2AcPal /%	1AcPol /%	2AcPol /%	1AcPol /%	AcA /%	Conv /%	REMARKS
16	Ligand E (P ₂):Rh = 1:1	Tol (4mL) 80°C, 40 bar	21	0.6	4.6	41.4 ee << 1%	29.3 ee << 1%	21.8 ee << 1%	29.3 ee << 1%	2.3	99.4	Good quality graph with no induction period. Double exponential fit of gas uptake data fits for two first order reactions, k = 5.0 × 10 ⁻⁴ s ⁻¹ (hydroformylation) and k = 1.8 × 10 ⁻⁴ s ⁻¹ (hydrogenation). Note that gas uptake essentially ceased after 8 hr before the complete hydrogenation of aldehyde into alcohol. This suggests the catalyst decomposition.

VA = Vinyl acetate; AA = Acetic acid; 2AcPal = 2-Acetoxypropanal; 2AcPol = 2-Acetoxy-1-propanol; 1AcPol = 1-Acetoxy-2-propanol & AcA = Acetoxyacetone.

The 2-Acetoxy-1-propanol (2AcPol) is from the direct hydrogenation of 2-Acetoxypropanal (2AcPal) whereas the 1-Acetoxy-2-propanol (1AcPol) is from the acetic acid catalysed isomerisation of 2AcPol (primary product) into 1AcPol (secondary product). The acetic acid (AA) probably arises from the thermal disproportionation of the expected linear aldehyde, 3-Acetoxypropanal into propenal (Acrolein) and acetic acid. This process has been seen at relatively low temperatures. The expected propenal is difficult to quantitate as it tends to overlap with the solvent peak in the chiral GC analyses, but does appear to be in similar quantities to that of the acetic acid. Thus, the amount of acetic acid can be taken as a measure of the n:i ratio of aldehyde formation (very low).

Conversion = 100 - % of residual vinyl acetate.

4.3 DENDRIMER BASED DIPHOSPHINE UNITS (IMPERIAL)

The catalytic hydroformylation of 1-hexene was carried out using the dendrimer based diphosphine catalyst precursors (Figure 46) synthesised by members of the group of Dr. T. Welton (Imperial College, London). The dendrimer core is illustrated in Figure 47.

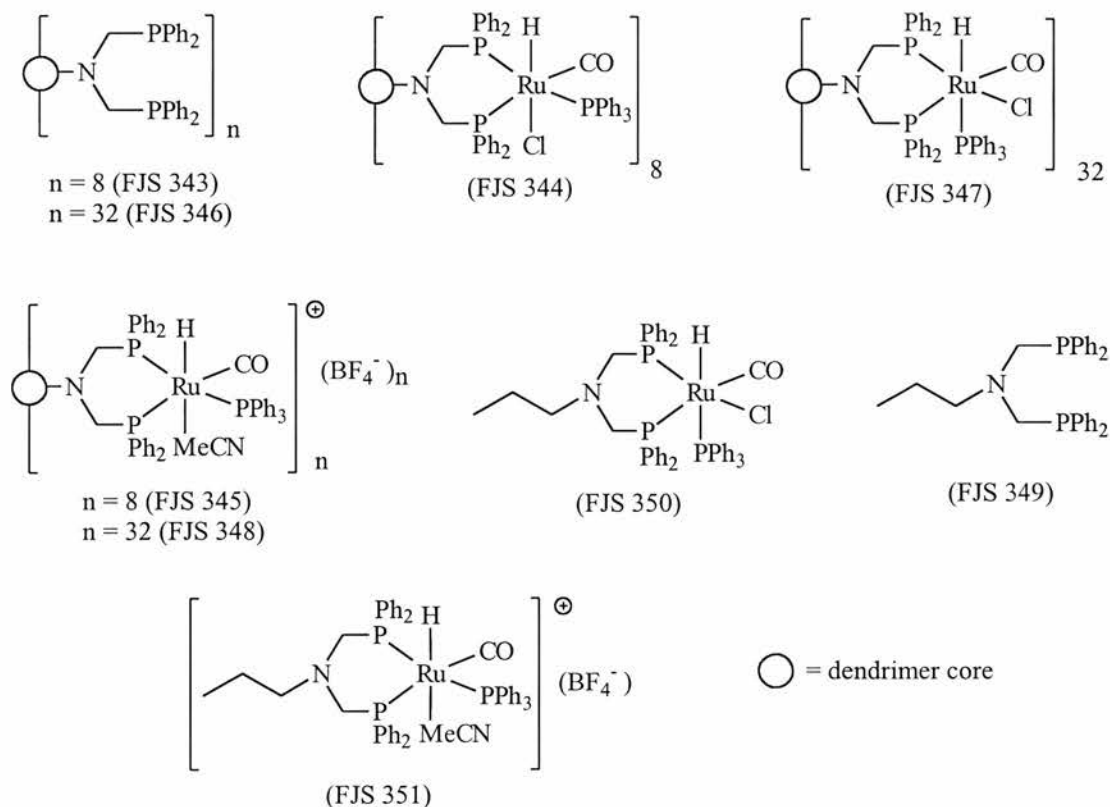


Figure 46: Catalyst precursors FJS 343 – FJS 351

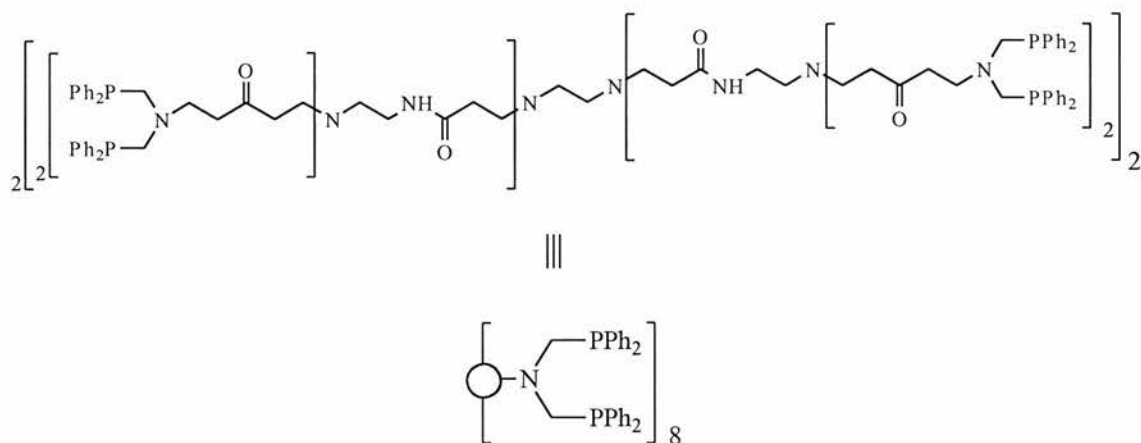


Figure 47: Dendrimer core for generation = 1 dendrimer ($n=8$). Generation =3 is not shown ($n = 32$)

The interest in these dendrimer compounds was focussed on their stability and on whether the steric constraints caused by the core, and/or the six membered ring which might give

bite angles close to 120° , would lead to high n/i ratios. Although the thrust of this type of research is towards longer chain alkene hydroformylation, hexene was used as the substrate as it is inexpensive and readily available.

All experiments are summarised in Table 8 and commentary on each reaction is included. After initial solvent test reactions, THF was deemed most suitable and was used for most experiments. The results for the preliminary reactions where alternative solvents were used were not significant and have not been included in the discussion.

The reactions were performed on the CATS kinetic rig fitted with a manual sampling tube. All samples were analysed using GC-MS.

RHODIUM COMPLEXES

The complexes were prepared *in situ* from $[\text{Rh}(\text{CO})_2(\text{acac})]$ and the diphosphine ligands. A Rh:(P₂) ratio of 1:1 was used in all cases. Generally, short induction periods were seen for the dendrimer bound rhodium catalysts, increasing when larger dendrimers were used. Induction times are not expected with normal rhodium catalysed reactions and this was seen with the simple diphosphine ligand in experiment 12 (FJS 349). The short inactive periods early in the reactions can be attributed to the fact that coordination may be slow with the dendrimers. It is surprising that there is essentially zero activity for up to 10 minutes before the catalyst activates (see Figure 48). The reaction then proceeds with first order activity. The pseudo first order rate constants, obtained from exponential curve fits on the early part of the reactions kinetic data, decrease as the dendrimer size increases.

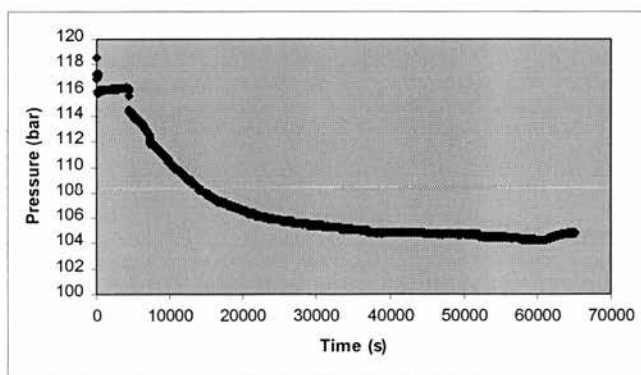


Figure 48: Kinetics Graph for Imperial Experiment 7.

Rates obtained from the kinetic data are all considerably lower than those obtained with simple monodentate phosphines (generally $> 10^{-3} \text{ s}^{-1}$ at 70°C). However, direct

comparisons with the normal standard, PPh_3 , are difficult as it gives zero order kinetics under the same reaction conditions as used here. The catalysts appear relatively stable, leading to full conversion of the substrate in time without changes in the general kinetic profile (Figure 48).

This smooth trend in the graph suggests that the catalyst is still active after the substrate has been exhausted. The slight rise in pressure seen at the end of the graph is due to there being no gas uptake whilst there is a slight ambient temperature increase around the ballast vessel at the end of the long run. Note that in some cases (experiments 2 and 3) there was some evidence of dendrimer-catalyst decomposition as a precipitate was visible at the end of the reaction.

The n/i ratios are low, which is surprising as the 6-membered ring formed by the coordinating metal complex should favour axial – equatorial coordination, which is important for high selectivities when using bidentate ligands.⁹³

RUTHENIUM COMPLEXES

The compounds were used as supplied for the hydroformylation of 1-hexene. There is a long induction period observed for all these reactions. This was first attributed to ligand decomposition of the dendrimer based complexes, but the simple diphosphine complexes (experiments 4 and 7) give long induction periods as well. Hence, the period of inactivity is thought to be due to the delay whilst the active species forms. In other studies using PPh_3 based ruthenium complexes, there is an induction period when starting with the $[\text{Ru}(\text{CO})_3(\text{PPh}_3)_2]$ complex, which has been attributed to the slow formation of the catalytic species, $[\text{RuH}_2(\text{CO})_2(\text{PPh}_3)_2]$.⁹⁴ The formation of the active species from the chloride based complexes is probably more difficult and the induction period is longer, particularly in the absence of added base. The product distributions from the related pairs of complexes (with either Cl^- or cationic) show that the catalyst precursors do not form the same species. This is deduced from the hydrogenation activity of the catalyst derived from the cationic complexes (experiments 7-9) and their superiority over the Cl^- derived precursors (experiments 4-6). However, the conversion of hexene is lower overall with the cationic based catalysts.

This activity is interesting, as there are few hydroformylation catalysts that will give alcohols as products under mild conditions. Other than the rhodium trialkylphosphine complexes mentioned in Section 2.4.2 that give alcohols when reacted in protic solvents,³¹ cobalt trialkylphosphine complexes also give alcohols albeit under forcing conditions.⁴ If the trinuclear complex $[\text{Ru}_3(\text{CO})_{12}]$ is reacted in the presence of trinaphthylphosphite it can also give significant quantities of C_7 alcohols from 1-hexene.⁹⁴ Mononuclear Ru complexes do not generally produce alcohols although they are often active for hydrogenation of aldehydes, especially if they have Cl^- present.^{94,95} In this case, the reaction is probably sequential, with the straight chain aldehyde being preferentially hydrogenated. This is common in sequential reactions,³¹ and is the reason the n/i ratio is high in the alcohol products but with overall $n/i < 3$ with the simple parent ligands giving the most selective reactions.

Once the induction period had passed, the activity of the ruthenium complexes are similar to that found for typical PPh_3 complexes. This is noteworthy as it is unusual because the $[\text{Ru}(\text{CO})_3(\text{Ph}_2\text{PCH}_2\text{CH}_2\text{PPh}_2)]$ complex has low activity,⁹⁴ even though the six membered rings would be expected to give more active catalysis. The runs using the dendrimer bound cations (experiments 8 and 9) are the only systems which do not show first order kinetics, but rather react at zero order. The actual values reported for the rate constants need to be treated with some caution as the reactions with ruthenium complexes lead to mixtures of aldehydes and alcohols (equivalent to 2 and 3 moles of gas uptake respectively). Hence, the rate constants expressed should be treated as correct only to the nearest order of magnitude. The catalyst derived from FJS350 (experiment 4, the Cl^- complex with the simple ligand) shows odd behaviour, suggesting that the active species is formed very slowly with a gradual concentration increase.

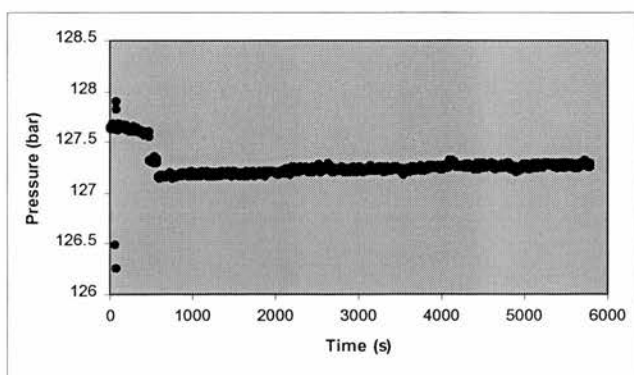


Figure 49: Graph of induction period for experiment 4.

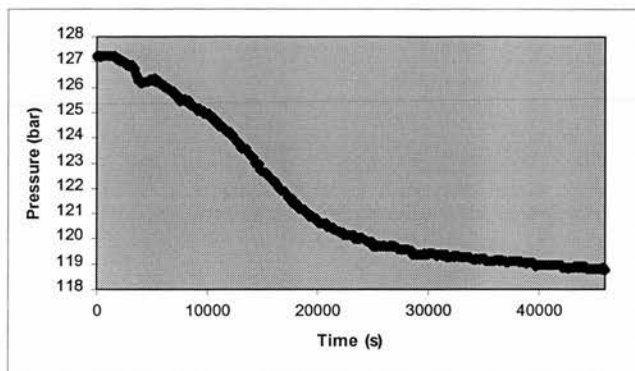


Figure 50: Graph of gas uptake for experiment 4 showing odd shape (note: induction period has been excluded).

This is the type of graph expected where there is an induction period forming a catalyst that follows first order kinetics in substrate. The sharp onset of activity in the other cases suggests some autocatalysis of the formation of the active species. Once started, all of the ruthenium becomes active very quickly.

The samples tested appear to show genuine dendrimer based catalysis. Although the rates and selectivities for the hydroformylation system are generally poor, there is potential for effective catalysis in other similar areas.

Table 8: Catalytic hydroformylation of 1-hexene using the catalyst precursors FJS 343 – FJS 351.



No.	CATALYST SYSTEM	CONDITIONS	t / hr	1-H / %	I-H / %	EtPa l / %	MeH al / %	Hal ol / %	MeH ol / %	Hol / %	al:ol	n:i al	n:i ol	Conv / %	REMARKS
1	Diphosphine / Rh (P ₂):Rh = 1:1 FJS 349	5x10 ⁻⁵ mol Rh THF 80°C 20 bar CO/H ₂	1	85.3	0.5	t	6.6	7.6	t	t	-	1.2	-	14.7	Good quality graph with no induction period and first order kinetics, k=2.7x10 ⁻⁴ s ⁻¹ . Gas uptake was continuing at steady rate when reaction stopped at 2hr and 55% conversion, strongly suggests the catalyst was still active.
			2	45.2	1.7	t	24.4	28.6	t	t	-	1.2	-	54.8	
2	(P-P)8 / Rh (P ₂):Rh = 1:1 FJS 343	As expt 1	2	59.4	4.9	t	11.5	24.2	t	t	-	2.1	-	40.6	Good quality graph with an induction period of several minutes, followed by first order kinetics, k=1.2x10 ⁻⁴ s ⁻¹ . Gas uptake had essentially ceased after 15 hr of 20 hr run. Suggests the catalyst was still active after virtually 100% conversion reached.
			20	0.2	4.8	0.9	30.6	63.3	t	0.2	>500	2.0	-	99.8	
3	(P-P)32 / Rh (P ₂):Rh = 1:1 FJS 346	As expt 1	1	No data collected										-	Good quality graph with an induction period of several minutes, followed by first order kinetics with k=6.4x10 ⁻⁵ s ⁻¹ . Gas uptake had essentially ceased after 14 hr of 20 hr run. Suggests the catalyst was still active after virtually 100% conversion reached.
			16	2.8	6.5	1.0	28.4	61.1	t	0.2	>450	2.1	-	97.2	
4	Ru(Cl) FJS 350	4x10 ⁻⁵ mol Ru THF 120°C 100 bar CO/H ₂	2	96.6	0.5	t	0.7	2.1	t	0.1	28	3.0	-	3.4	Graph has odd shape with an induction period of ca. ½ hr followed by first order kinetics with k=1.6x10 ⁻⁴ s ⁻¹ (over the period 15000 to 25000s). Gas uptake continuing at slow steady rate when reaction stopped at 20hr and 91% conversion, strongly suggests the catalyst was still active.
			20	8.6	3.4	0.7	27.6	57.0	0.6	2.1	32	2.0	3.5	91.4	
5	Ru(Cl) FJS 344	As expt 4	2	73.7	3.5	t	6.4	15.8	0.1	0.4	44	2.5	4.0	26.3	Good quality graph of gas uptake with an induction period of ca. 1/2 hr, followed by first order kinetics, k=9.8x10 ⁻⁵ s ⁻¹ (over the period 8000 to 25000s). Gas uptake essentially ceased after 8 hr of 20 hr run, suggesting the catalyst was still active after virtually 100% conversion.
			20	4.1	3.5	1.2	24.9	50.9	2.3	13.2	5	2.0	5.7	95.9	

Table 8: Continued

No.	CATALYST SYSTEM	CONDITIONS	t / hr	1-H / %	I-H / %	EtPal / %	MeHal / %	Hal / %	MeHol / %	Hal / %	al:ol	n:al	n:ol	Conv / %	REMARKS
6	Ru(Cl) FJS 347	As expt 4	2	87.4	1.8	t	2.8	7.2	0.1	0.6	14	2.6	6.0	12.6	Poor graph with an induction period of ca. 1&1/2 hr followed by first order kinetics, $k=7.3 \times 10^{-4} \text{ s}^{-1}$. The gas uptake had essentially ceased after 7 hr of 20 hr run with only 32% conversion at the end of the run (20 hr). This strongly suggests catalyst deactivation during run.
			20	68.3	5.3	0.1	7.1	16.7	0.4	2.2	9	2.3	5.5	31.7	
7	Ru(cation) FJS 351	4×10^{-5} mol Ru THF 120°C 100 bar CO/H ₂	2	93.5	1.1	t	1.3	2.7	0.2	1.2	2.9	2.1	6.0	6.5	Good quality graph with an induction period of ca. 1 hr followed by first order kinetics, $k=1.2 \times 10^{-4} \text{ s}^{-1}$ (over the period 10000 to 20000s). Gas uptake continuing at steady rate when reaction stopped at 20hr and 82% conversion, strongly suggests the catalyst was still active.
			20	18.5	5.7	0.1	5.4	2.4	14.8	53.1	0.1	0.4	3.6	81.5	
8	Ru(cation) FJS 345	As expt 7	2	91.3	3.1	t	1.5	3.4	0.1	0.6	7.0	2.3	6.0	8.7	Good quality graph with an induction period of ca. 1 hr, followed by zero order kinetics, $k=2.2 \times 10^{-5} \text{ mol dm}^{-3} \text{ s}^{-1}$. Gas uptake continuing at steady rate when reaction stopped at 20hr and 69% conversion, strongly suggests the catalyst was still active.
			20	31.1	9.4	0.2	14.8	27.0	2.6	14.9	2.5	1.8	5.7	68.9	
9	Ru(cation) FJS 348	As expt 7	2	< 0.5% conversion in total										Good quality graph with an induction period of ca. >2 hr, followed by zero order kinetics, $k=2.3 \times 10^{-5} \text{ mol dm}^{-3} \text{ s}^{-1}$. Gas uptake continuing at steady rate when reaction stopped at 20hr and 76% conversion, strongly suggests the catalyst was still active.	
			20	24.4	11.6	0.2	17.2	44.9	0.2	1.5	37	2.6	7.5		75.6

1-H = 1-Hexene; I-H = Isomerised Hexenes; EtPal = 2-Ethylpentanal; MeHal = 2-Methylhexanal; Hal = n-Heptanal; MeHol = 2-Methylhexanol & Hol = n-Heptanol.
t = trace (generally <0.03%); Conversion = 100 - % of residual 1-Hexene (i.e. isomerised hexenes are regarded as products).

4.4 ASYMMETRIC HYDROFORMYLATION (WARWICK)

The ESPHOS diphosphine and SEMI-ESPHOS monodentate phosphine (Figure 51) were tested under a variety of conditions to ascertain their ability for asymmetric hydroformylation of vinyl acetate and styrene, and were supplied by the research group of Dr. M. Wills (University of Warwick). The results are summarised and individually commented on in Tables 7 to 12.

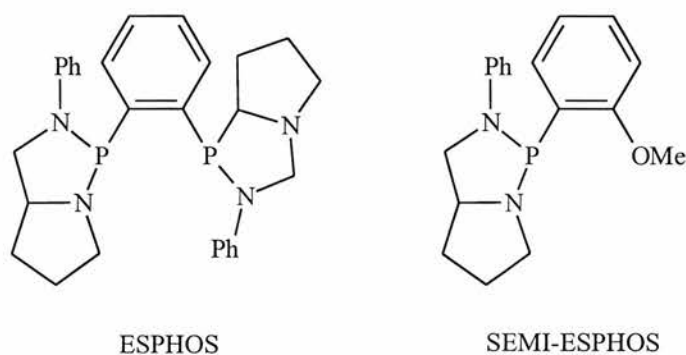


Figure 51: Structures of the ESPHOS and SEMI-ESPHOS ligands

Standard experimental techniques were used for the catalytic reactions. Samples were taken during the reactions using a device that allowed manual sample extraction via a tube immersed in the reaction mixture and fitted with a needle valve. The liquid products were analysed by GC-FID (quantitative) and GC-MS (qualitative) using a chiral capillary column. This was used so that the extent to which asymmetric synthesis had been achieved could be monitored. All peaks were verified by comparison to authentic samples which had either been purchased or synthesised.

At low pressure (8 or 10 bar) gas diffusion into the liquid phase can become rate determining. In the tables which follow, every experiment troubled by this phenomenon has a note describing the extent to which it is affected. It is particularly valuable to note the comparative experiments using PPh_3 for styrene hydroformylation in Table 14. When this mass transfer limitation occurs, the kinetics can give an erroneous zero order dependence on substrate concentration. The product distribution can also be misleading (see Table 14) since it changes when the reactant solution is 'starved' of CO during the reaction. The first step is the coordination of styrene followed by rhodium hydrogen transfer, yielding the straight and branched Rh-alkyl species. An equilibrium is established between these two products due to the reversibility of the hydrogen transfer.

(Figure 52). Carbon monoxide now acts as a ‘trapping agent’ to form a Rh-CO-alkyl species with both the straight and branched chain species. Oxidative addition of hydrogen followed by reductive elimination leads to the products (2- and 3-phenylpropanal) are formed after elimination. If the CO trapping rate is faster (or similar to) that of the hydrogen transfer, then increasing the concentration of carbon monoxide in solution will prefer trapping the kinetically favoured Rh-alkyl species. This would lead to more branched products. Conversely, if the solution was starved of carbon monoxide the production of straight chained product is encouraged (e.g. Experiment 21, Table 14). Therefore, due to diffusion limitations, the low pressure reactions reported later in this section appear to give a misleading zero order substrate concentration dependence and may reduce the selectivity to the derived branched chain (kinetic) product.

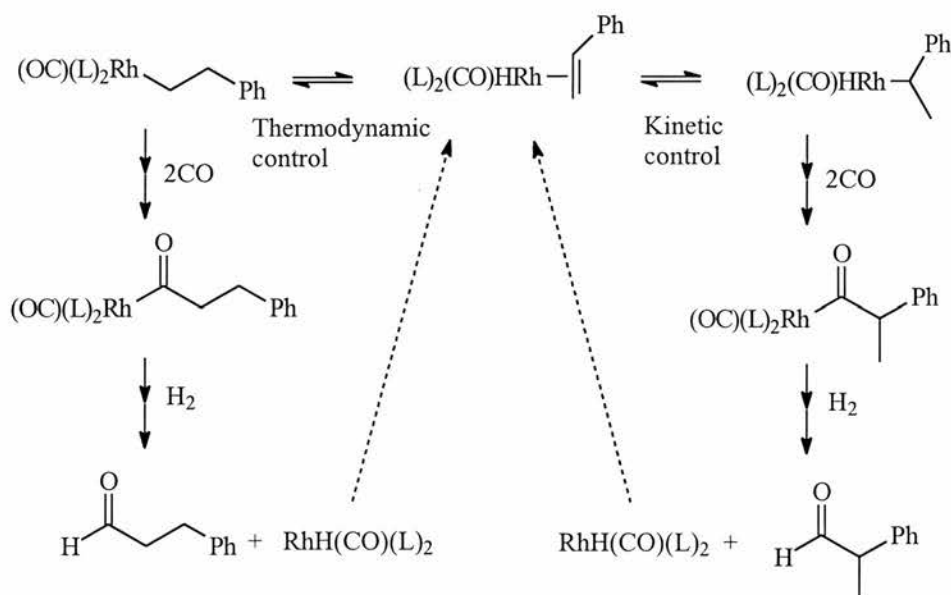


Figure 52: Scheme illustrating the formation of straight and branched Rh-Alkyl species.

VINYL ACETATE

Optically active aldehydes are very important precursors in biologically active compounds as well as new materials (e.g. biodegradable polymers and liquid crystals). The ESPHOS ligand has shown great potential for the asymmetric hydroformylation of vinyl acetate. The chiral branched aldehyde, 2-acetoxypropanal, is a precursor for the Strecker synthesis of the α -amino acid threonine (Figure 53).⁹⁶ The ratio of branched to straight chain aldehydes as well as the enantiomeric excesses resulting from using ESPHOS are similar to the best results found in the literature for BINAPHOS and BIHEMPOHOS.⁹⁷ The fact

that ESPHOS yields virtually racemic products after hydroformylation of styrene is surprising as other ligands such as BINAPHOS and BIHEMPHOS give large inductions when hydroformylating styrene and vinyl acetate. However, asymmetric induction is usually higher in heterofunctionalised alkenes such as vinyl acetate. This is presumably due to the additional binding of the C=O bond of the substrate to the catalyst. SEMI-ESPHOS did not produce a very effective hydroformylation catalyst even under forcing conditions.

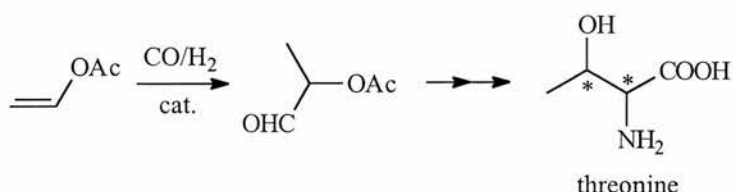


Figure 53: Vinyl acetate used as a building block for the synthesis of the α -amino acid threonine.

The major isomer produced when 2-acetoxypropanal is catalysed by the ESPHOS hydroformylation process is the S-(-) enantiomer. In contrast, the slight enantiomeric excess observed in one of the SEMI-ESPHOS catalytic processes is the R-enantiomer (experiment 11, Table 10). The 2-acetoxy-1-propanol (2Ac1ol) is produced by sequential hydroformylation of vinyl acetate to 2-acetoxypropanal (2Acal) followed by hydrogenation (Figure 54). This is illustrated by the fall of the 2Acal / total alcohol ratio over time in experiment 2, Table 9. The 1-acetoxy-2-propanol (1Ac2ol) is created when the primary product (2Ac1ol) is isomerised, deduced from the drop in the 2Ac1ol / 1Ac2ol ratio over time in the same experiment.

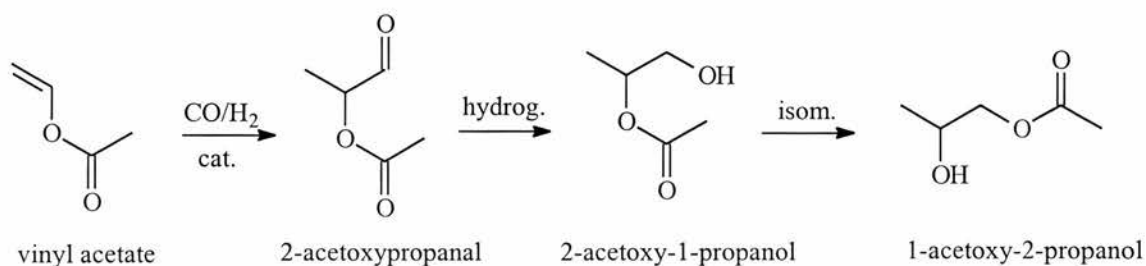


Figure 54: Production of 2Ac1ol and 1Ac2ol from vinyl acetate under hydroformylation conditions.

When the product samples were re-analysed after two months, the 2Ac1ol / 1Ac2ol ratio had fallen considerably relative to the results obtained from fresh products. This ratio presumably equilibrates to a steady ratio in time. Due to the fact that hydrogenation of the aldehyde does not affect the chiral centre, it is certain that the major enantiomer in the 2-

acetoxypropanol hydroformylation (and subsequent hydrogenation) is the S-product. However, various mechanisms can be suggested for the isomerisation of the 2-acetoxy-1-propanol into 1-acetoxy-2-propanol. Some invert the chiral centre and some do not. Hence, we cannot be certain which is the major enantiomer, but there are simple methods available which could be used to deduce it. This can be illustrated by the hydrolysis of a product mixture of large amounts of both 1-acetoxy-2-propanol and 2-acetoxy-1-propanol giving 1,2-propanediol (Figure 55). If both the acetoxypropanols are rich in the S enantiomer then (S)-1,2-propanediol will be the major product. However, if the 1-acetoxy-2-propanol has been formed through a process involving inversion of the chiral centre then both the R and S enantiomers will be produced in large amounts.

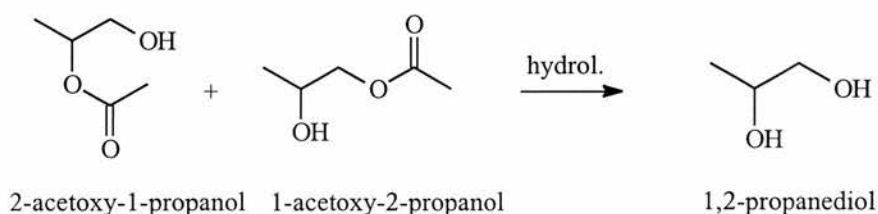


Figure 55: Hydrolysis of 1-acetoxy-2-propanol and 2-acetoxy-1-propanol to give 1,2-propanediol.

Acetic acid arises from the thermal decomposition of the expected linear aldehyde (3-acetoxypropanal) into propenal (acrolein) and acetic acid (Figure 56). This has been seen during these experiments at relatively low temperatures. Propenal is difficult to analyse quantitatively as it hydrogenates to propanal, which overlaps the solvent peak in the chiral GC analysis. It does, however, appear to be present in similar quantities to acetic acid. Hence, the amount of acetic acid can be a measure of the i:n ratio of aldehyde formation.

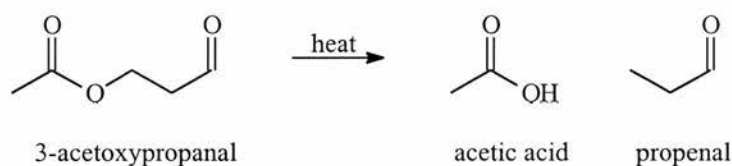


Figure 56: Thermal decomposition of 3-acetoxypropanal.

Experiment 6 is an example of the results obtained after the ideal experimental technique had been determined. Vinyl acetate was catalytically hydroformylated, resulting in 99% conversion with 90% yield of the branched aldehyde and 89% ee of the S enantiomer. These results along with the i:n ratio are competitive with effective catalysts already reported in the literature.

The formation of some alcohol is probably due to the presence of acetic acid in solution. It would be beneficial to follow up this work by performing the direct hydrogenation of the chiral branched aldehyde to chiral alcohol *in-situ*. This could be done by cooling and venting the autoclave after the hydroformylation, re-pressurising with hydrogen and performing the hydrogenation.

STYRENE

Asymmetric hydroformylation of vinyl aromatics lends itself (after aldehyde oxidation) to the synthesis of a number of optically active non-steroidal anti-inflammatory agents and 2-arylpropionic acids such as Naproxen and Ibuprofen (Figure 57).⁹⁸

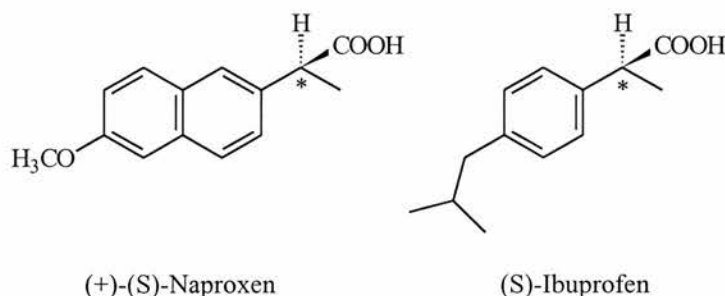


Figure 57: Structures of Naproxen and Ibuprofen

Styrene hydroformylation is a useful general model for this class of compounds. The results obtained (tables 10 and 11 with ESPHOS and SEMI-ESPHOS do not show particularly strong evidence for the effective asymmetric induction to the branched aldehyde product (2-phenylpropanal). Both ligand systems give the same initial rate, contrasting the results reported for vinyl acetate. The fact that ESPHOS produces a virtually racemic product from styrene was surprising when compared to the large inductions obtained using BINAPHOS and BIHEMPHOS from hydroformylation of both substrates. This deserves more attention in future work with this class of ligand.

The two ligands tested in these studies show very different activities. The SEMI-ESPHOS ligand, whilst not totally ineffective does not show potential for future applications. ESPHOS, on the other hand, has demonstrated great potential for asymmetric hydroformylation catalysis and deserves further attention. It is a stable ligand that deserves further tests on asymmetric hydrogenations as well as hydroformylations.

Table 9: Asymmetric hydroformylation of vinyl acetate using ESPHOS.

Conditions: ESPHOS dimer + Rh(CO)₂(acac), (P₂):Rh = 1.5:1, Vinyl acetate:Rh = 214:1, 5x10⁻⁵ mol Rh, Tol (4mL), Vinyl acetate (1mL), Stirrer rate ca. 500 rpm

No.	CATALYST SYSTEM	t / hr	VA / %	AA / %	2Acal / %	2Ac1ol / %	1Ac2ol / %	AcA / %	Conv. / %	al i:n	2Acal/ tot. ol	2Ac1ol/ 1Ac2ol	REMARKS
1	80°C & 40 bar CO/H ₂	2	0	5.7	41.0 75%ee	40.0 85%ee	13.1 81%ee	0.3	100	94:6	0.77	3.0	No induction period. Kinetics of gas uptake suggest the hydroformylation was zero order in substrate conc. with a rate throughout most of the reaction = 2.2 x 10 ⁻³ mol dm ⁻³ s ⁻¹ . The subsequent hydrogenation of the aldehyde to 2Ac1ol being an order of magnitude slower with a zero order rate = 1.6 x 10 ⁻⁴ mol dm ⁻³ s ⁻¹ . Gas uptake (hydrogenation) still proceeding at this rate when reaction halted at 3 hrs.
		3	0	5.9	34.9 76%ee	43.0 84%ee	15.8 82%ee	0.3	100	94:6	0.59	2.7	
2	80°C & 40 bar CO/H ₂	0.5	39.1	5.7	54.5 82%ee	0.3	t	0.3	60.9	91:9	182	-	In contrast to expt 1, this reaction had an induction period of ca. 15 min. (during which reaction was occurring at an increasing rate). Kinetics of gas uptake suggest that the hydroformylation was zero order in substrate conc. with a rate throughout most of the reaction = 8.1 x 10 ⁻⁴ mol dm ⁻³ s ⁻¹ . The hydrogenation step again being an order of magnitude slower with a zero order rate = 8.0 x 10 ⁻⁵ mol dm ⁻³ s ⁻¹ . Gas uptake (hydrogenation) still proceeding at this rate when reaction halted at 3 hrs. These rates should be treated with suspicion as they are not consistent with the rates from the identical reactions of expts 1 & 3, and, given the unexpected induction period for this expt suggest some discrepancy in the way the autoclave was loaded. The autoclave loading procedures was revised due to irregular results from this expt. Results clearly demonstrate the stepwise nature of the reaction i.e. hydroformylation followed by hydrogenation of the branched aldehyde to 2Ac1ol (with subsequent isomerisation to 1Ac2ol).
		1.0	19.5	6.0	73.5 81%ee	0.6	t	0.5	80.5	93:7	123	-	
		1.5	5.1	6.5	85.3 82%ee	2.5	0.2	0.5	94.9	93:7	32	12.5	
		2.0	0.3	5.8	82.0 80%ee	10.4 84%ee	1.2	0.5	99.7	94:6	7.0	8.7	
		2.5	0.3	8.2	75.3 78%ee	13.4 87%ee	2.2	0.6	99.7	92:8	4.8	6.1	
3	80°C & 40 bar CO/H ₂	3.0	0	8.0	66.0 75%ee	19.6 83%ee	5.8 81%ee	0.6	100	92:8	2.6	3.4	No induction period. Kinetics of gas uptake suggest the hydroformylation was zero order in substrate conc. with a rate throughout most of the reaction = 3.4 x 10 ⁻³ mol dm ⁻³ s ⁻¹ . The subsequent hydrogenation step being an order of magnitude slower with a zero order rate dependence on substrate conc. = 3.1 x 10 ⁻⁴ mol dm ⁻³ s ⁻¹ . Gas uptake (hydrogenation) still proceeding at this rate when reaction halted at 3 hrs. The rates from this expt are fairly consistent with expt 1 and should be treated as the most accurate as the loading of the autoclave and experimental set up was improved upon relative to earlier experiments.
		1.5	1.5	7.0	37.0 84%ee	44.3 88%ee	10.2 84%ee	0.1	98.5	93:7	0.67	4.3	

VA = vinyl acetate; AA = acetic acid; 2Acal = 2-acetoxypropanal; 2Ac1ol = 2-acetoxy-1-propanol; 1Ac2ol = 1-acetoxy-2-propanol & AcA = acetoxyacetone. al i:n = ratio of branched to linear aldehyde formation and is calculated as (2Acal + 2Ac1ol + 1Ac2ol) : AA. Conversion = 100 - % of residual vinyl acetate. The S(-) enantiomer (authentic product prepared *via* organic synthesis) is the major enantiomer observed for the 2-acetoxypropanal product from ESPHOS catalysed hydroformylations. The slight ee excess observed in one of the SEMI-ESPHOS catalysed hydroformylations (expt 11 of Table 8) is the R enantiomer. The S enantiomer is also the major enantiomer observed for both the 2-acetoxy-1-propanol product (from ESPHOS catalysed hydroformylations with subsequent hydrogenation of aldehyde to alcohol) and for 1-acetoxy-2-propanol (formed by isomerisation of 2-acetoxy-1-propanol) - authentic syntheses from (S)-1,2-propanediol - organic transformations.

Table 9: Continued

No.	CATALYST SYSTEM	t / hr	VA / %	AA / %	2Acal / %	2Acal / %	2Ac1ol / %	1Ac2ol / %	AcA / %	Conv. %	al i:n	2Acal / tot. ol	2Ac1ol / 1Ac2ol	REMARKS	
4	60°C & 8 bar CO/H ₂	1	94.4	0	5.6 / 86% ^{eee}	0	0	0	0	5.6	-	-	-	Kinetics for the three hydroformylation experiments at 60°C are more consistent than those at 80°C. All three 60°C expts. & 8 bar CO/H ₂ had induction periods, with some time variation. There was a 50 min. induction period in which there was very little gas uptake, followed by rapid reaction. Hydroformylation was zero order in substrate conc. with rate throughout most of the reaction = 1.8 x 10 ⁻⁴ mol dm ⁻³ s ⁻¹ . Slow gas uptake (hydrogenation) still proceeding when reaction stopped at 7 hrs. Note: At low reactor pressures (expts using 8 or 10 bar) it was found with the present reactor stirrer that gas diffusion into liquid phase can be rate limiting. This leads to pseudo zero order rate dependence on substrate conc. (see notes in Table 14). However, the rates determined for vinyl acetate hydroformylation at 60°C & 8 bar CO/H ₂ at ca. 2 x 10 ⁻⁴ mol dm ⁻³ s ⁻¹ are an order of magnitude slower than the rate of styrene hydroformylation at 80°C & 10 bar CO/H ₂ (expt 21, Table 14) where gas diffusion into the liquid phase is rate limiting. Thus, it may be that the rate determined for vinyl acetate hydroformylation at 60°C & 8 bar CO/H ₂ is genuinely zero order with respect to substrate conc., but requires verification with improved gas-liquid mixing efficiency.	
		2	80.3	t	19.7 / 88% ^{eee}	0	0	0	0	19.7	-	-	-		
		3	49.8	2.6	47.4 / 88% ^{eee}	0.1	0	0.1	0	0.1	50.2	95:5	474		-
		5	24.1*	3.8	71.3 / 87% ^{eee}	0.5	t	0.2	t	0.2	75.9	95:5	143		-
		7	4.8	4.8	87.5 / 86% ^{eee}	2.5 / 87% ^{eee}	0.1	0.6	0.1	0.6	95.2	95:5	34		25
		4	38.4*	3.6	57.2 / 87% ^{eee}	0.9	0	0	0	0	61.6	94:6	64		-
		7	0.8	5.4	82.2 / 87% ^{eee}	10.5 / 88% ^{eee}	0.5	0.5	0.5	0.5	99.2	95:5	7.5		21
6	60°C & 8 bar CO/H ₂	5	1.1*	5.4	90.3 / 89% ^{eee}	3.3	t	t	t	98.9	95:5	27	-	25 min. induction period during which there was an increasing rate of gas uptake until reaching constant rate. Hydroformylation zero order in substrate conc. with a rate throughout most of the reaction of 2.1 x 10 ⁻⁴ mol dm ⁻³ s ⁻¹ (see note in expt 4). Slow gas uptake (hydrogenation) still proceeding when reaction halted at 5 hrs.	
		21	1.4	5.7	75.8 / 88% ^{eee}	16.0 / 89% ^{eee}	1.1	t	t	98.6	94:6	4.4	15		
7	50°C & 8 bar CO/H ₂	21	1.4	5.7	75.8 / 88% ^{eee}	16.0 / 89% ^{eee}	1.1	t	t	98.6	94:6	4.4	15	90 min. induction period during which there was a very slow increase in gas uptake until reaching constant rate. Hydroformylation zero order in substrate conc. with a rate throughout most of the reaction of 7.2 x 10 ⁻⁵ mol dm ⁻³ s ⁻¹ (see note in expt 5). Slow gas uptake (hydrogenation) still proceeding when reaction halted at 21 hrs. Ideally, the product mixture should have been sampled after ca. 10 hrs when there would presumably have been little alcohol product.	

* The inconsistency in % of unreacted vinyl acetate at 4 or 5 hrs reaction time, since all three reactions have near identical initial rates, is due to an inappropriate sampling technique (expts 4 & 5). The sampling tube dips into the reaction mixture and has liquid forced up to the top when the autoclave is pressurised. The vinyl acetate substrate in this liquid does not undergo hydroformylation, and if not flushed out before sampling, gives a spiked value for vinyl acetate concentration. In earlier expts, including expts 4 & 5, this effect was noted until these tables were drawn up.

Table 10: Asymmetric hydroformylation of vinyl acetate using SEMI-ESPHOS.

Conditions: SEMI-ESPHOS + Rh(CO)₂(acac); Vinyl acetate:Rh = 214:1; 5x10⁻⁵ mol Rh; Tol (4mL); Vinyl acetate (1mL); Stirrer rate ca. 500 rpm

No.	CATALYST SYSTEM	t / hr	VA / %	AA / %	2Acal / %	2Ac1ol / %	1Ac2ol / %	AcA / %	Conv. %	al i:n	2Acal/ tot. ol	2Ac1ol/ 1Ac2ol	REMARKS
8	Rh:P = 1:3 80°C & 40 bar CO/H ₂	8	95.8	3.1	1.1	-	-	-	4.2	-	-	-	Poor graph - no kinetic data.
9	Rh:P = 1:2 80°C & 40 bar CO/H ₂	20	89.8	7.7	2.5	-	-	-	10.2	-	-	-	Poor graph - no kinetic data.
10	Rh:P = 1:2 120°C & 40 bar CO/H ₂	6	95.5	2.7	1.9	-	-	-	5.5	-	-	-	Poor graph - no kinetics data.
11	Rh:P = 1:2 120°C & 100 bar CO/H ₂	6	78.2	6.0	14.7 <2%ee	0.2	0.3	0.5	21.8	71:29	29	-	Poor graph - no kinetic data. Solid deposit in dark solution is evidence for catalyst decomposition. Note: small chiral induction into branched aldehyde is opposite to ESPHOS.

Table 11: Hydroformylation of vinyl acetate using PPh₃ for comparison

Conditions: PPh₃ + Rh(CO)₂(acac); Vinyl acetate:Rh = 214:1; 5x10⁻⁵ mol Rh; Tol (4mL); Vinyl acetate (1mL); Stirrer rate ca. 500 rpm

No.	CATALYST SYSTEM	t / hr	VA / %	AA / %	2Acal / %	2Ac1ol / %	1Ac2ol / %	AcA / %	Conv. %	al i:n	2Acal/ tot. ol	2Ac1ol/ 1Ac2ol	REMARKS
12	P:Rh = 3:1 80°C & 40 bar CO/H ₂	4.5	0.3	18.5	73.6 0%ee	1.4	2.7	3.6	99.7	81:19	18	0.5	No induction period. Hydroformylation has a first order dependence on the substrate concentration, with the rate constant $k = 4.8 \times 10^{-3} \text{ s}^{-1}$, giving an initial rate of hydroformylation of $1.0 \times 10^{-2} \text{ mol dm}^{-3} \text{ s}^{-1}$. This is an important experiment as it demonstrates that at 40 bar, for reactions with initial rates $< 1.0 \times 10^{-2} \text{ mol dm}^{-3} \text{ s}^{-1}$, gas diffusion into the liquid phase is not rate determining with the present gas-liquid mixing capability of our constant pressure autoclave. Thus, the zero order rate dependence on substrate conc. found for vinyl acetate hydroformylation employing ESPHOS at 80°C & 40 bar CO/H ₂ (expts 1-3) appear genuine. The gas uptake essentially stopped after 30 mins. when the hydroformylation reaction was complete i.e. little tendency to hydrogenate aldehyde.

Table 12: Asymmetric hydroformylation of styrene using ESPHOS diphosphine.

Conditions: ESPHOS dimer + Rh(CO)₂(acac), (P₂):Rh = 1.5:1, Styrene:Rh = 170:1, 5x10⁻⁵ mol Rh, Tol (4mL), Styrene (1mL), Stirrer rate ca. 500 rpm

No.	CATALYST SYSTEM	t /hr	STY / %	ACET / %	2PhPa / %	3PhPa / %	2PhPo / %	3PhPo / %	Other / %	Conv. %	al i:n	REMARKS
13	80°C & 10 bar CO/H ₂	2	0.2	0.8	80.8 <2%ee	16.4	0.8%	0.3	0.7	99.8	83:1 7	Odd graph shape - apparent induction period (where reaction accelerates) of > 35 min., whereas reaction was complete within 65 min. Not reliable for rate data. Again, suspect result and probably due to an error in autoclave loading in early experiments.
14	80°C & 10 bar CO/H ₂	1.5	0.4	0.7	76.9 0%ee	22.0	0	0	0	99.6	78:2 2	More comprehensible shape to graph. Small induction period of 4 min. during which no reaction took place, followed by kinetics of with an apparent (see notes in Table 14) zero order dependence on substrate conc. and a rate = 1.0 x 10 ⁻³ mol dm ⁻³ s ⁻¹ over most of the reaction. Gas uptake virtually stopped after 45 min. suggests little tendency to hydrogenate aldehyde. The lack of minor products, compared to expt 13, probably due to improved autoclave loading technique.

STY = styrene; ACET = acetophenone; 2PhPal = 2-phenylpropanal; 3PhPal = 3-phenylpropanal; 2PhPol = 2-phenyl-1-propanol; 3PhPol = 3-phenyl-1-propanol.

Conversion = 100 - % of residual styrene. al i:n = ratio of branched to linear aldehyde formation and for those reactions where some of the aldehyde has been hydrogenated to alcohol is defined as (2PhPal + 2PhPol) : (3PhPal + 3PhPol).

Table 13: Asymmetric hydroformylation of styrene using SEMI-ESPHOS.

Conditions: SEMI-ESPHOS + Rh(CO)₂(acac); 5x10⁻⁵ mol Rh; Rh:P = 1:2, Styrene:Rh = 170:1, Tol (4mL), Styrene (1mL), Stirrer rate ca. 500 rpm (no.15-17) 1000 rpm (no. 18-20)

No.	CATALYST SYSTEM	t / hr	STY / %	ACET / %	2PhPal / %	3PhPal / %	2PhPol / %	3PhPol / %	Other / %	Conv %	al i:n	REMARKS
15	80°C & 10 bar CO/H ₂	2	8.7	2.6	51.6 <1%ee	33.4	0.4%	0.7	2.7	91.3	60:40	No induction period. Virtually no further gas uptake after 1 hr confirming catalyst deactivation - there remained a considerable amount of unreacted substrate (although no visible evidence for decomposition). The catalyst deactivation / decomposition has the visual effect on the gas uptake graph of suggesting reaction was first order with respect to substrate concentration. However, accounting for catalyst deactivation, the reaction could have zero or first order rate dependence on substrate conc. or, is gas diffusion limited (see remarks in Table 14). In either case the initial rate of hydroformylation = 1.2 x 10 ⁻³ mol dm ⁻³ s ⁻¹ .
16	80°C & 10 bar CO/H ₂	0.8	64.1	t	23.9 <2%ee	12.0	-	-	-	35.9	67:33	Similar to expt 15. No induction period. No significant gas uptake beyond 30 min with 2/3 of styrene unreacted - catalyst deactivated (very dark coloured solution but no solid deposit). Initial rate = 7.0 x 10 ⁻⁴ mol dm ⁻³ s ⁻¹ .
17	80°C & 10 bar CO/H ₂	3.5	18.0	t	52.4 0%ee	29.5	-	-	-	82.0	64:36	No induction period. Kinetics give better fit to first order dependence on substrate conc. (than expts 15 or 16) with a rate constant k = 5.4 x 10 ⁻⁴ s ⁻¹ , giving an initial rate of hydroformylation = 9.4 x 10 ⁻⁴ mol dm ⁻³ s ⁻¹ . However, 18% of styrene remained with no further significant gas uptake beyond 2.8 hr, confirming that catalyst had again deactivated (very dark coloured reaction solution but no solid deposit).
18*	60°C & 10 bar CO/H ₂	1.5	4.7	0.5	88.2 2.3%ee	6.6	-	-	-	95.3	93:7	Induction period of ca. 10 min. after which reaction accelerates. Initial rate = 9.2 x 10 ⁻⁴ mol dm ⁻³ s ⁻¹ . Reaction appears to be still proceeding at a very slow rate when expt stopped.
19*	30°C & 10 bar CO/H ₂	18	48.3	0.1	50.2 <2%ee	1.4	-	-	-	51.7	97:3	Induction period and initial rate not accurate due to slow nature of reaction and room temperature fluctuations (overnight run) affecting ballast vessel pressure readings. Reaction still proceeding when run halted.
20*	30°C & 40 bar CO/H ₂	18	39.3	0.1	59.0 <1%ee	1.6	-	-	-	60.7	97:3	

STY = styrene; ACET = acetophenone; 2PhPal = 2-phenylpropanal; 3PhPal = 3-phenylpropanal; 2PhPol = 2-phenyl-1-propanol; 3PhPol = 3-phenyl-1-propanol.
*NEW TWIN SCREW STIRRER (ca. 1000 rpm) used for experiments 18-20.

Conversion = 100 - % of residual styrene. al i:n = ratio of branched to linear aldehyde formation and for those reactions where some of the aldehyde has been hydrogenated to alcohol is defined as (2PhPal + 2PhPol) : (3PhPal + 3PhPol).

Table 14: Hydroformylation of styrene using PPh₃ for comparison.

Conditions: PPh₃ + Rh(CO)₂(acac), P:Rh = 3:1, Styrene:Rh = 170:1, 5x10⁻⁵ mol Rh, Tol = 4mL, Vinyl acetate = 1mL

No.	CATALYST SYSTEM	t / hr	STY / %	ACET / %	2PhPal / %	3PhPal / %	Conv. %	al i:n	REMARKS
21	80°C & 10 bar CO/H ₂ Stirrer ca. 500 rpm	1	0.8	0.2	54.5 0%ee	44.6	99.2	55:45	No induction period followed by apparent zero order dependence on substrate conc. with a rate = 1.9 x 10 ⁻³ mol dm ⁻³ s ⁻¹ over most of the reaction. Hydroformylation complete within 29 min. However, changing the stirrer speed in (expt 22 & 23) causes the rate to change. In conclusion, the low pressures (8 and 10 bar) for styrene and vinyl acetate hydroformylation, gas diffusion into the liquid phase can be rate determining. The present gas-liquid mixing ability of the kinetics rig is unable to overcome diffusion control at low reactor pressures.
22	80°C & 10 bar CO/H ₂ Stirrer ca. 1000 rpm	0.75	1.4	0.2	72.9 0%ee	25.5	98.6	74:26	No induction period. Rate over most of the reaction ca. double the previous expt of 3.7 x 10 ⁻³ mol dm ⁻³ s ⁻¹ (ca. twice the stirring speed), with the hydroformylation complete within 15 min. Confirming the rate limited by gas diffusion into the liquid phase. Note: the diffusion control rate limited catalytic process can have a dramatic effect on product distribution, in this case the ratio of branched to straight chain aldehyde.
23	80°C & 10 bar CO/H ₂ Stirrer. ca. 500 rpm (for ca. 50% of conv.) Stirrer ca. 1000 rpm (for ca. 50% of conv.)	0.4	0.7	0.2	62.4 0%ee	36.7	99.3	63:37	No induction period. Rate 1 while stirring at ca. 500 rpm = 2.6 x 10 ⁻³ mol dm ⁻³ s ⁻¹ while rate 2 on increasing stirrer rate to ca. 1000 rpm = 4.6 x 10 ⁻³ mol dm ⁻³ s ⁻¹ i.e. ca. doubling in rate. The time taken to complete the hydroformylation falling between that taken in expts 22 and 23, at 18 min. Note: the i:n ratio of the aldehyde falls between those for expts 21 and 22.

Table 14: Continued.

Note: the following experiments use the twin screw stirrer.

No.	CATALYST SYSTEM	t / hr	STY / %	ACET / %	2PhPal / %	3PhPal / %	Conv %	al i:n	REMARKS
24	Stirrer rate <i>ca.</i> 500 rpm (for <i>ca.</i> 50% of conversion) Stirrer rate <i>ca.</i> 1000 rpm (for <i>ca.</i> 50% of conversion)	0.5	0.8	0.2	73.8 0%ee	25.3	99.2	75:25	No induction period followed by: Initial rate = $3.9 \times 10^{-3} \text{ mol dm}^{-3} \text{ s}^{-1}$ (500 rpm). Initial rate = $6.1 \times 10^{-3} \text{ mol dm}^{-3} \text{ s}^{-1}$ (1000 rpm).
25	Stirrer rate <i>ca.</i> 1000 rpm	0.5	0.6	0.2	81.3 0%ee	17.9	99.4	82:18	No induction period followed by: Initial rate = $7.3 \times 10^{-3} \text{ mol dm}^{-3} \text{ s}^{-1}$ (1000 rpm).
26	Stirrer rate <i>ca.</i> 1000 rpm	0.5	0.6	0.2	82.9 0%ee	16.4	99.4	83:17	No induction period followed by: Initial rate = $5.1 \times 10^{-3} \text{ mol dm}^{-3} \text{ s}^{-1}$ (1000 rpm).

STY = styrene; ACET = acetophenone. 2PhPal = 2-phenylpropanal; 3PhPal = 3-phenylpropanal; 3PhPol = 2-phenyl-1-propanol; 2PhPol = 3-phenyl-1-propanol; 3PhPol = 3-phenyl-1-propanol. Conversion = 100 - % of residual styrene. al i:n = ratio of branched to linear aldehyde formation and for those reactions where some of the aldehyde has been hydrogenated to alcohol is defined as (2PhPal + 2PhPol) : (3PhPal + 3PhPol).

4.5 OTHER REACTIONS

This section briefly describes some of the other experiments carried out on different systems. These are a break with the traditional hydroformylation reactions performed, but are examples of the different types of systems that are able to be tested. All the compounds studied in this section are sourced from researchers working at the University of St. Andrews School of Chemistry.

4.5.1 PALLADIUM CATALYSED COPOLYMERISATION

The bidentate phosphine ligands used to catalyse the alternating copolymerisation of ethylene and CO in this section were supplied by the research group of Professor J. D. Woolins. Table 15 lists the ligands tested and summarises the results obtained.

Shell research initially developed cationic palladium-tertiary phosphine complexes, containing weakly coordinating anions, to catalyse the alkoxy-carbonylation of ethene to methyl propanoate in methanol.⁹⁹ A surprising change in selectivity was seen when PPh₃ ligands were replaced by *cis*-chelating bidentate phosphines and the reaction done under the same conditions. No methyl propionate was formed, instead high molecular weight, alternating (CO/ethylene), polyketone was formed (Figure 58). The rates were very high (*ca.* 6000 g L⁻¹ hr⁻¹) and the reaction was performed under economical, mild conditions (85°C, 45 bar). One of the ligands was 1,3-bis(diphenylphosphino)propane (dppp) which forms a palladium catalyst which can produce TOF of over 10⁶.

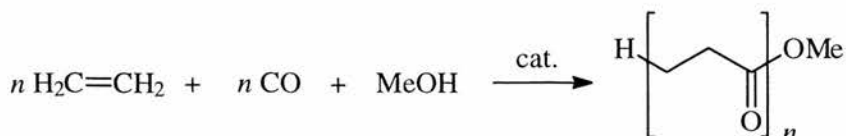


Figure 58: Copolymerisation of ethene and CO in methanol.

Variation of the bidentate ligand leads to changes in both the reaction rate and molecular weight of the products. The counteranions also have an effect on rates with the weakly or non-coordinating (e.g. OTs⁻) examples being the most active. Protic solvents, such as lower alcohols, yield the best results but some aprotic solvents are also useful.

Although the copolymer end-group analysis by ¹³C-NMR generally shows the presence of 50% ester (-COOMe) and 50% ketone (-COCH₂CH₃) groups suggesting keto-ester

formation, some products, when analysed by GC-MS show the presence of diester and diketone products as well (Figure 59).^{99d}

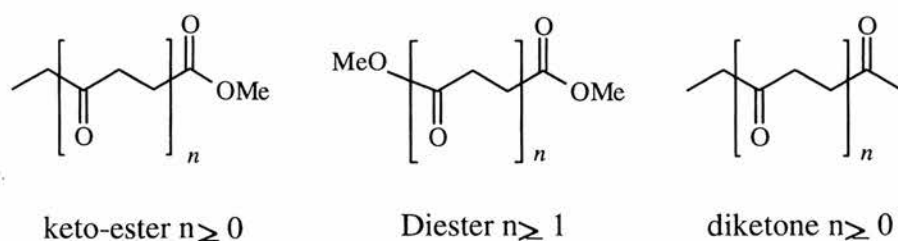


Figure 59: End groups of the copolymerisation products.

At low temperatures ($< \sim 85^\circ\text{C}$) the majority of the products are keto-esters. At higher temperatures the products are present in a keto-ester:diester:diketone ratio of around 2:1:1.

All reactions for this study were carried out in 250 mL batch autoclaves fitted with a glass liner and magnetic stirrer. The catalysts were prepared *in-situ* from $\text{Pd}(\text{OAc})_2$, the diphosphine and *p*-toluenesulphonic acid. The CATS kinetic rig was not used due to the nature of the reaction.

Experiment 1 (Table 15), was done to provide a reference reaction. All other reactions had such small amounts of solid present (in $\mu\text{g} - \text{mg} / \text{mL}$) that it was difficult to measure the yields quantitatively. Although no polymer was visible in these subsequent experiments there were low levels of oligomers ($n = 0-2$). The results, whilst not outwardly encouraging do have some interesting aspects. The results from experiments 6-8 (the piperazine backboned ligand) show that the diester oligomers are formed in preference to the normally favoured keto-esters (diester:keto-ester ratio of up to 20:1).

Metallic residues, as well as varying amounts of $\text{Ph}_2\text{P}(\text{O})\text{OMe}$ and other unidentified decomposition products, were visible in the glass liners after all the experiments. It can thus be deduced that the ligands are unstable in methanol and undergo some kind of methanolysis of the P-N bond. Temperature reduction (85 to 65°C) did not affect ligand stability (experiment 8).

The ligands did not form successful catalysts under these conditions. However, further tests may be useful, especially for the piperazine backboned ligand. These tests should be carried out in aprotic solvents to avoid ligand decomposition.

Table 15: Copolymerisation of ethylene and CO using diphosphine ligands.

Conditions: Pd(OAc)₂ (5.0x10⁻⁵mol) (5x10⁻³ mol L⁻¹), (P-P) (5.0x10⁻⁵mol), *p*-toluenesulphonic acid (11x10⁻⁵ mol), MeOH (10 mL), 45 bar CO/C₂H₄ (1:1), 85°C, 17 hrs.

No.	Ligand	n = 0		n = 1		n = 2		Comments		
		Me-propionate	Diethylketone	Keto-ester	Diester	Diketone	Keto-ester		Diester	Diketone
1 ^a		0.8	5.7	8.4	2.4	2.3	1.7	0.6	.04	Reaction product a solid mass of polymer (6.8g)
2		3.8	0.6	6.3	0.5	0.1	0.6	0.3	-	Dark coloured solid residue (0.2g). Traces of Ph ₂ P(O)OMe plus other ligand decomposition products detected in GC-MS
3		1.2	0.2	1.2	2.3	-	-	0.6	-	Dark coloured solid residue. Traces of Ph ₂ P(O)OMe plus other ligand decomposition products detected in GC-MS
4		0.2	0.3	-	-	-	-	-	-	Dark coloured solid residue. Traces of Ph ₂ P(O)OMe detected in GC-MS
5		2.7	-	2.1	0.5	-	-	-	-	Dark coloured solid residue. Traces of Ph ₂ P(O)OMe and large amounts of Ph ₂ P(S)OMe or Ph ₂ P(O)SMe detected in GC-MS
6		0.1	-	0.1	2.2	-	-	0.6	-	Dark coloured solid residue. Large amounts of Ph ₂ P(O)OMe detected in GC-MS
7 ^a		0.2	-	0.3	5.5	-	-	1.1	-	Dark coloured solid residue. Large amounts of Ph ₂ P(O)OMe detected in GC-MS
8 ^b		trace	-	0.2	2.8	-	0.5	1.7	-	Dark coloured solid residue. Large amounts of Ph ₂ P(O)OMe detected in GC-MS

^a Concentration = 2.0 x10⁻³ mol L⁻¹, reaction time 5 hrs.

^b Concentration = 2.0 x10⁻³ mol L⁻¹, 50 mL MeOH, 65°C, 5 hrs.

Note: the units are relative amounts recorded by the GC-MS and are arbitrary.

4.5.2 COBALT BASED METHANOL CARBONYLATION CATALYSIS

The ability of $[\text{Cp}^*\text{Co}(\text{CO})_2]$ in the presence of PEt_3 and MeI to catalyse the carbonylation of methanol has been studied.¹⁰⁰ Some kinetics runs were carried out using the CATS service to provide supplementary results for previous work. Although this work was done in conjunction with a wide ranging study, only the results gleaned from the CATS runs are reported here.

Ethanoic acid is a bulk chemical of major importance in the polymer, paints and other industries. The dominant manufacturing process is currently the carbonylation of methanol in the presence of iodomethane.¹⁰¹ The first process of this kind used $[\text{Co}_2(\text{CO})_8]$ as the catalyst precursor, but the low activity and selectivity meant that forcing conditions (200°C , 600 bar) were needed and the selectivity to methanol was low.¹⁰²

The discovery that rhodium¹⁰³ and iridium¹⁰⁴ based catalysts operate more selectively under much milder conditions (180°C , 30 bar) led to them being favoured commercially. However, due to its much lower cost, there would be considerable interest in cobalt based systems that operate with high activity and selectivity under mild conditions. The system summarised in Figure 60 has shown potential as an effective catalyst (experiment 3 & 4, Table 16).

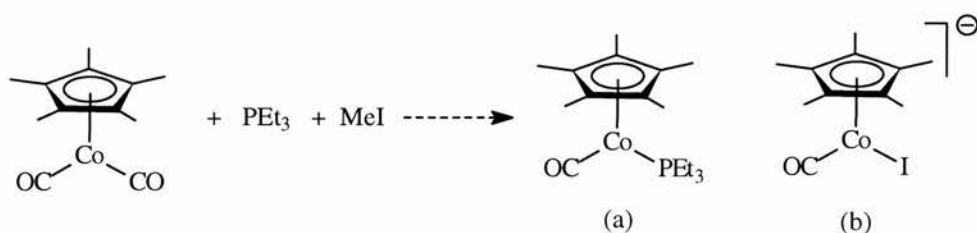


Figure 60: The catalyst precursors and active catalytic cobalt species (a & b).

$[\text{Cp}^*\text{Co}(\text{CO})_2]$ in methanol containing methyl iodide shows relatively low activity, but if 10 equivalents of PEt_3 are added, a dramatic increase in catalytic activity is seen. The reaction profile shows a very fast initial phase followed by a period of no activity and a further period where the activity is restored but to a level lower than the original phase. This effect is reproducible. When water is added a similar reaction profile is observed but the overall rates are higher.

A stock solution was made up and used for all the reactions. This was made up of acetic acid (64.0g), methyl acetate (15.0g) and water (7.0 g). The autoclave was loaded with 4 mL of the stock solution and the catalyst precursor. A MeI / stock solution mixture was injected into the reaction when the required conditions were reached and the kinetic data plotted. The reactions done are summarised in Table 16.

When PEt_3 and MeI were not used in the same reaction (experiments 1-3) no catalytic activity was observed. The reaction products in experiment one did, however yield dark brown crystals that were characterised as $[\text{Cp}^*\text{Co}(\text{CO})\text{I}_2]$ by X-ray crystal analysis.

The kinetic graph of experiment 4 shows two distinct areas of activity (Figure 61). The reaction profile shows a very fast initial phase followed by a period of inactivity and a further area where the activity is restored but to a lower level to that seen in the initial phase.

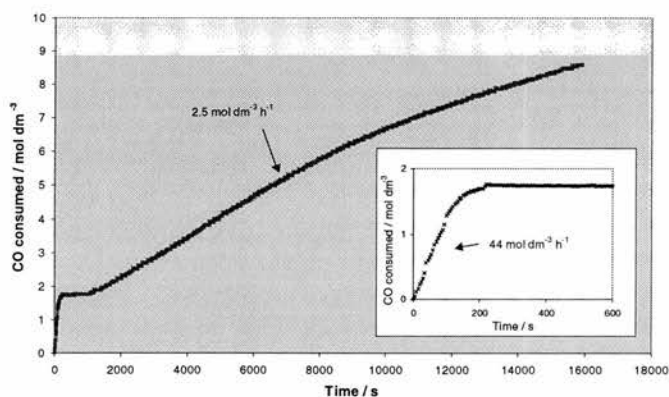


Figure 61: Kinetic graph of methanol carbonylation (experiment 4)

The build up of $[\text{Cp}^*\text{Co}(\text{CO})\text{I}_2]$ observed in the absence of catalytic activity in the earlier experiments, suggests that the catalytic activity is low because there is a low concentration of Co (I) in solution. The concentrations of $[\text{Cp}^*\text{Co}(\text{CO})_2]$ and PEt_3 and the conditions were kept constant from experiment 3 so that the only change was the replacement of acetic acid and methyl acetate by methanol.

The results obtained were very encouraging. The composition of the solution in experiments 4 and 5 were very similar in order to get some idea of experimental error. Clearly the valve between the ballast and reaction vessels was working far better in the case of experiment 4 and these results should be considered as a closer representation of the catalytic activity. The initial rate was measured at 300 turnovers per hour. This rate is

far in excess of any other rates measured for cobalt catalysts or for rhodium catalysts under these mild conditions. The first catalytic system suddenly stops carbonylating and a slower rate takes over. The rate of carbonylation for this system is still good ~ 20 turnovers per hour and better than the measurement made in the absence of water.^{100a} This could be because water helps maintain a high concentration of the active catalyst. The second region of carbonylation shows a first order decay and the second catalytic system shows a first order dependence on the concentration of methanol.

The products detected by GC analysis were methyl acetate 1.83 mol dm^{-3} , acetic acid and a tiny quantity of 1,1-dimethoxyethane $1.2 \times 10^{-3} \text{ mol dm}^{-3}$. From the total CO uptake 8.87 mol dm^{-3} carbonylated products were produced and the selectivity was $> 99.9\%$ towards acetates. The GC-MS revealed that triethyl phosphine, triethyl phosphine oxide and pentamethyl cyclopentadiene were also in solution.

The $[\text{Cp}^*\text{Co}(\text{CO})_2] + \text{PEt}_3$ catalytic system operates very well in methanol and water with two regions of activity. The first catalytic species, $[\text{Cp}^*\text{Co}(\text{CO})(\text{PEt}_3)]$, carbonylates at a very rapid rate but soon rearranges to a slower, more stable catalyst, $[\text{Cp}^*\text{Co}(\text{CO})\text{I}]^-$. The resultant solutions contain the desired products almost exclusively.

Careful design of cobalt based catalysts can give activities and selectivities that are comparable with those of their rhodium analogues and because of the high solubility and low cost, this type of catalyst holds exciting prospects for the continuing use of cobalt as a homogeneous catalyst.

Table 16: Kinetic runs for Cobalt Based Methanol Carbonylation Catalysis.Conditions: $[\text{Cp}^*\text{Co}(\text{CO})_2] = 0.602$ mmoles, 100bar CO, 120°C

No.	[LiI] / mmols	[PEt ₃] / mmols	MeOH	MeI / g	H ₂ O / mL	Rate / mol dm ⁻³ hr ⁻¹	TOF	Comments
1	-	-	-	0.7	-	no rate	-	Dark brown needles: $[\text{Cp}^*\text{Co}(\text{CO})_2]$
2	5.983	-	-	0.7	-	no rate	-	No catalytic activity
3	-	5.911	-	1.0	-	no rate	-	No catalytic activity
4	-	6.065	2.0487g	1.0	0.35	43.9, 2.5	314, 18	Kinetic graph shows very fast initial phase followed by no activity and then a second phase of activity, orange final solution.
5	-	6.058	2.0546g	1.0	0.36	- , 3.41	- , 25	Kinetic graph shows very fast initial phase followed by no activity and then a second phase of activity, orange final solution.

4.5.3 RHODIUM CATALYSED CARBONYLATION OF METHYL ACETATE

As a comparison to the cobalt based chemistry mentioned in section 4.5.2, further tests were carried out using the $[\text{Cp}^*\text{Rh}(\text{CO})_2]$ and $[\text{Cp}^*\text{Rh}(\text{CO})\text{I}_2]$ systems.^{100a} The results for the runs done as part of the CATS service are reported here.

Acetic anhydride is an important bulk chemical used mainly in the synthesis of cellulose acetate for photographic film and other acetates. It is prepared by dehydrating acetic acid, or by the direct rhodium catalysed carbonylation of methyl acetate (Figure 62).¹⁰⁵

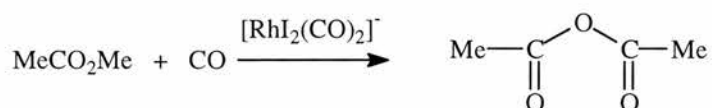


Figure 62: Rhodium Catalysed carbonylation of methyl acetate

A problem that is encountered is the simultaneous catalysis of the water gas shift reaction. Thus, HI in the system can lead to the formation of H_2 and the catalytically inactive $[\text{RhI}_4(\text{CO})_2]^-$. In methanol carbonylation this rhodium (III) complex is reduced back to $[\text{RhI}_2(\text{CO})_2]^-$ by reaction with added water, this releases CO_2 and completes the water gas shift reaction cycle. For acetic anhydride production water cannot be present, so the reaction is performed in the presence of hydrogen to avoid the formation of $[\text{RhI}_4(\text{CO})_2]^-$. This does have drawbacks, mainly the production of side products such as methane, ethanal, ethanol and methyl propanoate.

The catalytic system briefly introduced here produces acetic anhydride without added hydrogen. This is partly due to the rhodium (III) complex formed by the water gas shift reaction being catalytically active for methyl acetate carbonylation as well.

Following on from the work described in section 4.5.2, above, $[\text{Cp}^*\text{Rh}(\text{CO})_2]$ was tested (189°C, 36 bar CO). It was found that in the presence of lithium iodide, under anhydrous conditions, it catalyses the carbonylation of methylacetate with a rate of $6.9 \text{ mol dm}^{-3} \text{ h}^{-1}$ (experiment 1, Table 17), with 58% conversion of methyl acetate after one hour. The reaction shows zero order kinetics in methyl acetate over the first 20 minutes and then starts to slow. This is probably due to the active species conversion (by the water gas shift reaction) to $[\text{Cp}^*\text{Rh}(\text{CO})\text{I}_2]$. This is deduced from the fact that after cooling and opening the reactor, this complex had crystallised from the solution.

The reaction does not stop completely as $[\text{Cp}^*\text{Rh}(\text{CO})\text{I}_2]$ is itself active for carbonylation of methyl acetate (experiment 2, Table 17) albeit at a lower rate ($1.19 \text{ mol dm}^{-3} \text{ h}^{-1}$). This reaction also retains activity for prolonged periods (39% conversion of methyl acetate after one and a half hours).

This work, has been elaborated on further^{100a} and together the results suggest that the electron rich complex is a highly active catalyst for methyl acetate carbonylation, in part due to the formation of $[\text{Cp}^*\text{Rh}(\text{CO})\text{I}_2]$ which is formed by the water gas shift reaction which is active in the same system and apparently stable for proposed periods.

Table 17: Rhodium Catalysed Methyl Acetate Carbonylation runs.

No	Catalyst	Conc./mol dm ⁻³	Temp. / °C	Press. / bar	AcOH / g	AcOAc / g	LiI / g	MeI / g	MeOAc / g	Total volume / mL	Rate/ mol dm ⁻³ hr ⁻¹	Rate/ turnover hr ⁻¹
1	Cp*Rh(CO) ₂	0.0065	189	36	3.100	0.032	0.7314	0.912	1.529	5.4	6.9	1062
2	Cp*Rh(CO) ₂	0.0065	189	36	3.100	0.032	0.7314	0.912	1.529	5.4	1.19	182



CHAPTER FIVE:
EXPERIMENTAL

CHAPTER FIVE: EXPERIMENTAL

5.1 GENERAL EXPERIMENTAL

Due to the nature of the work involved in the testing and optimisation of catalytic systems there is a lot of repetition of experimental procedure. As such this chapter gives the general techniques and conditions used and then outlines some specific conditions particular to that set of reactions. The laboratory is set up so that all reaction, write up and analyses are done in the same area. All reactions are written up directly into the CATS-PC and a hard copy is printed and filed with the GC data and other paperwork for each section. Hardware specifications not mentioned here are described in chapter one and other experimental techniques in chapter four and are not repeated here.

All experiments were carried out under a dry nitrogen / argon atmosphere, dried through a Cr (II) / silica packed glass column. Liquids were handled using gas tight syringes. Sensitive solids were handled under inert atmosphere using Schlenk techniques¹⁰⁶ and/or a glove box. Liquids were predried and treated according to literature procedures.¹⁰⁷

Reactions were carried out on vacuum lines. Liquids were transferred under inert atmosphere by syringe or canula through suba seals. Solids were transferred directly from one Schlenk tube to another or weighed out in a glove box under argon.

Carbon monoxide, synthesis gas and ethylene were purchased from BOC gases. Solvents, metal complexes, liquids and other reagents were purchased from Aldrich, Fisher, Strem or similar sources. These were purified by standard methods, and liquids were stored over A4 molecular sieves. All reactants not available commercially were provided by individual researchers and used as supplied. Unless specifically stated they were treated as air sensitive and handled in a glove box or using Schlenk lines.

Most specific conditions for each set of reactions are listed in the accompanying tables following each section in chapter four.

5.2 CHARGING THE AUTOCLAVE

AIR SENSITIVE COMPOUNDS

All apparatus was washed, rinsed in acetone or dichloromethane and dried in an oven. The autoclave was run at high temperature with a suitable solvent to ensure that no residues from the previous run remain, and rinsed. Before fitting the clean reaction in its bay, the autoclave was heated above 100°C in an oven to ensure no moisture or solvent was present. It is assembled and allowed to cool with argon flowing .

Pressurising the injection port was usually done before the reaction vessel was charged. If a different substrate was used in the previous experiment the vessel was flushed with gas from the ballast vessel to ensure it was as dry as possible. It was then flushed 3 times with 1mL of the new substrate before being flushed again and charged with the required volume.

If the reactant solids were not particularly soluble in the chosen solvent the reaction vessel was unscrewed from its bay and the solids were carefully inserted with a steady stream of argon. After refitting the vessel and having allowed argon to flush through for ca. 2-5 minutes, solvent was injected through the side port with gas flowing and the system was sealed. This method was preferred to avoid concentration changes due to insolubility when dissolving the solids before injection. Care needs to be taken when loading solids into the reaction vessel and especially when flowing gas over powders as they may be blown around by excessive gas flow which could affect the concentrations once in solution. If the solids were soluble, they were dissolved and transferred into the autoclave through the side port. The procedure ensured that any time the vessels were not sealed there was a substantial flow of argon or reactant gas.

The reaction vessel was flushed with the reactant gas. Three cycles of pressurising and depressurising is done by filling with ca. 15 bar of gas and releasing slowly. On the 4th cycle the gas was brought to the pressure required by the experiment and was sealed.

The solution in the reaction vessel was then stirred and heat applied. Once the required internal temperature was achieved, and was stable, the data logger was activated. After 60 seconds of logging the substrate was injected and reaction vessel pressure set.

The reaction was allowed to proceed for the required time after which the vessel was cooled rapidly in a water bath with stirring. Once cooled the gas was slowly released and the products were extracted with a Pasteur pipette and analysed. The resulting solutions were stored in stoppered sample tubes in a cool dark cupboard.

NON-AIR SENSITIVE COMPOUNDS

All procedures for the non-air sensitive compounds were identical to those for air sensitive compounds except for the loading of the reaction vessel. The solid reactants were placed in the reaction vessel with very little or no gas flow and the solvents and substrates had not necessarily been treated under inert atmosphere and specially dried.

5.3 ANALYSIS

The GC-MS and FID system owned by CATS was the main source of analysis. Reaction products were diluted if they were to be injected into the column leading to the mass spectrometer. Typically, this dilution was by a factor of 20-50. This dilute solution was injected in 1 μ L quantities. The syringe was first rinsed with pure solvent, with the solution 5 times and then refilled for injection. Afterwards the syringe was rinsed with clean solvent and stored.

Solvents used were of HPLC grade or similar purity, otherwise they were purified and redistilled according to literature methods.¹⁰⁷ The columns owned by the service are: two HP-5MS 5% phenyl methyl siloxane (30.0m x 250 μ m x 0.25 μ m nominal) capillary columns, one Supelco Beta-dex 225 (60.0m x 250 μ m x 0.25 μ m nominal) chiral capillary column, a Supelco Beta-dex 120 (30.0m x 250 μ m x 0.25 μ m nominal) chiral capillary column and one Supelco MDN-35 (30.0m x 250 μ m x 0.25 μ m nominal) chiral capillary column. The two HP5-MS columns were both usually fitted, but a chiral column was installed when required (usually the Beta-dex 225).

The columns were calibrated using standard solutions made up in the laboratory with the required liquids for specific reactions.

CHAPTER FIVE: EXPERIMENTAL

5.1 GENERAL EXPERIMENTAL

Due to the nature of the work involved in the testing and optimisation of catalytic systems there is a lot of repetition of experimental procedure. As such this chapter gives the general techniques and conditions used and then outlines some specific conditions particular to that set of reactions. The laboratory is set up so that all reaction, write up and analyses are done in the same area. All reactions are written up directly into the CATS-PC and a hard copy is printed and filed with the GC data and other paperwork for each section. Hardware specifications not mentioned here are described in chapter one and other experimental techniques in chapter four and are not repeated here.

All experiments were carried out under a dry nitrogen / argon atmosphere, dried through a Cr (II) / silica packed glass column. Liquids were handled using gas tight syringes. Sensitive solids were handled under inert atmosphere using Schlenk techniques¹⁰⁶ and/or a glove box. Liquids were predried and treated according to literature procedures.¹⁰⁷

Reactions were carried out on vacuum lines. Liquids were transferred under inert atmosphere by syringe or canula through suba seals. Solids were transferred directly from one Schlenk tube to another or weighed out in a glove box under argon.

Carbon monoxide, synthesis gas and ethylene were purchased from BOC gases. Solvents, metal complexes, liquids and other reagents were purchased from Aldrich, Fisher, Strem or similar sources. These were purified by standard methods, and liquids were stored over A4 molecular sieves. All reactants not available commercially were provided by individual researchers and used as supplied. Unless specifically stated they were treated as air sensitive and handled in a glove box or using Schlenk lines.

Most specific conditions for each set of reactions are listed in the accompanying tables following each section in chapter four.

5.2 CHARGING THE AUTOCLAVE

AIR SENSITIVE COMPOUNDS

All apparatus was washed, rinsed in acetone or dichloromethane and dried in an oven. The autoclave was run at high temperature with a suitable solvent to ensure that no residues from the previous run remain, and rinsed. Before fitting the clean reaction in its bay, the autoclave was heated above 100°C in an oven to ensure no moisture or solvent was present. It is assembled and allowed to cool with argon flowing .

Pressurising the injection port was usually done before the reaction vessel was charged. If a different substrate was used in the previous experiment the vessel was flushed with gas from the ballast vessel to ensure it was as dry as possible. It was then flushed 3 times with 1mL of the new substrate before being flushed again and charged with the required volume.

If the reactant solids were not particularly soluble in the chosen solvent the reaction vessel was unscrewed from its bay and the solids were carefully inserted with a steady stream of argon. After refitting the vessel and having allowed argon to flush through for ca. 2-5 minutes, solvent was injected through the side port with gas flowing and the system was sealed. This method was preferred to avoid concentration changes due to insolubility when dissolving the solids before injection. Care needs to be taken when loading solids into the reaction vessel and especially when flowing gas over powders as they may be blown around by excessive gas flow which could affect the concentrations once in solution. If the solids were soluble, they were dissolved and transferred into the autoclave through the side port. The procedure ensured that any time the vessels were not sealed there was a substantial flow of argon or reactant gas.

The reaction vessel was flushed with the reactant gas. Three cycles of pressurising and depressurising is done by filling with ca. 15 bar of gas and releasing slowly. On the 4th cycle the gas was brought to the pressure required by the experiment and was sealed.

The solution in the reaction vessel was then stirred and heat applied. Once the required internal temperature was achieved, and was stable, the data logger was activated. After 60 seconds of logging the substrate was injected and reaction vessel pressure set.

The reaction was allowed to proceed for the required time after which the vessel was cooled rapidly in a water bath with stirring. Once cooled the gas was slowly released and the products were extracted with a Pasteur pipette and analysed. The resulting solutions were stored in stoppered sample tubes in a cool dark cupboard.

NON-AIR SENSITIVE COMPOUNDS

All procedures for the non-air sensitive compounds were identical to those for air sensitive compounds except for the loading of the reaction vessel. The solid reactants were placed in the reaction vessel with very little or no gas flow and the solvents and substrates had not necessarily been treated under inert atmosphere and specially dried.

5.3 ANALYSIS

The GC-MS and FID system owned by CATS was the main source of analysis. Reaction products were diluted if they were to be injected into the column leading to the mass spectrometer. Typically, this dilution was by a factor of 20-50. This dilute solution was injected in 1 μ L quantities. The syringe was first rinsed with pure solvent, with the solution 5 times and then refilled for injection. Afterwards the syringe was rinsed with clean solvent and stored.

Solvents used were of HPLC grade or similar purity, otherwise they were purified and redistilled according to literature methods.¹⁰⁷ The columns owned by the service are: two HP-5MS 5% phenyl methyl siloxane (30.0m x 250 μ m x 0.25 μ m nominal) capillary columns, one Supelco Beta-dex 225 (60.0m x 250 μ m x 0.25 μ m nominal) chiral capillary column, a Supelco Beta-dex 120 (30.0m x 250 μ m x 0.25 μ m nominal) chiral capillary column and one Supelco MDN-35 (30.0m x 250 μ m x 0.25 μ m nominal) chiral capillary column. The two HP5-MS columns were both usually fitted, but a chiral column was installed when required (usually the Beta-dex 225).

The columns were calibrated using standard solutions made up in the laboratory with the required liquids for specific reactions.



AFTERWORD

AFTERWORD

The ability to test catalytic systems, plot the kinetic data, and analyse the resulting products, is a valuable tool. The information gleaned can be used to optimise and evaluate processes so that their actual potential is tapped. Industry and academia can both benefit from test reactions of the type studied herein. The procedures developed can be used not only for the systems tested, but can also be applied to similar types of reactions. Hence, the fundamental possibilities of homogeneous catalysis can be brought one step closer to fruition.

The findings of this research programme indicate that the service provided by CATS can facilitate advancements in the field of catalysis. In time, if further research is properly supported, this field has the potential to yield great benefits in both the economic and ecological spheres.



REFERENCES

REFERENCES

- ¹ H. Adkins, G. Krsek, *J. Am. Chem. Soc.*, **1948**, *70*, 383
- ² a) Chemische Verwertungsgesellschaft Oberhausen m.b.H (O.Roelen), DE 89.548 (1938/1952) and US2.327.066(1943).
b) O.Roelen, *Chem. Exp. Didakt.*, **1977**, *3*, 119.
- ³ a) B. Cornils, W.A. Herrmann, C. W. Kolpaitner, *Nachr. Chem. Tech. Lab.*, **1993**, *41*, 544.
b) B. Cornils, W.A. Herrmann, M. Rasch, *Angw. Chem., Int. Ed. Engl.*, **1994**, *33*, 2144.
- ⁴ B. Cornils in *New Syntheses with Carbon Monoxide*, (Ed.: J. Falbe), Springer, Berlin, **1980**, Chapter 1.
- ⁵ Anon., *Celanese Corp. Annual Business Report*, **1974**, p.9.
- ⁶ W.A. Herrmann, B. Cornils, *Angew. Chem. Int. Ed. Engl.*, **1997**, *36*, 1048.
- ⁷ W.A. Herrmann, C.W. Kohlpainter, *Angew. Chem. Int. Ed. Engl.*, **1993**, *32*, 1524.
- ⁸ B. Cornils, *Angew. Chem. Int. Ed. Engl.*, **1995**, *34*, 1575.
- ⁹ a) B. Cornils, E.G. Kuntz, *J. Organomet. Chem.*, **1995**, *502*, 177.
b) F. Joó, Á. Kathó, *J. Mol. Catal.*, **1997**, *116*, 3.
- ¹⁰ E. Bayer, V. Schuring, *Angew. Chem. Int. Ed. Engl.*, **1975**, *14*, 493.
- ¹¹ M. Reggelin, *Nachr. Chem. Tech. Lab.*, **1997**, *45*, 1196, and references therein.
- ¹² B.E. Hanson, *Coord. Chem. Rev.*, **1999**, *185-186*, 795
- ¹³ W.A. Herrmann, B. Cornils, *Angew. Chem. Int. Ed. Engl.*, **1997**, *36*, 1049.
- ¹⁴ D. Koch, W. Leitner, *J. Am. Chem. Soc.*, **1998**, *120*, 13398.
- ¹⁵ G. Kraupp, *Angew. Chem. Int. Ed. Engl.*, **1994**, *33*, 1452.
- ¹⁶ F.P. Pruchnik in *Organometallic Chemistry of Transition Elements*, Plenum Press, New York, **1990**, p. 691
- ¹⁷ R.L. Pruett, *Adv. Organomet. Chem.*, **1979**, *17*, 1.
- ¹⁸ B.Cornils, W.A. Herrmann (Eds.), *Applied Homogeneous Catalysis with Organometallic Compounds: A Comprehensive Handbook in Two Volumes*, VCH-Weinheim, New York/Basel/Cambridge/Tokyo, **1996**
- ¹⁹ I.Tkatchenko, in: G. Wilkinson (Ed.), *Comprehensive Organometallic Chemistry*, vol. 8, Pergamon Press, Oxford, **1982**, p. 101.
- ²⁰ P.Kalk, Y. Peres, J. Jenck, *Adv. Organomet. Chem.*, **1991**, *32*, 121
- ²¹ H. Bahrmann, H. Bach, *Ullmann's Encycl. Ind. Chem. 5th ed.*, **1991**, Vol. A18, p. 321.
- ²² a) G.K.I. Magomedov, L.V. Morozova, *Zh. Obsch. Khim.*, **1981**, *51*, 2226
b) T.E Nalesnik, J.H. Freudenberger, M. Orchin, *J. Organomet. Chem.*, **1982**, *236*, 95
c) Z. He., N. Luga, D. Neibecker, R. Methieu, J.J. Bonnet, *J. Organomet. Chem.*, **1992**, *426*, 247.
d) R.A. Sanchez-Delgado, M. Rosales, M.A. Esteruelas, L.A. Oro, *J. Mol. Catal. A: Chemical*, **1995**, *96*, 231.
e) L.A. Oro, M.T. Pinillos, M. Royo, E. Pastor, *J. Chem. Res, Synop.*, **1984**, 206; *Chem. Abstr.* **1984**, *101*, 191096.
- ²³ L. Alvila, T.A. Pakkanen, T.T. Pakkanen, O. Krause, *J. Mol. Catal.*, **1992**, *73*, 325.
- ²⁴ D.T. Brown, T. Eguchi, B.T. Heaton, J.A Iggo, R. Whyman, *J. Chem. Soc., Dalton Trans.*, **1991**, 677.

- ²⁵ a) A.D. Harley, G.J. Guskey, G.L. Geoffroy, *Organometallics*, **1983**, 2, 53
b) C. Mahe, H. Patin, J.Y. Le Marouille, A. Benoit, *Organometallics*, **1983**, 2, 1051
c) A. Ceriotti, L. Garlaschelli, G. Longoni, M.C. Malatesta, D. Strumolo, A. Fumagalli, S. Martinengo, *J. Mol. Catal.*, **1984**, 24, 309
d) S. Xue, Y. Luo, H. Fu, Y. Yin, *Ranliao Huaxue Xuebao*, **1986**, 14, 354; *Chem Abstr.*, **1987**, 107, 9264.
e) T. Hayashi, Z. H. Gu, T. Sakaura, M. Tanaka, *J. Organomet. Chem.*, **1988**, 352, 373.
f) A.R. El'man, V.I. Kurkin, EV. Slivinskii, S.M. Loktev, *Neftekhimiya*, **1990**, 30, 46; *Chem. Abstr.*, **1990**, 112, 197383.
- ²⁶ L.H. Pignolet (Ed.) *Homogeneous Catalysis with Metal Phosphine Complexes*, Plenum, London, **1983**.
- ²⁷ a) C.A. Tolman, W.C. Seidel, L.W. Gosser, *J. Am. Chem. Soc.*, **1974**, 96, 53
b) C.A. Tolman, *Chem. Rev.*, **1977**, 77, 313
- ²⁸ a) C.P. Casey, G.T. Whiteker, *Isr. J. Chem.*, **1990**, 30, 299
b) C.P. Casey, G.T. Whiteker, C.F. Campana, D.R. Powell, *Inorg. Chem.*, **1990**, 29, 3376
c) C.P. Casey, G.T. Whiteker, M.G. Melville, L.M. Petrovich, J.A. Gavney, Jr., D.R. Powell, *J. Am. Chem. Soc.*, **1992**, 114, 5535.
- ²⁹ C.P. Casey, L.M. Petrovich, *J. Am. Chem. Soc.*, **1992**, 114, 5535.
- ³⁰ C.P. Casey, E.L. Paulsen, E.W. Beuttenmueller, B.R. Proft, B. A. Matter, D.R. Powell, *J. Am. Chem. Soc.*, **1999**, 121, 63.
- ³¹ J.K. MacDougall, M.C. Simpson, M.J. Green, D.J. Cole-Hamilton, *J. Chem.Soc., Dalton Trans.*, **1996**, 1161.
- ³² a) P.W.N.M van Leeuwen, C.F. Roobeek, *J. Organomet. Chem.*, **1983**, 258, 343
b) A. Polo, J. Real, C. Claver, S. Castillion, J.C. Bayon, *J. Chem. Soc., Chem. Commun.*, **1990**, 600
c) A. van Rooy, E.N. Orij, P.C.J. Kamer, F. van den Aardweg, P.W.N.M. van Leeuwen, *J. Chem. Soc., Chem. Commun.*, **1991** 1096
d) T. Jongsma, G. Challa, P.W.N.M. van Leeuwen, *J. Organomet. Chem.*, **1991**, 421, 121.
- ³³ A.M. Trzeciak, J. J. Ziólkowski, *Coord. Chem. Rev.*, **1999**, 190, 883.
- ³⁴ a) A.G. Abatjoglou, E. Billing, D.R. Bryant, *Organometallics*, **1984**, 3, 923.
b) A.G. Abatjoglou, D.R. Bryant, *Organometallics*, **1984**, 3, 932.
c) R.A. Dubois, *Organometallics*, **1984**, 3, 649.
- ³⁵ R.M. Deshpande, S.S. Divekar, R.V. Gholap, R.V. Chaudhari, *J. Mol. Catal.*, **1991**, 67, 333
- ³⁶ a) W. Keim, *J. Organomet. Chem.*, **1968**, 14, 649.
b) G. Wilkinson, M. Yagupsky, C.K. Brown, G. Yagupsky, *J. Chem. Soc. A*, **1970**, 937.
- ³⁷ J. Falbe, *Carbon Monoxide in Organic Synthesis*, Springer, Berlin, **1970**.
- ³⁸ C. Botteghi, R. Ganzerla, M. Lenarda, G. Moretti, *J. Mol. Catal.*, **1987**, 40, 129.
- ³⁹ N. Noujiri, M. Misono, *Appl. Catal. A: General*, **1993**, 93, 103.
- ⁴⁰ N. Nagato in *Encycl. Chem. Technol. (Kirk-Othmer)*, 4th ed., **1991**, Vol.2, p. 144.
- ⁴¹ a) BASF AG (W. Himmele, W. Aquila), US 3.840.589, **1974**.
b) Hoffmann La Roche (P. Fitton, H. Moffet), US 4.124.619, **1978**.
- ⁴² M. Barber, *Stereotechnol. Pharm. Manuf. Int.*, **1990**, 137.

- ⁴³ C.Y. Hsu, M. Orchin, *J. Am. Chem. Soc.*, **1975**, *97*, 3553.
- ⁴⁴ J.K. Stille, H. Su, P. Brechot, G. Parrinello, L.S. Hegedus, *Organometallics*, **1991**, *10*, 1183.
- ⁴⁵ I. Tóth, I. Guo, B.E. Hanson, *Organometallics*, **1993**, *12*, 848.
- ⁴⁶ a) N. Sakai, S. Mano, K. Nozaki, H. Takaya, *J. Am. Chem. Soc.*, **1993**, *115*, 7033.
b) G.J.H. Buisman, E.J. Vos, P.C.J. Kamer, P.W.N.M. van Leeuwen, *J. Chem. Soc., Dalton Trans.*, **1995**, 409.
- ⁴⁷ a) D.S. Breslow, R.F. Heck, *Chem. Ind. (London)*, **1960**, 467.
b) R.F. Heck, D.S. Breslow, *J. Am. Chem. Soc.*, **1961**, *83*, 4023.
- ⁴⁸ F. Piacenti, M. Bianchi, P. Frediani, G. Menchi, U. Matteoli, *J. Organomet. Chem.*, **1991**, *417*, 77.
- ⁴⁹ M.S. Borovikov, I. Kovács, F. Ungváry, A. Sisak, L. Markó, *Organometallics*, **1992**, *11*, 1576.
- ⁵⁰ F.H. Jardine, *Polyhedron*, **1982**, *1*, 569.
- ⁵¹ a) S.S. Bath, L. Vaska, *J. Am. Chem. Soc.*, **1963**, *85*, 3500.
b) S.J. LaPlaca, J.A. Ibers, *J. Am. Chem. Soc.*, **1963**, *85*, 3500.
- ⁵² a) D. Evans, J. A. Osborn, G. Wilkinson, *J. Chem. Soc. (A)*, **1968**, 3133.
b) C.K. Brown, G. Wilkinson, *Tetrahedron Lett.*, **1969**, 1725.
c) C.K. Brown, G. Wilkinson, *J. Chem. Soc. (A)*, **1970**, 2753.
- ⁵³ a) Shell Oil(E.F. Lutz), US 4.528.416, **1985**
a). Shell (E.F. Lutz, P.A. Gautier), EP 177.999, **1986**
b) E.F. Lutz, *J. Chem. Educ.*, **1986**, *63*, 202.
- ⁵⁴ J.K. Stille in *Comprehensive Organic Synthesis* (Eds. B.M. Trost, I. Fleming, M.F. Semmelhack), Pergamon, Oxford, **1991**, pg. 913.
- ⁵⁵ a) G. Natta, R. Ercoli, S. Castellano, F.H. Barbieri, *J. Am. Chem. Soc.*, **1954**, *76*, 4049.
b) F.E. Paulik, *Catal. Rev.*, **1972**, *6*, 49.
c) B. Heil, L. Markó, *Chem. Ber.*, **1968**, *101*, 2209.
d) G. Gregorio, G. Montrasi, M. Tampieri, P. Cavalieri d'Oro, G. Pagani, A. Andreetta, *Chim. Ind. (Milan)*, **1980**, *62*, 389.
e) S.S. Divekar, R.M. Deshpande, R.V. Chaudhari, *Catal. Lett.*, **1993**, *21*, 191.
- ⁵⁶ a) G. Natta, R. Ercoli, S. Castellano, F.H. Barbieri, *J. Am. Chem. Soc.*, **1954**, *76*, 4049.
b) B. Heil, L. Markó, *Chem. Ber.*, **1968**, *101*, 2209.
- ⁵⁷ I.T. Horváth, G. Kiss, R.A. Cook, J.E. Bond, P.A. Stevens, J. Rábai, E. J. Mozeleski, *J. Am. Chem. Soc.*, **1998**, *120*, 3133
- ⁵⁸ R. Martin, *Chem. Ind. (London)*, **1954**, 1536.
- ⁵⁹ F. Piacenti, P. Pino, R. Lazzaroni, M. Bianchi, *J. Chem. Soc. (C)*, **1966**, 488.
- ⁶⁰ S. Brewis, *J. Chem. Soc.*, **1964**, 5014.
- ⁶¹ W.R. Moser, C.J. Papile, D. A. Brannon, R. A. Duwell, S.J. Weininger, *J. Mol. Catal.*, **1987**, *41*, 271.
- ⁶² M.G. Voronkov, V.L. Lavrent'yev, *Top. Curr. Chem.*, **1992**, *102*, 199.
- ⁶³ a) A. Tsuchida, C. Bolln, F. G. Sernetz, H. Frey, and R. Mulhaupt, *Macromolecules*, **1997**, *30*, 2818.
b) J. Lichtenhan, *Comments Inorg. Chem.*, **1995**, *17*, 115.
- ⁶⁴ a) R.H. Baney, M. Itoh, A. Sakakibara, T. Suzuki, *Chem. Rev.*, **1995**, *95*, 1409.
b) A.R. Bassindale, T.E. Gentle, *J. Mater. Chem.*, **1993**, *3*, 1319.

- ⁶⁴ a) R.H. Baney, M. Itoh, A. Sakakibara, T. Suzuki, *Chem. Rev.*, **1995**, 95, 1409.
b) A.R. Bassindale, T.E. Gentle, *J. Mater. Chem.*, **1993**, 3, 1319.
- ⁶⁵ a) F.J. Feher, T.A. Budzichowski, R.L. Blanski, K.J. Weller, J.W. Ziller, *Organometallics*, **1991**, 10, 2526.
b) F.J. Feher, D. Soulivong, G.T. Lewis, *J. Am. Chem. Soc.*, **1997**, 119, 11323.
c) F.J. Feher, S.H. Phillips, *J. Organomet. Chem.*, **1996**, 521, 401.
d) V. Ruffieux, G. Schmid, P. Braunstein, J. Rosé, *Chem. Eur. J.*, **1996**, 3, 900.
- ⁶⁶ F.J. Feher, S.H. Phillips, J.W. Ziller, *Chem. Commun.*, **1997**, 829.
- ⁶⁷ F.J. Feher, D. Soulivong, A.G. Eklund, *Chem. Commun.*, **1998**, 399.
- ⁶⁸ D.A. Loy, K.J. Shea, *Chem. Rev.*, **1995**, 95, 1431.
- ⁶⁹ F.J. Feher, D. Soulivong, A.G. Eklund, K.D. Wyndham, *Chem. Commun.*, **1997**, 1185.
- ⁷⁰ a) T.N. Voronkov, R.G. Martynova, V.I. Belyi, *Zh. Obshch. Khim.*, **1979**, 49, 1522.
b) T.N. Martynova, V.P. Korchkov, *Zh. Obshch. Khim.*, **1982**, 52, 1585.
c) F.J. Feher, T.A. Budzichowski, *Polyhedron*, **1995**, 14, 3239.
- ⁷¹ F.T. Edelman, *Angew. Chem. Int. Ed. Engl.*, **1992**, 31, 586.
- ⁷² F.J. Feher, T.L. Tajima, *J. Am. Chem. Soc.*, **1994**, 116, 2145.
- ⁷³ F.J. Feher, J.F. Walzer, *Inorg. Chem.*, **1991**, 30, 1689.
- ⁷⁴ F.J. Feher, T.A. Budzichowski, *J. Organomet. Chem.*, **1989**, 379, 33.
- ⁷⁵ a) N. Ardoin, D. Astruc, *Bull. Soc. Chim. Fr.*, **1995**, 132, 875.
b) D.A. Tomalia, A.M. Naylor, W.A. Goddard III, *Angew. Chem. Int. Ed. Engl.*, **1990**, 29, 138.
c) H. Meikelburger, W. Jaworek, F. Vögtle, *Angew. Chem. Int. Ed. Engl.*, **1992**, 31, 1571
- ⁷⁶ R. Dagani, *Chem. Eng. News*, **1996**, June 3.
- ⁷⁷ a) L.A. van de Kuil, H. Luitjes, D.M. Grove, J.W. Zwikker, J.G.M. van der Linden, A.M. Roelofsen, L.W. Jenneskens, W. Drenth, G. van Koten, *Organometallics*, **1994**, 13, 468.
b) L.A. van de Kuil, D.M. Grove, J.W. Zwikker, L.W. Jenneskens, W. Drenth, G. van Koten, *Chem. Mater.*, **1994**, 6, 1675.
- ⁷⁸ J.W.J. Knappen, A.W. van der Made, J.C. de Wilde, P.W.M.N. van Leeuwen, P. Wijkens, D.M. Grove, G. van Koten, *Nature*, **1994**, 372, 659.
- ⁷⁹ Meschmeyer T., Rey F., Sankar G., Thomas J. M., *Nature*, **1995**, 378, 159.
- ⁸⁰ R.E. Morris. personal communication.
- ⁸¹ R.E. Morris, P.A. Jaffres, *J. Chem. Soc., Dalton Trans.*, **1998**, 16, 2767.
- ⁸² U. Dittmar, B.J. Hendan, U. Flörke, H.C. Marsmann, *J. Organomet. Chem.*, **1995**, 489, 185.
- ⁸³ B. Hong, T.P.S. Thomas, H.J. Murfee, M.J. Lebrun, *Inorg. Chem.*, **1997**, 36, 6146.
- ⁸⁴ F.J. Feher, T.A. Budzichowski, *Organometallics*, **1991**, 10, 812.
- ⁸⁵ F.J. Feher, S.H. Phillips, *J. Organomet. Chem.*, **1996**, 521, 401.
- ⁸⁶ K.J. Weller, J.J. Schwab, *Organometallics*, **1995**, 14, 2009.
- ⁸⁷ L. Ropartz, *First Year Ph.D. Report, University of St. Andrews*, **1999**.
- ⁸⁸ J.K. MacDougall, M.C. Simpson, M.J. Green, D.J. Cole-Hamilton, *J. Chem. Soc. Dalton Trans.*, **1996**, 1161.
- ⁸⁹ I.T. Horváth, J. Rábai, *Science*, **1994**, 72, 266.

- ⁹⁰ a) E. Lindner, T. Schneller, F. Auer, H.A. Mayer, *Angw.Chem. Int. Ed.*, **1999**, 38, 2154.
b) D.P. Curran, *Angw.Chem. Int. Ed.*, **1998**, 37, 1175.
c) B. Cornils, *Angw.Chem. Int. Ed.*, **1997**, 36, 2057
d) E.G. Hope, A.M. Stuart, *Chem. Ind.*, **1999**, 755.
e) I. Klement, H. Lütjens, P. Knochel, *Angw.Chem. Int. Ed.*, **1997**, 36, 1454.
- ⁹¹ a) J. G. Riess, M. Le Blanc, *Pure Appl. Chem.*, **1982**, 54, 2383.
b) J.G. Riess, *New J. Chem.*, **1995**, 19, 893.
c) V. W. Sadtler, M.P. Krafft, J.G. Riess, *Angw.Chem. Int. Ed.*, **1996**, 35, 1976.
- ⁹² I.T. Horváth, G. Kiss, R.A. Cook, J.E. Bond, P.A. Stevens, J. Rábai, E. J. Mozeleski, *J. Am. Chem. Soc.*, **1998**, 120, 3133.
- ⁹³ C.P. Casey, E.L. Paulsen, E.W. Beuttenmueller, B.R. Proft, L.M. Petrovich, B.A. Matter, D.R. Powell, *J. Am. Chem. Soc.*, **1997**, 119, 11817.
- ⁹⁴ R.A. Sanchez-Delgado, J.S. Bradley, D.J. Cole-Hamilton, *J. Chem. Soc., Dalton Trans.*, **1976**, 399.
- ⁹⁵ R.A. Sanchez-Delgado, A. Andriollo, O.L. de Ochoa, T. Suarez, N. Valencia, *J. Organomet. Chem.*, **1981**, 209, 77.
- ⁹⁶ P. Eilbracht in, *Stereoselective Synthesis*, Eds. G. Helmchen, R.W. Hoffmann, J. Mulzer, E. Schaumann, Theime, Stuttgart, Ed. E21, vol. 4, **1996**.
- ⁹⁷ a) N. Sakai, S. Mano, K. Nozaki, H. Takaya, *J. Am. Chem. Soc.* **1993**, 115, 7033.
b) T. Higashizima, N. Sakai, K. Nozaki, H. Takaya, *Tetrahedron Lett.*, **1994**, 35 2023.
- ⁹⁸ G. Parrinello, J.K. Stille, *J. Am. Chem. Soc.*, **1987**, 109, 7122
- ⁹⁹ a) E. Drent, *European Patent Appl.*, 121,965 (**1984**) and 181,014 (**1986**).
b) J.A.M. van Broekhoven, E. Drent, E. Klei, *Eur. Pat.*, 213 671, **1987**.
c) J.A.M. van Broekhoven, E. Drent, *Eur. Pat.*, 235 865, **1987**.
d) E. Drent, J.A.M. van Broekhoven, M.J. Doyle, *J. Organomet. Chem.*, **1991**, 417, 235.
- ¹⁰⁰ a) A.C. Marr, PhD Thesis, University of St. Andrews, **1998**.
b) A.C. Marr, E.J. Ditzel, A.C. Benyei, P. Lightfoot, D.J. Cole-Hamilton, *Chem. Commun.*, **1999**, 1379.
- ¹⁰¹ M.J. Howard, M.D. Jones, M.S. Roberts, S.A. Taylor, *Catal. Today*, **1993**, 18, 325.
- ¹⁰² T. W. Dekleva, D. Forster, *Adv. Catal.*, **1986**, 34, 100.
- ¹⁰³ F.E. Paulik, J. Roth, *Chem. Commun.*, **1968**, 1578
- ¹⁰⁴ C. S. Garland, M.F. Giles, J.G. Sunley, *Eur. Pat.*, 643 034, **1995**; *Chem. Abstr.*, **1995**, 123, 86573g.
- ¹⁰⁵ M.J.Howard, M.D. Jones, M.S. Robersts, S.A. TAYlor, *Catalysis Today*, **1993**, 18, 325.
- ¹⁰⁶ D.F. Shriver, M. A. Drezdson, *The Manipulation of Air-Sensitive Compounds*, 2nd Ed, John Wiley & Sons, New York, **1986**.
- ¹⁰⁷ D.D. Perrin, W.L.F. Armarego, *Purification of Laboratory Chemicals*, 3rd Ed., Pergamon Press, Oxford, **1988**.